Maatgevende golfrandvoorwaarden Fort Ellewoutsdijk

OPDRACHTGEVER: Rijkswaterstaat Zeeland

PROJECTNUMMER: 05i045

VERSIE: definitief

13-05-2005

INFRAM

Projectgegevens

Titel:	Maatgevende golfrandvoorwaarden Fort Ellewoutsdijk
Versie:	Definitief
Opdrachtgever:	Rijkswaterstaat Zeeland
Projectnummer:	05i045
Omschrijving project:	De primaire waterkering bij Fort Ellewoutsdijk wordt gedeeltelijk beschermd door een buitendijk met een hoogte vrijwel gelijk aan de maatgevende waterstand. Bij een maatgevende storm loopt de "badkuip" al vol bij het getij voorafgaand aan het getij met de maatgevende condities. De waterstand is dan verder constant ter plaatse van de primaire kering. De maatgevende golfcondities worden dan vooral bepaald door golftransmissie over de voorliggende dijk. De hoek ten westen van het fort wordt het zwaarst aangevallen, omdat de andere hoek redelijk in de luwte van het fort ligt en de golven schever inkomen. Dit rapport geeft de maatgevende golfcondities bij de primaire kering. Daarbij is rekening gehouden met het stormverloop en met maatregelen om de golftransmissie te beperken.
Uitgevoerd door:	[redacted]

Inhoudsopgave

Lijst van symbolen ii

1 Inleiding, probleemstelling en gegevens 1
1.1 Opdracht 1
1.2 Probleemstelling 1
1.3 Gegevens 2

2 Fysisch gebeuren bij maatgevend stormverloop 6
2.1 Stormverloop 6
2.2 De badkuip loopt vol 7
2.3 Golftransmissie over de voorliggende kering 8
2.4 Locale golfgroei en reflectie 9

3 Maatgevende golfcondities bij de primaire kering 12
3.1 Huidige situatie 12
3.2 Voorliggende waterkering 0,5 m verhoogd 13
3.3 Voorliggende waterkering 1,0 m verhoogd 14
3.4 Andere maatregelen om de golftransmissie te beperken 14

4 Conclusies en aanbevelingen 16

Referenties

Lijst van symbolen

duur = gedeelte van storm waarbij omstandigheden constant worden verondersteld (uur)
g = versnelling van de zwaartekracht (m/s^2)
H_i = inkomende significante golfhoogte (m)
H_{m0} = significante golfhoogte op basis van spectrale energie (m)
$H_{m0}(1)$ = golfhoogte na transmissie behorende bij de piekperiode (m)
$H_{m0}(2)$ = golfhoogte behorende bij frequenties groter dan 1,5 piekfrequentie (m)
transmissie $H_{m0}(2)$ = alleen voor transmissie
totaal $H_{m0}(2)$ = transmissie en locale golfgroei
H_s = significante golfhoogte (m); $H_s = H_{m0}$
H_t = transmissiegolfhoogte (m)
K_t = H_t/H_i = transmissiecoëfficiënt (-)
lengte = lengte van de voorliggende dijk waarover golfoverslag plaats vindt
q = gemiddeld overslagdebiet (l/s per m breedte)
R_c = vrije kruinhoogte boven de waterstand (m)
s = $2\pi H_i/(gT_p^2)$ = golfsteilheid (-)
T_p = piekperiode (s)
$T_p(1)$ = periode behorende bij energie met frequenties < 1,5 piekfrequentie (s)
$T_p(2)$ = periode behorende bij energie met frequenties > 1,5 piekfrequentie (s)
T_{peq} = equivalente periode, samengesteld uit $T_p(1)$ en $T_p(2)$; gelijk aan T_p bij de dijk
T_s = significante golfperiode (s)
Volume = volume water dat in een bepaalde tijd de "badkuip" (gedeeltelijk) vult (m^3)
VTV = Voorschrift Toetsen op Veiligheid
U_{10} = windsnelheid op 10 m hoogte (m/s)
X = strijklengte (m)

α = hoek van buitentalud (°)
β = hoek van golfaanval ten opzichte van normaal van de dijk (°)
β-dijk = hoek van golfaanval op primaire waterkering (°)
β-noord = hoek van golfaanval ten opzichte van noord (°)
β_t = hoek van transmissiegolven ten opzichte van normaal van overslaande dijk (°)
ξ = $\tan\alpha/s^{0.5}$ = brekerparameter (-)
ξ_{op} = brekerparameter berekend met T_p (-)

1 Inleiding, probleemstelling en gegevens

1.1 Opdracht

Met de brief van 16 maart 2005 en kenmerk PZST-B-05058 werd aan Infram opdracht gegeven een geavanceerde berekening uit te voeren naar de maatgevende golfcondities bij Fort Ellewoutsdijk. Dit rapport maakt deel uit van opdracht met kenmerk ZLAO 35050040.

1.2 Probleemstelling

Fort Ellewoutsdijk ligt in het uiterste zuiden van Zuid-Beveland, zie figuur 1.1. Aan de achterzijde van het historische fort ligt de primaire kering. Het fort en ook de primaire kering, worden onder dagelijkse omstandigheden beschermd door een voorliggende dijk, zie foto 1.1.

Figuur 1.1 Locatie Fort Ellewoutsdijk

Foto 1.1 Luchtfoto Fort Ellewoutsdijk met te berekenen dijkvakken

Onder maatgevende omstandigheden komt de waterstand net boven deze dijk uit, loopt de "badkuip" tussen de beide dijken vol en kunnen er golven bij de primaire kering komen. Het buitentalud van deze kering bestaat alleen uit klei en gras. De vraag is nu welke maatgevende condities bij de primaire kering kunnen ontstaan, zodat kan worden nagegaan of de bekleding met gras voldoende sterk is, of dat een harde bekleding moet worden aangelegd. Het traject waarvoor de maatgevende golfcondities moeten worden bepaald is ook in foto 1.1 aangegeven.

1.3 Gegevens

Door de opdrachtgever zijn de golfrandvoorwaarden toegeleverd, welke door RIKZ zijn berekend en welke later zijn geactualiseerd. Fort Ellewoutsdijk wordt gekenmerkt door twee dijkvakken genaamd 32a en 32 b. Figuur 1.3 geeft de plattegrond van de situatie met de dijkvakken.

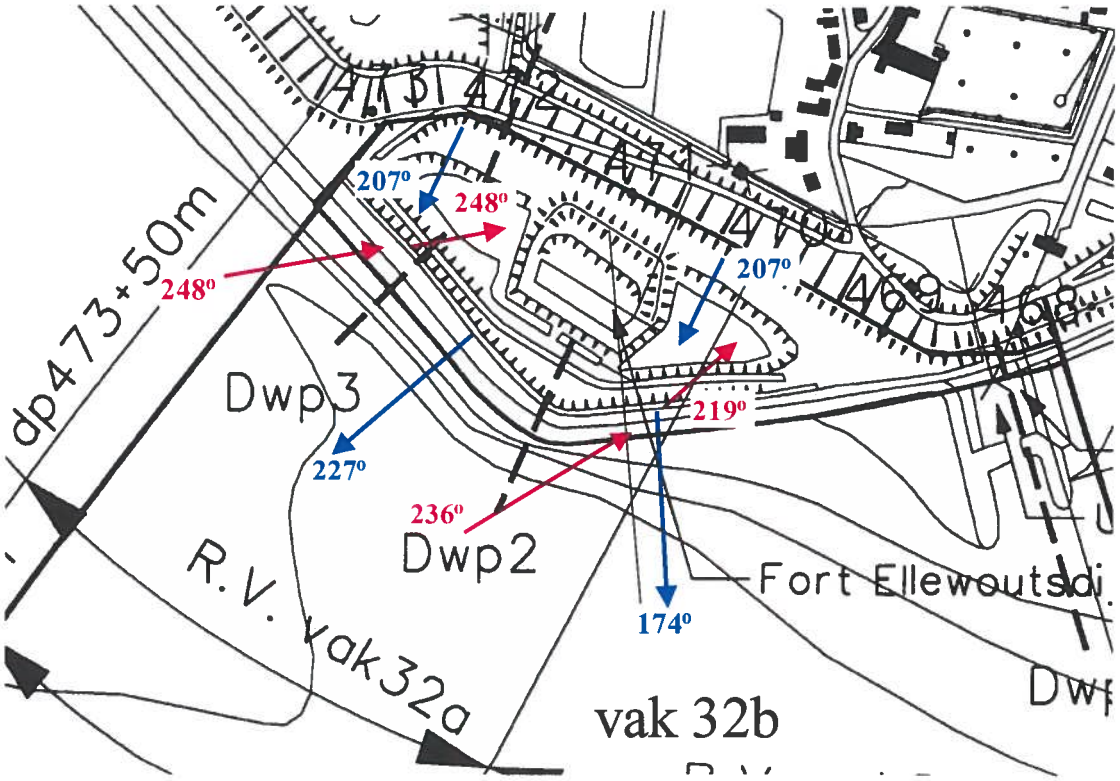

Figuur 1.2 Plattegrond Ellewoutsdijk met de normalen voor de diverse dijkvakken en de maatgevende golfrichtingen

Dijkvak 32a betreft met name de meest westelijke van de voorliggende waterkering. De voorliggende kering heeft een normaal van 227°, terwijl de primaire kering een normaal heeft van 207°. Dit is de voorliggende kering die het zwaarst wordt aangevallen. Dijkvak 32b ligt oostelijk hiervan heeft een normaal van 174°. Alhoewel de overgang tussen de beide vakken niet precies ligt op de hoek van de voorliggende kering, is hier voor de eenvoud toch van uit gegaan.

De toegeleverde golfrandvoorwaarden zijn gegeven in tabel 1.1 en zijn gevonden voor een maatgevende windrichting van 270° (zie figuur 1.1) en een windsnelheid van 33 m/s. De golfcondities worden voor 3 waterstanden gegeven.

Tabel 1.1 Toegeleverde en door RIKZ berekende golfrandvoorwaarden

Dijkvak	Golfrichtingsband (°)	Waterstand					
		NAP +2 m		NAP +4 m		NAP +6 m	
		H_s (m)	T_p (s)	H_s (m)	T_p (s)	H_s (m)	T_p (s)
32a	223-273	2,5	5,8	2,8	6,2	3,1	6,7
32b	212-260	2,0	5,5	2,3	5,8	2,6	6,3

Voor andere waterstanden kan worden geïnterpoleerd of geëxtrapoleerd om de golfcondities te berekenen. De golfrichtingsband is gedefinieerd als de gemiddelde richting van de golven op 50 m voor de teen van de dijk met als bandbreedte +/- 0,5σ van het richtingspreidingsspectrum. De maatgevende golfrichting is dus het midden van de golfrichtingsband. Dit is 248° voor vak 32a en 236° voor vak 32b en de golven zijn dus bijgedraaid ten opzichte van de windrichting 270°. Door de oplopende vooroever draaien de golven ook nog iets bij voor vak 32b (zie ook figuur 1.2).

De geëxtrapoleerde golfrandvoorwaarden behorend bij het Ontwerppeil 2060 zijn in tabel 1.2 gegeven.

Tabel 1.2 Toegeleverde golfrandvoorwaarden bij Ontwerppeil 2060

Dijkvak	Ontwerppeil 2060 (NAP + m)	Golfparameters	
		H_s (m)	T_p (s)
32a	6,20	3,13	6,75
32b	6,20	2,63	6,35

Om het stormverloop te kunnen construeren is het gemiddelde getijverloop nodig. De slotgemiddelden 1991.0, zoals deze in bestekken worden gebruikt, zijn voor Terneuzen 2.29 m + NAP en 1.90 m – NAP. Terneuzen ligt precies aan de overkant van de Westerschelde ten opzichte van Ellewoutsdijk, zodat deze waarden voldoende nauwkeurig zijn.

Ook zijn plattegronden ontvangen en profielen van dijkdoorsneden. De doorsneden van Dwp 2 en 3 (zie voor locatie figuur 1.2) geven de westelijke voorliggende dijk en zijn schematisch weergegeven in figuren 1.3 en 1.4. Het buitentalud is 1:3.6, de kruinhoogte is 6.1 m + NAP en de kruinbreedte is ongeveer 6 m.

Het profiel van de achterliggende primaire kering is gegeven in figuur 1.5. De kruinhoogte van deze dijk is ongeveer 10,4 m + NAP. Tussen 5,85 m + NAP en 6,25 m + NAP bevindt zich een berm met een talud 1:11. Deze berm bevindt zich precies rondom het ontwerppeil 6,20 m + NAP.

In figuur 1.6 is de doorsnede van het fort gegeven. De bovenkant van het fort ligt op ongeveer 5.5 m + NAP, dit is ongeveer 0,6 – 0,7 m beneden de maatgevende waterstand.

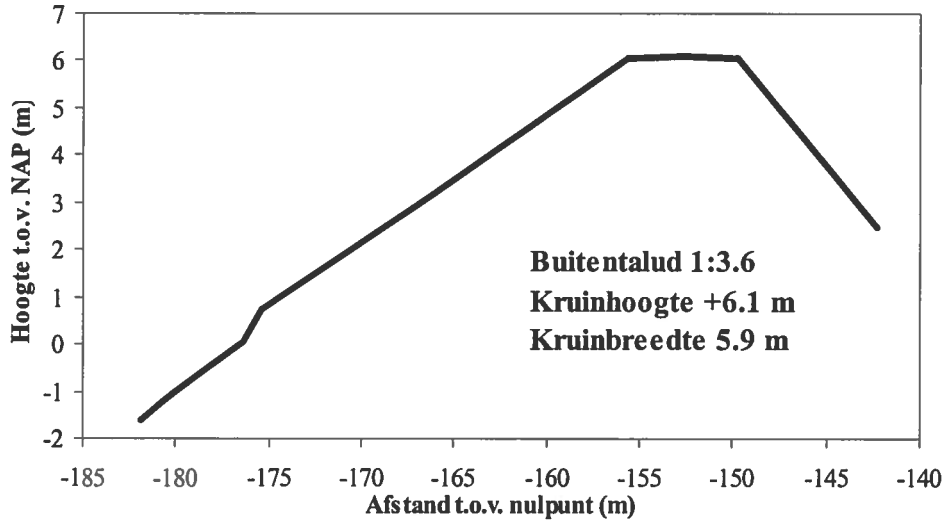

Figuur 1.3 Doorsnede Dwp 2, westelijke voorliggende dijk

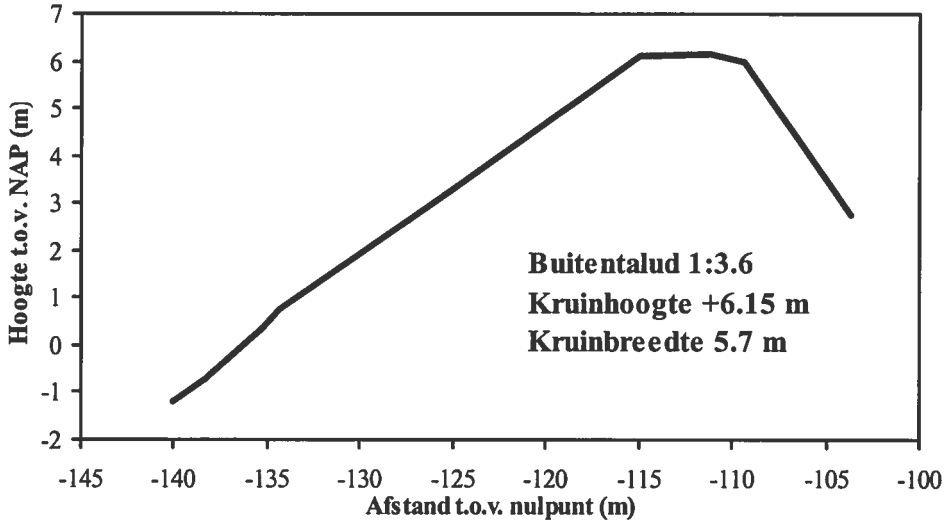

Figuur 1.4 Doorsnede Dwp 3, westelijke voorliggende dijk

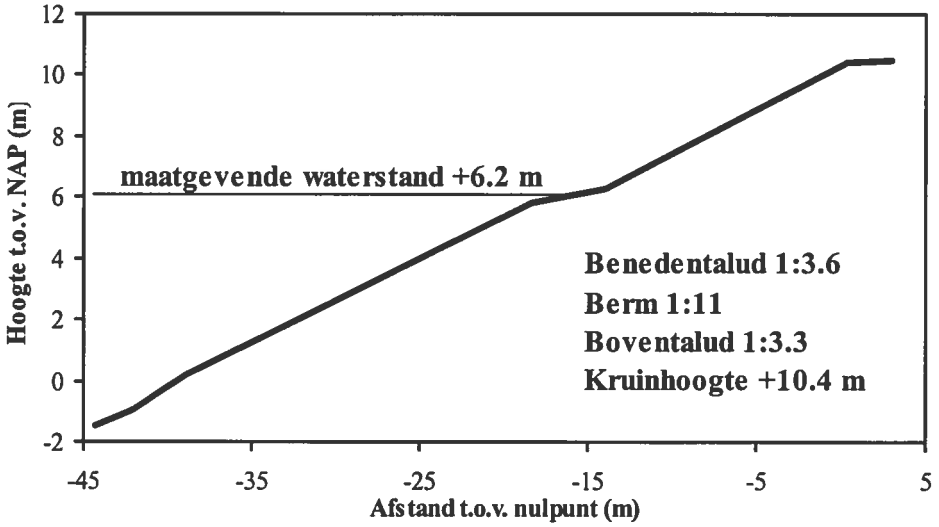

Figuur 1.5 Doorsnede achterliggende primaire kering

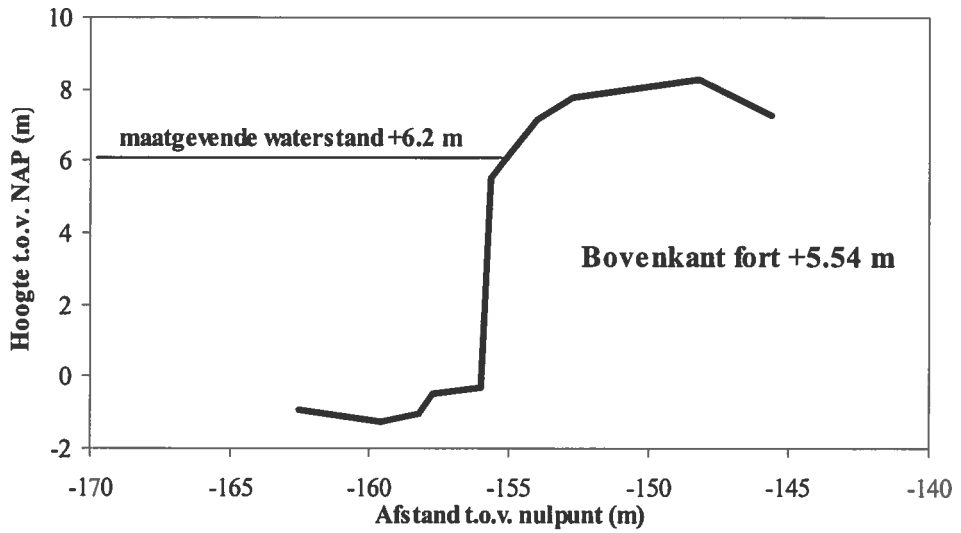

Figuur 1.6 Doorsnede ter plaatse van het fort

2 Fysisch gebeuren bij maatgevend stormverloop

2.1 Stormverloop

De zwaarste belastingen op de primaire kering zullen ongetwijfeld ontstaan als de "badkuip" is volgelopen en het ontwerppeil is bereikt met bijbehorende golfcondities. Maar ook voor en na de situatie op ontwerppeil kunnen er nog zware belastingen bestaan. Verder is het van belang na te gaan wanneer en in welke tijd het gebied tussen de twee dijken vol loopt. Hierbij is het stormverloop van belang.

In de VTV (paragraaf 3.3.4) wordt het verloop van de waterstand beschreven voor maatgevende toetssituaties. Langs de Noordzeekust geldt een stormopzetduur van 35 uur. Een gemiddelde getijkromme moet op deze stormopzet worden gesuperponeerd, zodanig dat het tijdstip van een top van de getijkromme samenvalt met dat van de top van de opzet. De maximale waterstand wordt hiermee gelijk aan Toetspeil (in ons geval ontwerppeil).

Met een ontwerppeil van 6,2 m +NAP en een gemiddelde getijamplitude van (2,29 + 1,90)/2 = 2.1 m is de maximale stormopzet 4,1 m +NAP. Het verloop van de stormopzet en het verloop van de totale waterstand is in figuur 2.1 uitgezet.

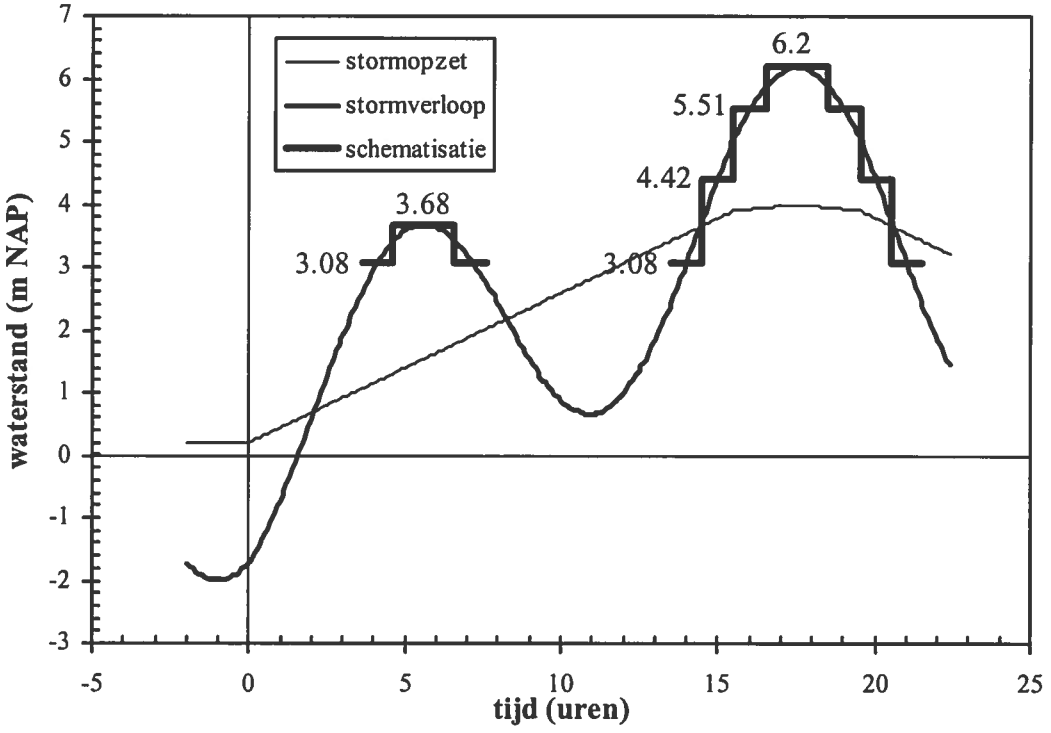

Figuur 2.1 Stormopzet en waterstandsverloop voor ontwerpomstandigheden

Het getij voorafgaand aan het getij met het ontwerppeil komt tot een maximale waterstand van ongeveer 3,7 m +NAP. Om de gevolgen van de variërende waterstand na te gaan zijn in figuur 2.1 perioden van 1 uur aangegeven, waarbij de waterstand ongeveer constant mag worden verondersteld. Voor de top van het getij geldt dat deze 2 uur duurt. Bij het voorafgaand getij duurt de maximale waterstand van 3,68 m +NAP 2 uur en voor en na dit maximum komt de waterstand (geschematiseerd) van 3,08 m +NAP ook in totaal 2 uur voor. In het getij daarna

komen waterstanden van 3,08 m, 4,42 m, 5,51 m +NAP voor gedurende 2 maal 1 uur en een ontwerpwaterstand van 6,2 m +NAP gedurende 2 uur.

2.2 De badkuip loopt vol

Als zowel de waterstand en de golven hoog genoeg zijn dan zal op een gegeven moment water over de voorliggende dijk slaan. Dit water kan niet weglopen. Bij stijgende waterstand zal steeds meer water over de kruin slaan, totdat het totale gebied tussen de beide dijken (de badkuip) vol is. Op dat moment ontstaat er een constante waterstand in de badkuip die vrijwel gelijk is aan de kruinhoogte van de voorliggende dijk (6,1 m +NAP). Deze hoogte is ook vrijwel gelijk aan het ontwerppeil. Als de badkuip eenmaal is volgelopen, zal een variërende waterstand wel effect hebben op de golven in de badkuip, maar niet meer op de waterstand. Het water kan immers niet meer weg.

De inhoud van de badkuip en de golfoverslag tijdens de aanloop van de ontwerpstorm zijn bepalend voor wanneer de badkuip helemaal vol is. Op basis van de gedetailleerde plattegrond van het gebied en de verschillende doorsneden van de dijken is de inhoud van de badkuip vrij nauwkeurig berekend. Deze inhoud bedraagt 116.000 m^3. De lengte van het westelijke dijkvak 32a is 230 m en die van het oostelijke dijkvak 32b is 180 m.

Met TAW (2002), het rapport omtrent golfoploop en golfoverslag bij dijken, kan de golfoverslag over de voorliggende dijk worden berekend. Voor deze studie is het bijbehorende programma PC-OVERSLAG gebruikt. Het buitentalud van de voorliggende dijk is geschematiseerd tot een 1:3,6 talud met een ruwheidsfactor 1.

In paragraaf 1.3 zijn de maatgevende golfrichtingen bij de dijk besproken en in paragraaf 2.1 is het waterstandsverloop tijdens de ontwerpstorm gegeven. Allereerst is berekend in hoeverre tijdens het getij voorafgaand aan het getij met het ontwerppeil de badkuip al vol loopt. Tabel 2.1 geeft de resultaten.

Tabel 2.1 Volume golfoverslag bij de aanloop naar ontwerppeil tijdens ontwerpstorm

Dijkvak	waterstand	H_s	T_p	β-noord	β	R_c	ξ_{op}	q	lengte	duur	Volume
	m NAP	m	s	graden	graden			l/s per m	m	uur	m^3
32a	3.08	2.66	6.02	248	21	3.02	1.28	22.24	230	2	36829
32b	3.08	2.16	5.67	236	62	3.02	1.34	3.09	180	2	4005
32a	3.68	2.75	6.14	248	21	2.42	1.29	65.29	230	2	108120
32b	3.68	2.25	5.75	236	62	2.42	1.33	13.27	180	2	17198
										totaal	166152

Bij een waterstand van 3,08 m +NAP begint golfoverslag al te spelen. In 1 uur zal ongeveer 20.000 m^3 water in de badkuip lopen (het andere uur van de duur van 2 uur ligt na hoog water). Het voorafgaand getij heeft ongeveer gedurende 2 uur een waterstand van 3.68 m +NAP. Tijdens deze twee uur gaat er ongeveer 125.000 m^3 over de kruin van de voorliggende dijk. Dit is al meer dan de inhoud van de badkuip.

De conclusie is dat de badkuip al volgelopen is tijdens het getij voorafgaand aan het getij met het ontwerppeil. Voor, tijdens en na de situatie op ontwerppeil kan daarom worden uitgegaan van een constant waterpeil in de badkuip van ongeveer 6,1 - 6,2 m +NAP.

Foto 2.1 geeft een idee van de waterstand in het westelijk gedeelte. De vrijwel constante waterstand zit rond de berm op de primaire kering en net boven de verticale muur van het fort.

Foto 2.1 Westelijk deel met de waterstand nadat de badkuip is vol gelopen

2.3 Golftransmissie over de voorliggende kering

In Van der Meer et al. (2004) worden formules gegeven voor golftransmissie over lage en gladde dammen bij scheve golfaanval. Deze formules zijn rechtstreeks te gebruiken voor de voorliggende dijk. De formule voor golftransmissie is:

$$K_t = [-0.3R_c/H_i + 0.75[1 - \exp(-0.5\xi)]] \cos^{2/3}\beta \qquad (1)$$

met als minimum $K_t = 0.075$ en maximum $K_t = 0.8$.

en toepassingsgebied: $1 < \xi_{op} < 3$ $\quad 0° \leq \beta \leq 70°$ $\quad 1 < B/H_i < 4$

Hierbij is:

$K_t = H_t/H_i$ = transmissiecoëfficiënt (-)
R_c = vrije kruinhoogte boven de waterstand (m)
H_i = inkomende significante golfhoogte (m)
H_t = transmissiegolfhoogte (m)
$\xi = \tan\alpha/s^{0.5}$ = brekerparameter (-)
α = hoek van buitentalud (°)
$s = 2\pi H_i/(gT_p^2)$ = golfsteilheid (-)
T_p = piekperiode (s)
β = hoek van golfaanval

Voor de maatgevende windrichting van 270° en de maatgevende golfrichtingen bij de dijk (paragraaf 1.3) en de 4 waterstanden rondom de getijpiek met de ontwerpwaterstand, kan de golftransmissie over elk dijkvak worden berekend. De *linker* helft van tabel 2.2 geeft de resultaten voor golftransmissie alleen, met in het midden van de tabel de transmissie golfhoogte H_t en de hoek van transmissie met de normaal van de dijk β_t. De rechter helft van de tabel geeft de resultaten voor locale golfgroei (volgende paragraaf) en de totale resultaten (hoofdstuk 3).

Tabel 2.2 Golftransmissie en locale golfgroei bij huidige situatie

Randvoorwaarden					Transmissie						Locale golfgroei				Resultaat primaire kering		
Dijkvak	waterstand m NAP	H_s m	T_p s	β-noord graden	β graden	R_c	ξ_{op}	K_t	H_t	β_t graden	$H_{m0}(1)$ m	transmissie $H_{m0}(2)$ m	totaal $H_{m0}(2)$ m	$T_p(2)$ s	H_{m0} m	T_p s	β-dijk graden
32a	**6.2**	3.1	6.75	248	21	-0.1	1.32	0.356	1.11	21	0.86	0.70	0.76	2.56	**1.15**	**4.92**	**41**
32b	**6.2**	2.6	6.35	236	62	-0.1	1.36	0.230	0.61	45	0.47	0.38	0.46	1.84	**0.66**	**4.15**	**12**
32a	**5.51**	3	6.56	248	21	0.59	1.31	0.288	0.87	21	0.68	0.55	0.62	2.25	**0.92**	**4.58**	**41**
32b	**5.51**	2.5	6.18	236	62	0.59	1.35	0.180	0.46	45	0.35	0.29	0.43	1.77	**0.56**	**3.53**	**12**
32a	**4.42**	2.9	6.31	248	21	1.68	1.30	0.173	0.50	21	0.38	0.31	0.43	1.77	**0.58**	**3.77**	**41**
32b	**4.42**	2.4	5.91	236	62	1.68	1.34	0.092	0.22	45	0.17	0.14	0.30	1.38	**0.34**	**2.48**	**12**
32a	**3.08**	2.7	6.02	248	21	3.02	1.28	0.075	0.20	21	0.15	0.13	0.33	1.48	**0.36**	**2.30**	**41**
32b	**3.08**	2.2	5.66	236	62	3.02	1.34	0.075	0.16	45	0.13	0.10	0.28	1.33	**0.31**	**2.05**	**12**

De golftransmissie over het westelijke dijkvak 32a heeft dezelfde richting als de inkomende golf ($\beta = \beta_t$ in tabel 2.2). Bij het oostelijke dijkvak verandert de richting van transmissiegolven. De golven komen onder een hoek van $\beta = 62°$ aan en gaan gemiddeld onder een hoek van $\beta_t = 45°$ met de voorliggende dijk weg (zie Van der Meer et al., 2004). Bij de ontwerpwaterstand treden natuurlijk de hoogste golven op. Voor het dijkvak 32a is dit een golfhoogte van $H_t = 1{,}11$ m (zie midden van de tabel). Over het oostelijk dijkvak is dit niet meer dan 0,61 m. Maar dit is *alleen de golfhoogte door transmissie*. Locale golfgroei en eventueel reflectie kunnen de golfhoogte bij de primaire kering nog verhogen. Dit wordt behandeld in de volgende paragraaf.

2.4 Locale golfgroei en reflectie

In het kader van het ontwerp van een nieuwe waterkering in het stedelijk gebied van Harlingen is in detail gekeken naar locale golfgroei bij hele korte strijklengtes en extreme windsnelheden. Bij Harlingen beschermen de havendammen deels de waterkering, net als de voorliggende dijk bij Ellewoutsdijk, en is er 100 – 400 m ruimte tussen de havendammen en de waterkering. Ondanks deze korte lengte wordt golfenergie opgewekt omdat onder maatgevende omstandigheden de windsnelheid extreem hoog is. Dit effect moet worden meegenomen bij de bepaling van de golfcondities bij de primaire kering van Ellewoutsdijk. Overigens is de ruimte achter de voorliggende kering bij Ellewoutsdijk niet meer dan 120 m (dijkvak 32a) en 90 m (dijkvak 32b), dus minder dan in Harlingen.

In Van der Meer (2002) wordt de problematiek rond Harlingen beschreven met de juiste formule voor locale golfgroei. De studie naar de juiste golfgroeiformule is beschreven in Ris et al. (2002). Dit is de formule van Wilson (1955):

Assuming that $U=U_{10}$, $H=H_s$ and $c=gT_s/2\pi$ in Wilson's formulations, the following formulations for wave growth in deep water were derived by Wilson (1955):

$$\frac{H_s g}{U_{10}^2} = \overbrace{0.26\tanh\left(0.01\left(\frac{gX}{U_{10}^2}\right)^{0.5}\right)}^{10^{-1}<\frac{gX}{U_{10}^2}} \quad \overbrace{2.6\times10^{-3}\left(\frac{gX}{U_{10}^2}\right)^{0.5}}^{\frac{gX}{U_{10}^2}\to 0}$$

$$\frac{T_s g}{U_{10}} = 1.4\,2\pi\tanh\left(0.0436\left(\frac{gX}{U_{10}^2}\right)^{0.33}\right) \quad 6.02\times10^{-2}\,2\pi\left(\frac{gX}{U_{10}^2}\right)^{0.33} \tag{2}$$

where: H_s = significant wave height; g = acceleration of gravity U_{10} = wind speed at 10 m height; T_s = significant period and X = fetch length.

Er speelt echter nog een effect. Door golftransmissie verandert de vorm van het golfspectrum. Overslaande golven genereren vaak 2 of meer golven, die noodzakelijkerwijs een kortere periode hebben. Alhoewel de piekperiode wel ongeveer gelijk blijft, wordt de gemiddelde golfperiode veel korter. Er gaat veel meer energie in de hogere frequenties zitten. In Van der Meer et al. (2002) wordt de methode beschreven. Ongeveer 60% van de golfenergie blijft rondom de piekperiode zitten en de resterende 40% gaat naar de hogere frequenties. En locale golfgroei vindt vooral plaats bij deze hogere frequenties.

Met andere woorden, er is al golfenergie bij de hogere frequenties en de extreme wind zal juist deze energie nog laten toenemen. Uiteindelijk ontstaat bij de primaire kering een tweetoppig spectrum: een deel van de energie zit bij de oorspronkelijke piekperiode van de inkomende golven en een deel bij een veel kortere periode. De methode om de uiteindelijke golfhoogte bij de primaire kering te berekenen is als volgt:

- Verdeel de transmissiegolfhoogte in twee aparte golfhoogtes:
  - $H_{m0}(1)$ met 60% van de energie en met de oorspronkelijke piekperiode
  - $H_{m0}(2)$ met 40% van de energie
- Bereken met formule 2 welke strijklengte nodig is om $H_{m0}(2)$ te genereren
- Voeg deze strijklengte bij de werkelijke strijklengte en bereken de totale locale golfgroei. Deze levert een nieuwe totale $H_{m0}(2)$ op met een periode $T_p(2)$
- Herleid het tweetoppig spectrum tot een equivalent enkeltoppig spectrum

De formule om het tweetoppig spectrum te herleiden tot een uiteindelijke H_{m0} en T_p is:

$$H_{m0} = \sqrt{H_{m0,1}^2 + H_{m0,2}^2} \tag{3}$$

$$T_{peq} = \left(\frac{H_{m0,1}}{H_{m0}}\right)^2 T_{p,1} + \left(\frac{H_{m0,2}}{H_{m0}}\right)^2 T_{p,2} \tag{4}$$

De rechter helft van tabel 2.2 geeft de uiteindelijke resultaten van de hele exercitie met betrekking tot de locale golfgroei, zoals boven omschreven. De drie meest rechtse kolommen geven de maatgevende golfcondities bij primaire kering. Dit zijn de significante golfhoogte $H_{m0} = H_s$, de piekperiode $T_p = T_{peq}$ (formule 4) en de hoek van golfaanval ten opzichte van de normaal van de dijk, β-dijk.

De locale golfgroei heeft bij de wat hogere transmissiegolfhoogtes niet veel effect: de golfhoogte wordt orde 5 cm groter. De golfperiode wordt echter wel kleiner. Bij de lagere waterstanden en lagere transmissiegolfhoogtes (bijvoorbeeld bij een waterstand van 3,08 m +NAP) wordt de golfhoogte bij de primaire kering vrijwel uitsluitend bepaald door locale golfgroei. De golfhoogte zelf blijft dan echter beperkt tot orde 0,3 m.

Golfreflectie van dijken is door het meestal flauwe talud vrij laag. Het fort heeft echter een vrijwel verticale muur (zie figuur 1.6) en golven reflecteren volledig van een verticale muur. De golven die over het westelijke dijkvak 32a gaan, komen ongeveer onder 45° in op de westelijke zijde van het fort. Als deze golven volledig reflecteren, wordt de golfhoogte op de primaire kering hoger. In werkelijkheid zit echter de maatgevende waterstand van +6,2 m +NAP behoorlijk ver boven de bovenzijde van de muur van het fort. Zie figuur 1.6 en ook foto 2.1 en 2.2.

Foto 2.2 Maatgevende waterstand bij het fort

Het gedeelte boven het fort is bedekt met vrij willekeurig talud met gras. De reflectie van dit talud zal lang niet zo hoog zijn als van een verticale muur en ook meer gespreid. Ingeschat wordt dat deze reflectie niet van belang is voor de maatgevende condities bij de primaire kering net ten westen van het fort.

3 Maatgevende golfcondities bij de primaire kering

3.1 Huidige situatie

Hoe maatgevende condities zijn berekend is in hoofdstuk 2 gegeven. Het uiteindelijk resultaat voor de huidige situatie is samengevat in tabel 3.1 (gelijk aan tabel 2.2). De tabel geeft de maatgevende condities bij 4 waterstanden die elk ongeveer 2 uur duren. Voor de ontwerpwaterstand is dit in totaal 2 uur, voor de andere waterstanden geldt dat het eerste uur vóór hoog water valt en het tweede uur na hoog water. Bij de ontwerpwaterstand van 6,2 m +NAP ontstaat voor het westelijk deel een golfhoogte van 1,15 m met een piekperiode van 4,9 s. Het uur voor en na hoog water is de golfhoogte lager dan 1 m (0,92 m). Bij waterstanden lager dan 4,5 m +NAP wordt de golfhoogte veel lager en wordt deze voor een groot gedeelte bepaald door locale golfgroei met kleine en korte golven. De golfhoogte is dan lager dan 0,5 m. De golfhoogte H_{m0} is gelijk aan H_s.

Tabel 3.1 Maatgevende golfcondities bij huidige situatie

Randvoorwaarden					Transmissie						Locale golfgroei				Resultaat primaire kering		
Dijkvak	waterstand m NAP	H_s m	T_p s	β-noord graden	β graden	R_c	ξ_{op}	K_t	H_t	β_t graden	$H_{m0}(1)$ m	transmissie $H_{m0}(2)$ m	totaal $H_{m0}(2)$ m	$T_p(2)$ s	H_{m0} m	T_p s	β-dijk graden
32a	6.2	3.1	6.75	248	21	-0.1	1.32	0.356	1.11	21	0.86	0.70	0.76	2.56	1.15	4.92	41
32b	6.2	2.6	6.35	236	62	-0.1	1.36	0.230	0.61	45	0.47	0.38	0.46	1.84	0.66	4.15	12
32a	5.51	3	6.56	248	21	0.59	1.31	0.288	0.87	21	0.68	0.55	0.62	2.25	0.92	4.58	41
32b	5.51	2.5	6.18	236	62	0.59	1.35	0.180	0.46	45	0.35	0.29	0.43	1.77	0.56	3.53	12
32a	4.42	2.9	6.31	248	21	1.68	1.30	0.173	0.50	21	0.38	0.31	0.43	1.77	0.58	3.77	41
32b	4.42	2.4	5.91	236	62	1.68	1.34	0.092	0.22	45	0.17	0.14	0.30	1.38	0.34	2.48	12
32a	3.08	2.7	6.02	248	21	3.02	1.28	0.075	0.20	21	0.15	0.13	0.33	1.48	0.36	2.30	41
32b	3.08	2.2	5.66	236	62	3.02	1.34	0.075	0.16	45	0.13	0.10	0.28	1.33	0.31	2.05	12

De condities voor het oostelijk deel zijn veel lager dan voor het westelijk deel. Dit komt vooral doordat de golven veel schever invallen en daardoor de golftransmissie veel lager is. Bij de ontwerpwaterstand is de golfhoogte bij de primaire kering 0,66 m met een periode van 4,1 s.

Alle condities vinden plaats bij een waterstand in de buurt van 6,1 – 6,2 m +NAP, want als eenmaal de badkuip is volgelopen, dan kan het water niet weg. De golfcondities variëren dus met de waterstand op de Westerschelde, maar de waterstand in de badkuip zelf is constant. De belasting op de primaire kering vindt dan ook plaats rondom een constante waterstand en niet over het hele talud. Dit is afwijkend ten opzichte van dijkvakken die direct aan zee liggen.

Figuur 1.5 geeft de doorsnede van de primaire kering. Precies rondom de maatgevende waterstand ligt een berm. In figuur 1.5 is dit een berm met een talud 1:11 en een hoogte tussen 5,85 en 6,25 m +NAP. De breedte varieert van 4 m op het meest westelijk deel tot ongeveer 6 m in de buurt van het fort. Foto 3.1 geeft een idee van dit stuk primaire kering en de hoogte van de maatgevende waterstand.

Alhoewel dit rapport de maatgevende golfcondities geeft en niet de toetsing van de sterkte van de grasdijk, kan wel worden opgemerkt dat het effect van een berm precies rondom een constante maatgevende waterstand een positief effect heeft op de sterkte van de grasmat met onderliggende kleilaag. Daarnaast heeft de dijk in dit gebied zelf een grote overhoogte en is er dus een grote reststerkte aanwezig.

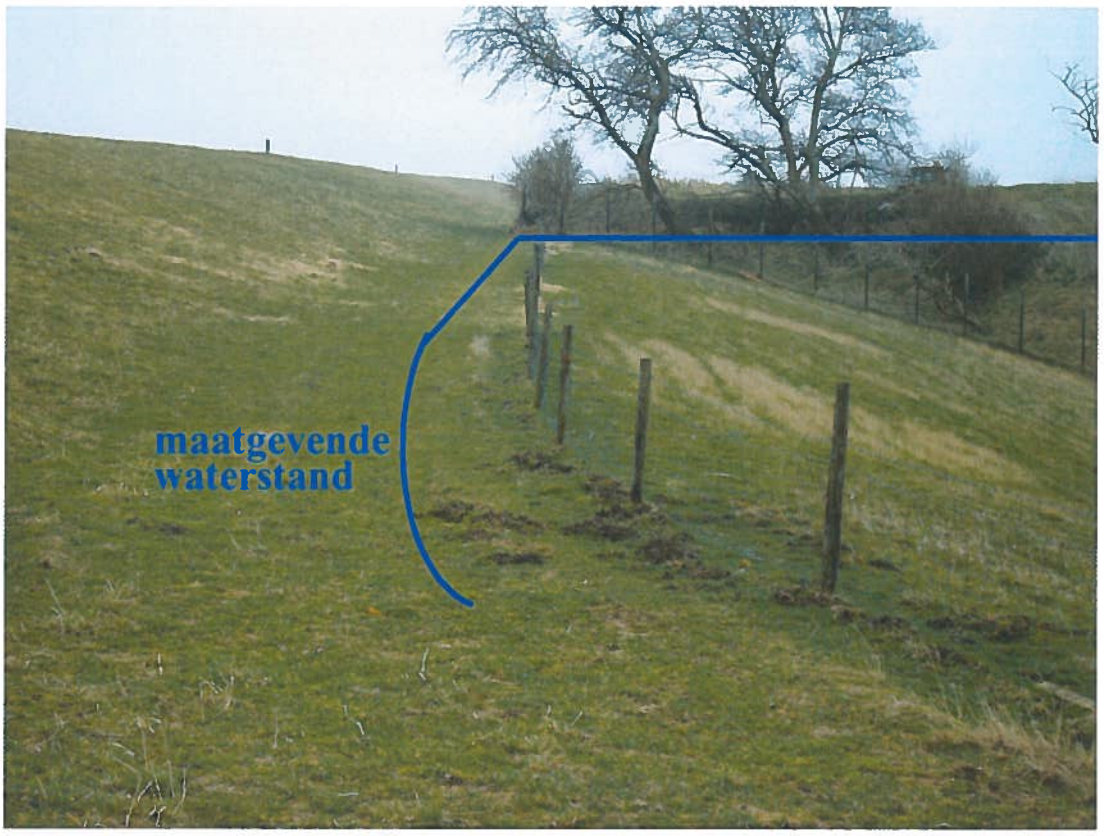

Foto 3.1 Het westelijke dijkvak 32a met de constante maatgevende waterstand op de berm

3.2 Voorliggende waterkering 0,5 m verhoogd

In het geval de huidige situatie dermate hoge golfcondities bij de primaire kering oplevert dat de grasmat met onderliggende kleilaag hier niet voldoende tegen bestand is, kan worden nagedacht over mogelijke maatregelen om de golfcondities te beperken. Als eerste wordt gekeken naar een verhoging van de voorliggende waterkering van 0,5 m. In feite is deze verhoging alleen nodig voor dijkvak 32a, het meest westelijke dijkvak, en niet voor het oostelijk deel, want daar zijn de golfcondities nu al niet zo hoog. Toch wordt ook voor dit dijkvak het effect berekend. Tabel 3.2 geeft de uiteindelijke resultaten.

Tabel 3.2 Maatgevende condities bij een voorliggende dijk die 0,5 m is verhoogd

Randvoorwaarden					Transmissie						Locale golfgroei				Resultaat primaire kering		
Dijkvak	waterstand	H_s	T_p	β-noord	β	R_c	ξ_{op}	K_t	H_t	β_t	$H_{m0}(1)$	transmissie	totaal	$T_p(2)$	H_{m0}	T_p	β-dijk
	m NAP	m	s	graden	graden					graden	m	$H_{m0}(2)$ m	$H_{m0}(2)$ m	s	m	s	graden
32a	6.2	3.1	6.75	248	21	0.4	1.32	0.310	0.97	21	0.75	0.61	0.68	2.39	**1.02**	**4.78**	**41**
32b	6.2	2.6	6.35	236	62	0.4	1.36	0.196	0.52	45	0.40	0.33	0.42	1.73	**0.58**	**3.92**	**12**
32a	5.51	3	6.56	248	21	1.09	1.31	0.241	0.73	21	0.57	0.46	0.55	2.06	**0.79**	**4.38**	**41**
32b	5.51	2.5	6.18	236	62	1.09	1.35	0.144	0.36	45	0.28	0.23	0.35	1.53	**0.45**	**3.38**	**12**
32a	4.42	2.9	6.31	248	21	2.18	1.30	0.123	0.35	21	0.27	0.22	0.37	1.60	**0.46**	**3.24**	**41**
32b	4.42	2.4	5.91	236	62	2.18	1.34	0.075	0.18	45	0.14	0.11	0.28	1.33	**0.31**	**2.21**	**12**
32a	3.08	2.7	6.02	248	21	3.52	1.28	0.075	0.20	21	0.15	0.13	0.33	1.47	**0.36**	**2.30**	**41**
32b	3.08	2.2	5.66	236	62	3.52	1.34	0.075	0.16	45	0.13	0.10	0.28	1.33	**0.31**	**2.05**	**12**

De hoogste golfcondities voor het westelijk deel tijdens de ontwerpwaterstand worden nu beperkt tot ongeveer 1 m in plaats van 1,15 m. Bij een waterstand van 5,5 m +NAP is de golfhoogte nog geen 0,8 m.

3.3 Voorliggende waterkering 1,0 m verhoogd

Mocht een verhoging van 0,5 m van de westelijke voorliggende kering niet genoeg zijn, dan zou een verhoging van 1,0 m overwogen kunnen worden. In plaats van de dijk zelf te verhogen, is het ook mogelijk een stevige muur van 1 m hoog op de dijk te plaatsen. Dit heeft vrijwel hetzelfde effect op de golftransmissie. Bij de eerder genoemde verbetering van de waterkering van Harlingen is dit onderzocht, omdat daar op de havendam een muur van ongeveer 1 m hoog aanwezig is. Proeven in de Deltagoot van WL hebben aangetoond dat zo'n muur stabiel kan zijn en dat transmissie overeenkomstig een verhoogde dijk is.

De maatgevende golfcondities zijn in tabel 3.3 gegeven. De golfhoogte bij de ontwerpwaterstand wordt nu 0,88 m in plaats van 1,15 zonder verhoging.

Tabel 3.3 Maatgevende condities bij een voorliggende dijk die 1,0 m is verhoogd

Randvoorwaarden					Transmissie						Locale golfgroei				Resultaat primaire kering		
Dijkvak	waterstand m NAP	H_s m	T_p s	β-noord graden	β graden	R_c	ξ_{op}	K_t	H_t	β_t graden	$H_{m0}(1)$ m	transmissie $H_{m0}(2)$ m	totaal $H_{m0}(2)$ m	$T_p(2)$ s	H_{m0} m	T_p s	β-dijk graden
32a	6.2	3.1	6.75	248	21	0.9	1.32	0.265	0.83	21	0.64	0.52	0.60	2.19	**0.88**	**4.62**	**41**
32b	6.2	2.6	6.35	236	62	0.9	1.36	0.161	0.42	45	0.33	0.27	0.38	1.62	**0.50**	**3.66**	**12**
32a	5.51	3	6.56	248	21	1.59	1.31	0.194	0.59	21	0.45	0.37	0.47	1.88	**0.66**	**4.12**	**41**
32b	5.51	2.5	6.18	236	62	1.59	1.35	0.108	0.27	45	0.21	0.17	0.31	1.43	**0.38**	**2.93**	**12**
32a	4.42	2.9	6.31	248	21	2.68	1.30	0.075	0.21	21	0.17	0.14	0.33	1.49	**0.37**	**2.45**	**41**
32b	4.42	2.4	5.91	236	62	2.68	1.34	0.075	0.18	45	0.14	0.11	0.28	1.34	**0.31**	**2.20**	**12**
32a	3.08	2.7	6.02	248	21	4.02	1.28	0.075	0.20	21	0.15	0.13	0.33	1.48	**0.36**	**2.30**	**41**
32b	3.08	2.2	5.66	236	62	4.02	1.34	0.075	0.16	45	0.13	0.10	0.28	1.33	**0.31**	**2.05**	**12**

3.4 Andere maatregelen om de golftransmissie te beperken

Verhoging van een constructie, zoals in paragrafen 3.2 en 3.3 besproken, leidt tot lagere maatgevende condities bij de primaire kering, maar de resultaten zijn niet spectaculair. Het is mogelijk aan maatregelen te denken waarbij de ruwheid van het talud groter wordt gemaakt en daardoor de golfdissipatie op het talud wordt verhoogd. Zo'n maatregel is bijvoorbeeld het overlagen van de bestaande voorliggende dijk (alleen het westelijk deel) met breuksteen. In principe is alleen breuksteen nodig op het bovenste deel van de dijk. Uitvoeringstechnisch gezien kan het echter aantrekkelijker zijn om het hele talud te overlagen. Het voordeel is dat de huidige steenbekleding niet hoeft te worden vervangen. Om toch over de dijk te kunnen blijven lopen is het mogelijk aan de achterzijde van de kruin een pad over te houden en de breuksteen tegen een muurtje te laten eindigen. Wel moet het binnentalud dan nog overslagbestendig worden gemaakt. Precieze uitwerking van dit alternatief past niet in het kader van deze opdracht. Wel zal het effect van een breuksteenoverlaging worden gegeven.

Eenzelfde problematiek heeft gespeeld bij de (asfalt)dammen die in het IJsselmeer liggen. Om een mogelijk niet voldoende sterke asfaltdam te beschermen is daar gedacht aan overlaging en zijn proeven in een golfgoot uitgevoerd, zowel omtrent de stabiliteit van de overlaging als

de transmissie. Dit werk is beschreven in Alkyon (1998). Het betrof een glad 1:4 buitentalud, een kruinbreedte van 2 m en maatgevende golfhoogtes van ongeveer 2,2 m. De overlaging bestond uit een 0,75 m dikke laag 60-300 kg breuksteen. Rondom een golfhoogte van 2 m ontstond er enige (toelaatbare) schade.
Bij Ellewoutsdijk zijn de golfcondities ongeveer 1,5 maal zo hoog, wat betekent dat de steendiameter ook ongeveer 1,5 maal zo groot zou moeten zijn. Dit betekent globaal een overlaging met 300-1000 kg steen, met een laagdikte van ongeveer 1,25 m. Als alternatief valt te denken aan zwaardere steen die eventueel in een enkele laag wordt gelegd, maar dat wordt hier verder niet uitgewerkt.

Figuur 3.1 geeft de transmissieresultaten zoals deze zijn gevonden voor de dammen in het IJsselmeer (Alkyon, 1998). Dammen 1, 3 en 4 waren gladde dammen met verschillende kruinbreedtes. Dam 2 is de dam met de overlaging. De punten liggen veel lager dan voor een gladde dam, bij dezelfde kruinhoogte. Op basis van de metingen voor de overlaging, wordt de volgende transmissieformule voorgesteld:

$$K_t = -0{,}3R_c/H_i + 0{,}23 \qquad (5)$$

met een minimum van $K_t = 0{,}05$

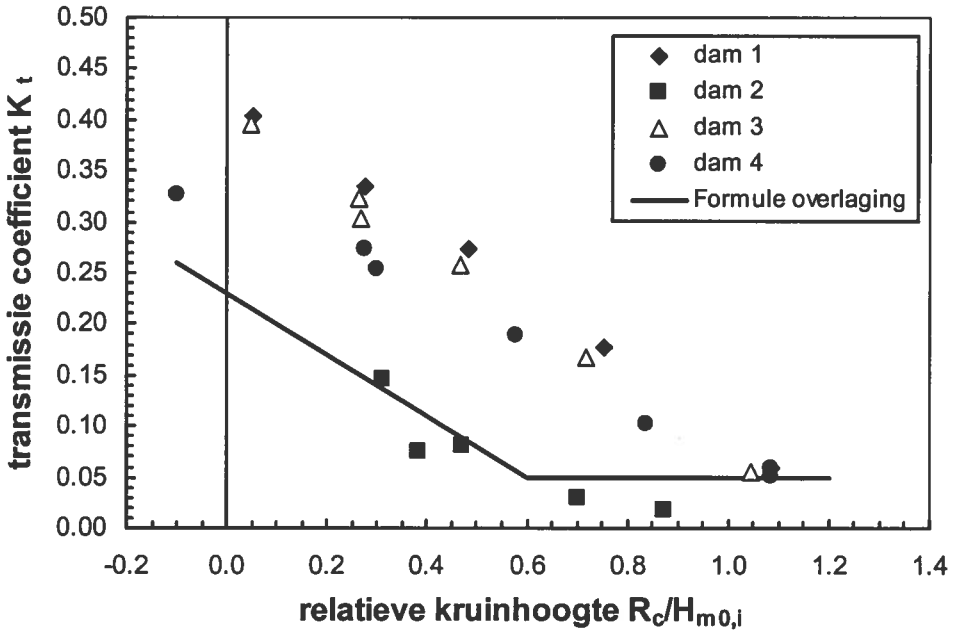

Figuur 3.1 Golftransmissie voor gladde dammen en met een overlaging

De maatgevende golfhoogte bij de ontwerpwaterstand voor de westelijke dijk is 3,13 m. De kruinhoogte met een overlaging van 1,25 m dik wordt 7,35 m +NAP. Met een ontwerpwaterstand van 6,2 m +NAP wordt de vrije kruinhoogte $R_c = 1{,}15$ m. Met formule 5 wordt een transmissiecoëffciënt gevonden van $K_t = 0{,}12$ en een transmissiegolfhoogte van $H_t = 0{,}37$ m. Hier komt de locale golfgroei nog bij, maar de golfhoogte blijft zeker beperkt tot lager dan 0,5 m. De overlaging is daarmee zeer effectief. Een nadere uitwerking met bijvoorbeeld zwaardere steen, maar in een enkele laag, is daarmee ook een mogelijkheid. De kruin kan dan waarschijnlijk iets lager worden gemaakt.

4 Conclusies en aanbevelingen

Bij het getij voorafgaand aan het getij met de ontwerpwaterstand loopt het gedeelte tussen de voorliggende dijk en de primaire kering, de badkuip, al vol door golfoverslag. Bij het getij met de ontwerpwaterstand is er in de badkuip dus een constante waterstand van ongeveer 6,1 – 6,2 m +NAP. Alle golfbelastingen op de primaire waterkering vinden plaats rondom deze waterlijn en niet over het hele talud van de dijk.

Het westelijk deel van de primaire kering wordt het zwaarst aangevallen. Golftransmissie is de bepalende factor voor de golfcondities bij de primaire kering. Een minder bepalende factor is locale golfgroei door de extreme windsnelheid. De maatgevende golfcondities bij de ontwerpwaterstand op het westelijk deel zijn: H_s = 1,15 m, T_p = 4,9 s en een hoek van aanval van 41°. Deze condities duren ongeveer 2 uur. Daarna zakt de golfhoogte tot beneden 1 m. Voor het oostelijk deel zijn de maatgevende condities: H_s = 0,66 m, T_p = 4,5 s en een hoek van aanval van 12°.

Rondom de constante waterstand van 6,1 – 6,2 m +NAP ligt een 4 – 6 m brede berm in het profiel van de primaire kering. De golven breken op deze berm en de berm is een positief element in de sterkte van de grasmat met onderliggende kleilaag. Door de toch redelijk beperkte golfhoogte heeft de primaire kering een grote overhoogte en daarmee ook een behoorlijke reststerkte, zeker in combinatie met de berm.

Verhogingen van de voorliggende dijk (in principe alleen het westelijk deel) met 0,5 m of 1,0 m leiden tot maatgevende golfhoogtes van 1,02 m en 0,88 m in plaats van 1,15 m. Een muurtje op de dijk met dezelfde hoogte heeft ongeveer hetzelfde effect.

Een overlaging met breuksteen 300 – 1000 kg en een laagdikte van 1,25 m leidt tot een maatgevende golfhoogte van hooguit 0,5 m. Deze optie heeft een groot effect op de maatgevende condities bij de primaire kering. Een vergelijkbare optie is een enkele laag zwaardere steen. In beide gevallen zou een wandelpad aan de achterkant van de kruin kunnen blijven bestaan. Door een overlaging hoeft de huidige steenbekleding niet te worden vervangen. Wel moet het binnentalud overslagbestendig worden gemaakt.

Referenties

Alkyon, 1998. Golfrandvoorwaarden voor dijkontwerp in door dammen afgeschermde gebieden. Band B. Beschrijving golftransmissie en dubbeltoppige spectra. Projectrapport A314/i181.

Ris, R.C., D.P. Hurdle, G.Ph. van Vledder, L.H. Holthuijsen. 2001. Deep water wave growth at short fetches for high wind speeds. *WL|Delft Hydraulics report H3817.*

TAW, 2002. Technisch Rapport Golfoploop en Golfoverslag bij Dijken.

Van der Meer, J.W., H.J. Regeling and J.P. de Waal. 2000. Wave transmission: spectral changes and its effects on run-up and overtopping. *Proc. 27th ICCE, Sydney, Australia*, ASCE, 2156-2168.

Van der Meer, J.W., R. Briganti, B. Wang and B. Zanuttigh, 2004. Wave transmission at low-crested structures, including oblique wave attack. *Proc. 29th ICCE, Lisbon, Portugal*, ASCE

Wilson, B.W., 1955. Graphical approach to the forecasting of waves in moving fetches. *Beach Erosion Board*. US Corps of Engineers, Department of the Army. Technical Memo 73.

Spectral changes due to wave transmission and effects of bi-modal wave spectra on overtopping

J.W. van der Meer; Infram; jentsje.vandermeer@infram.nl

H.J. Regeling; Ministry of Transport, Public Works and Water Management, IJsselmeer District, the Netherlands; e.regeling@rdij.rws.minvenw.nl

A.B. Mendez Lorenzo; Ministry of Transport, Public Works and Water Management, Road and Hydraulic Engineering Division, POBox 5044, 2600 GA Delft, the Netherlands; a.mendezlorenzo@dzh.rws.minvenw.nl

J.P. de Waal; Ministry of Transport, Public Works and Water Management, RIZA, the Netherlands; h.dwaal@riza.rws.minvenw.nl

P.J. Hawkes; HR Wallingford, Howbery Park, Wallingford, Oxfordshire, OX10 8BA, United Kingdom; pjh@hrwallingford.co.uk

Reprints of two papers published in Proceedings of 27th International Conference on Coastal Engineering, ASCE, Sydney, Australia

Wave transmission: spectral changes and its effects on run-up and overtopping

J.W. van der Meer[1], H.J. Regeling[2] and J.P. de Waal[3]

Introduction

Most research work on wave transmission over low-crested structures has been concentrated on establishing the wave transmission coefficient, i.e. the ratio between transmitted and incident significant wave height. It is clear that such structures decrease the wave height, but there is more!

Goda (1985), Tanimoto et al. (1987), Raichlen et al. (1992) and Van der Meer (1990) all conclude that also the mean period reduces to 0.4-1.0 of the incident mean period. The conclusion is that overtopping generates more waves. Further, Raichlen et al. (1992) and Lee (1994) give examples of measured spectra of transmitted waves. Both examples show the peak of the spectrum similar to the incident spectrum, but with much more energy at the higher frequencies.

A good estimation of the wave height in front of a structure is required for design or assessment of such a structure. But also wave period and sometimes spectral shape may have influence on the design. Wave run-up, for example, depends largely on the wave period. In order to establish the required dike height for acceptable run-up, both wave height and period should be known. In situations where a low-crested structure in front of such a dike gives some protection, wave period and spectral changes should be studied.

A local situation in the Netherlands was the reason for the research presented in this paper. Figure 1 gives a schematised layout. A large lake is situated on the west side (left side in the figure) and NW wind may generate waves up to a significant wave height of over 2 m. The dikes on the eastern side are partly protected by a system of various low-crested structures or dams, including some openings.

[1]Infram, PO Box 81, 3890 AB, Zeewolde, the Netherlands;
jentsje.vandermeer@infram.nl;
[2]Public Works Department, IJsselmeer District, the Netherlands;
e.regeling@rdij.rws.minvenw.nl;
[3]Public Works Department, RIZA, the Netherlands; h.dwaal@riza.rws.minvenw.n

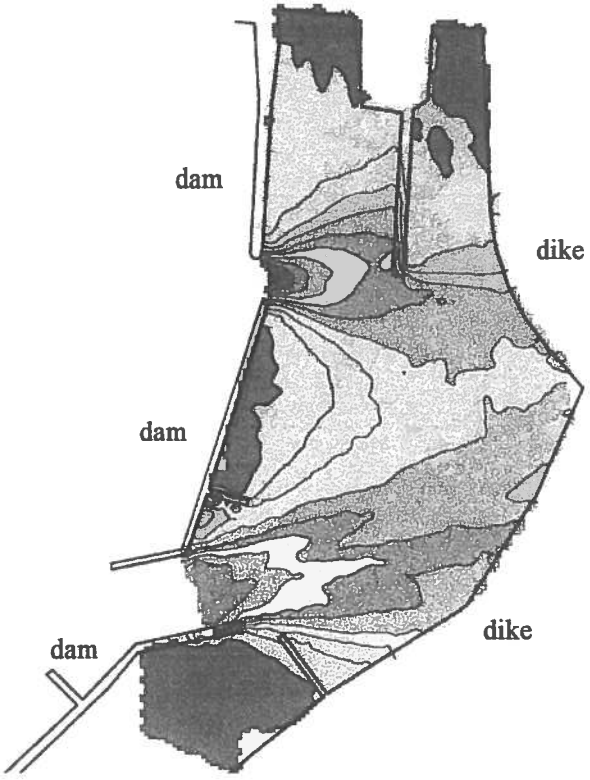

Figure 1. Schematised layout of dikes protected by low-crested structures or dams. The figure shows the results of wave penetration through two openings. The lake is on the left side of the figure.

The figure shows the results of a calculation on wave penetration. Such calculations were performed by Alkyon. Besides wave penetration, wave transmission is generated over the low-crested dams. The area is about 1 km by 2.5 km. This means that with a fetch of more than 1 km also locally generated (short) waves will be present during extreme conditions. The wave climate in front of the dikes can be described as a combination of wave penetration, wave transmission and locally generated wind waves. This paper deals with wave transmission only, but the effect on the total wave climate is discussed at the end.

Model tests

A model investigation was performed in a wave flume of Delft Hydraulics and the results were analysed by Infram. The model scale was 1:15 and all results are given in prototype values. In total five different structures were tested: smooth (asphalt) with various crest widths, smooth covered with rock and a very wide caisson. Figures 2-6 give the cross-sections of these structures. Dams 1 and 2 are similar, except that for dam 2 a 0.75 m thick rock layer of 60-300 kg rock was placed on top of the asphalt slope. All slopes were 1:4, both seaward and landward of the crest.

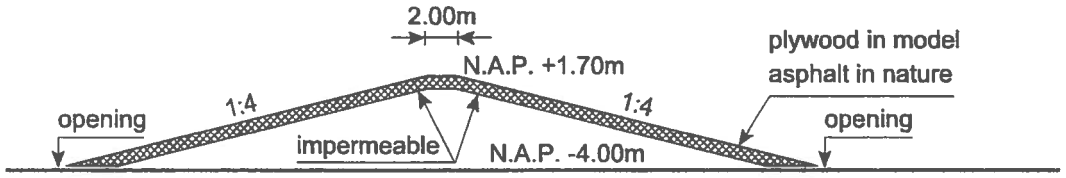

Figure 2. Dam 1. Smooth 1:4 slopes with crest width of 2 m

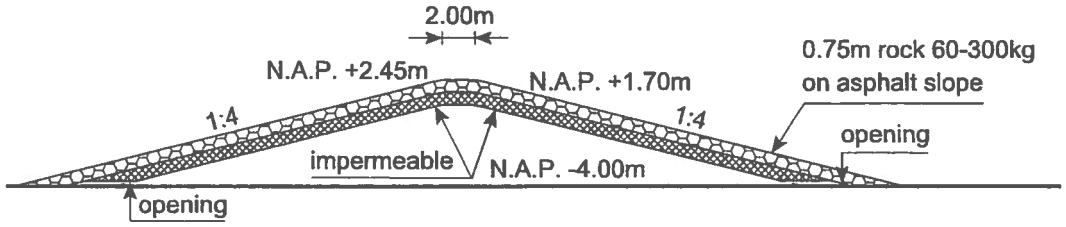

Figure 3. Dam 2. As dam 1, but covered with 60-300 kg rock

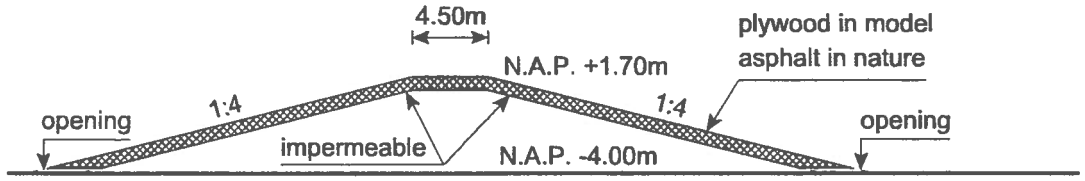

Figure 4. Dam 3. Smooth 1:4 slopes with crest width of 4.5 m

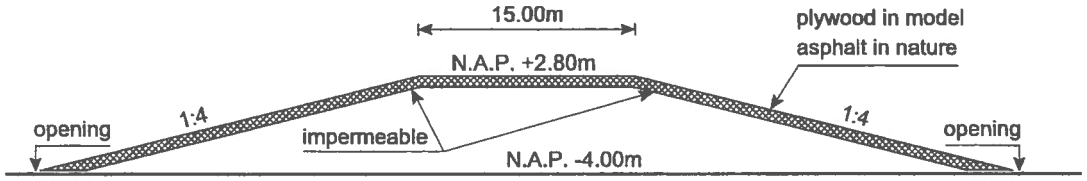

Figure 5. Dam 4. Smooth 1:4 slopes with crest width of 15 m

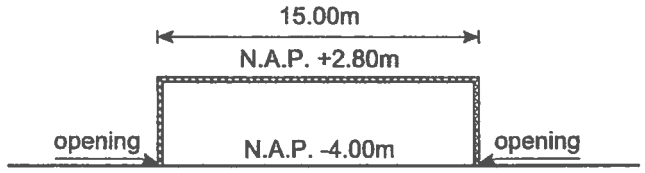

Figure 6. Low-crested caisson with wide crest

The main difference between dams 1, 3 and 4 is the crest width. The models were made of plywood and an opening was left near the bottom of the flume in order to maintain the same water level in front and behind the model. Various wave gauges measured the incident and reflected waves and the wave transmission. The model was placed in the middle of the flume with a spending 1:10 beach at the end.

In total 28 tests were performed. The water depth ranged between 4.5 and 7 m and the wave heights between H_{m0}=1.3-2.2 m with peak periods between T_p=5-7 s. Actually, the wave steepness was kept constant at s_{op}=0.03. The relative crest height ranged between R_c/H_{m0}=0-1.0, which means low-crested structures with the crest just above the still water level. The wave transmission coefficients measured varied between K_t=0-0.4. Table 1 gives the main results.

Table 1. Main test results

test	type	B	h_c	swl	incident			C_r	transmitted			K_t
		m	m	m	H_{m0} m	T_p s	T_m s		H_{m0} m	T_p s	T_m s	
1	dam 1	2	1.7	0.30	1.29	5.24	4.34	0.216	0.08	6.97	3.84	0.060
2	dam 1	2	1.7	0.60	1.46	5.70	4.61	0.233	0.26	6.68	3.37	0.178
3	dam 1	2	1.7	0.90	1.66	5.95	4.91	0.245	0.46	6.10	3.37	0.275
4	dam 1	2	1.7	1.20	1.83	6.37	5.13	0.244	0.61	6.62	3.41	0.335
5	dam 1	2	1.7	1.60	2.02	6.71	5.38	0.217	0.81	6.80	3.75	0.403
6	dam 2	2.5	2.45	1.71	1.94	6.44	5.23	0.204	0.14	7.28	3.03	0.074
7	dam 2	2.5	2.45	1.80	2.10	6.76	5.41	0.196	0.30	6.94	3.14	0.145
8	dam 2	3.5	2.6	1.10	1.72	6.05	4.92	0.187	0.04	6.72	6.15	0.024
9	dam 2	3.5	2.6	1.27	1.89	6.37	5.09	0.210	0.06	6.90	5.14	0.029
10	dam 2	3.5	2.6	1.67	1.97	6.71	5.41	0.202	0.16	6.98	3.41	0.080
11	dam 3	4.5	1.7	0.30	1.34	5.29	4.31	0.206	0.07	7.00	3.30	0.056
12	dam 3	4.5	1.7	0.60	1.53	5.71	4.60	0.235	0.25	6.87	3.15	0.167
13	dam 3	4.5	1.7	0.90	1.72	6.06	4.88	0.244	0.44	6.40	3.28	0.259
14	dam 3	4.5	1.7	1.20	1.90	6.45	5.13	0.238	0.61	6.62	3.39	0.322
14a	PM	4.5	1.7	1.20	1.87	6.62	4.81	0.244	0.57	7.06	3.32	0.304
15	dam 3	4.5	1.7	1.60	2.07	6.67	5.39	0.213	0.82	6.94	3.60	0.396
16	dam 4	15	2.8	1.20	1.91	6.41	5.09	0.255	0.19	8.56	2.85	0.102
17	dam 4	15	2.8	1.60	2.07	6.65	5.34	0.264	0.39	7.94	3.02	0.188
18	dam 4	15	2.8	0.90	1.75	5.99	4.90	0.225	0.09	6.94	3.43	0.052
18a	closed	15	2.8	0.90	1.75	5.99	4.87	0.242	0.10	7.04	6.38	0.059
19	dam 4	15	2.8	2.20	2.18	6.70	5.45	0.220	0.60	7.34	3.25	0.273
20	dam 4	15	2.8	2.20	2.02	6.35	5.25	0.212	0.51	7.09	3.13	0.254
20a	dam 4	15	2.8	3.00	2.01	6.33	5.24	0.148	0.66	6.62	3.39	0.326
21	caisson	20	1.5	0.83	1.24	4.00	3.59	0.766	0.11	4.25	3.37	0.085
22	caisson	20	1.5	0.78	1.47	5.68	4.67	0.749	0.20	5.74	4.30	0.133
23	caisson	20	1.5	1.17	0.59	6.37	5.28	0.837				0.000
24	caisson	20	1.5	1.14	1.04	3.99	3.51	0.754	0.09	4.38	3.40	0.089
25	caisson	20	1.5	1.41	0.84	6.64	5.52	0.755	0.13	6.55	3.47	0.149

In Table 1, B= the crest width, h_c = the crest height relative to NAP (chart datum), swl is the water level relative to NAP, H_{m0} = the incident spectral wave height, T_p = the peak period, T_m = the mean period $\sqrt{m_0/m_2}$, C_r = the reflection coefficient and K_t = the wave transmission coefficient $\sqrt{m_0 t/m_0 i}$ with t and i respectively for transmitted and incident values.

Analysis of results

Wave transmission coefficients. The transmission coefficients are not the main item of this paper, but may be valuable for other applications. They will be treated briefly. The main results are shown in Figure 7 where the wave transmission coefficient K_t is given as a function of the relative crest height R_c/H_{m0}. A few conclusions can be drawn.

First of all there is very little difference between the results of dams 1, 3 and 4, which only differ in crest width. For rubble mound structures a large influence of crest width is present, see for instance Van der Meer and Daemen (1994). The small influence for the tested dams can be explained by the way of wave breaking and the smooth surface. Due to the gentle slope of 1:4 waves break and the up-rushing wave tongue jumps over the smooth crest. In this process the width of the crest plays hardly a role as the surface is smooth without friction or permeability to reduce energy.

The difference in results between dam 1 and 2 is large. The permeable rock layer reduces the transmission by about a constant value of 0.15 and this for the same *relative* crest height!

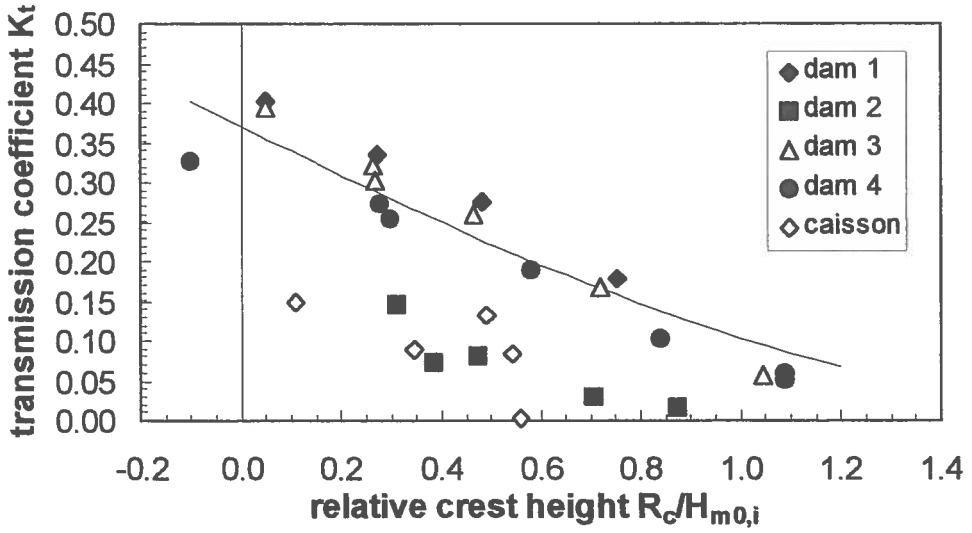

Figure 7. Wave transmission for the 5 tested structures

An efficient formula for fitting wave transmission results is described by Goda (1969). The formula is governed by two fitting coefficients α and β:

$$\frac{R_c}{H_i} \le -\alpha - \beta: \qquad K_t = 1$$

$$-\alpha - \beta \le \frac{R_c}{H_i} \le \alpha - \beta: \qquad K_t = \frac{1}{2}\left(1 - \sin\left(\frac{\pi}{2}\frac{\frac{R_c}{H_i} + \beta}{\alpha}\right)\right) \qquad (1)$$

$$\frac{R_c}{H_i} \ge \alpha - \beta \qquad K_t = 0$$

The fitted formula for the smooth dams is shown in Figure 7. Here α=2.4 and β=0.4. For dam 2 (rock layer) and the wide and low caisson the coefficients were α=1.6 and β=0.5, respectively α=1.8 and β=0.6.

Wave spectra. In most cases Jonswap spectra were generated in the flume. Only in test 14a a wider Pierson Moskowitz spectrum was used. Figure 8 shows three spectra which were measured offshore. The wave heights were respectively 1.34 m, 1.72 m and 2.07 m.

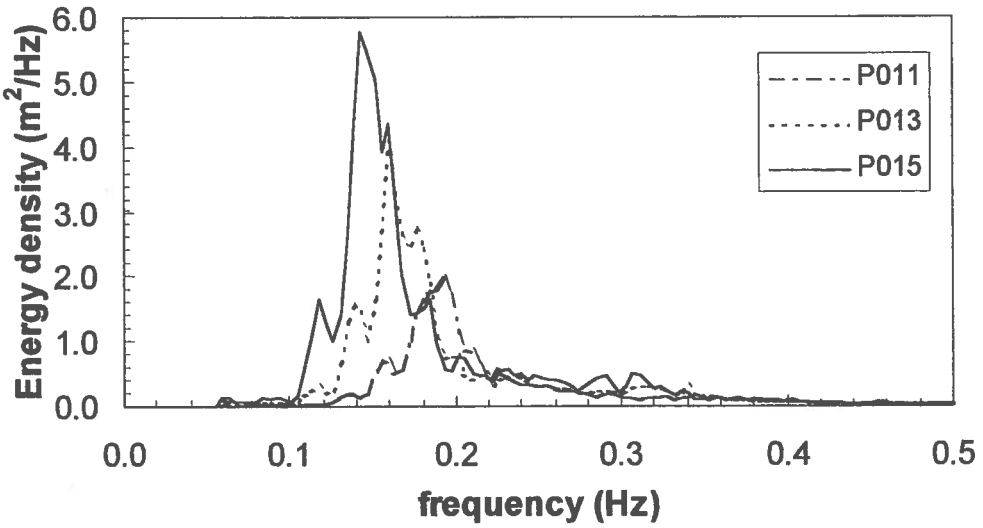

Figure 8. Example of measured spectra offshore

In Figure 9 two spectra are shown which are characteristic for transmitted spectra. The transmitted wave heights here were 0.61 m and 0.81 m, respectively. There is still a clear peak, sometimes even more narrow than the incident spectrum, but there is also energy present for larger frequencies. This energy is fairly constant over a wide frequency range. A more thorough analysis showed that this range was in average close to 1.5 f_p to 3.5 f_p, where f_p is the peak frequency.

Peak period. The transmitted spectra showed that the peak period remained more or less the same. In order to analyse this in a more objective way the ratio between peak

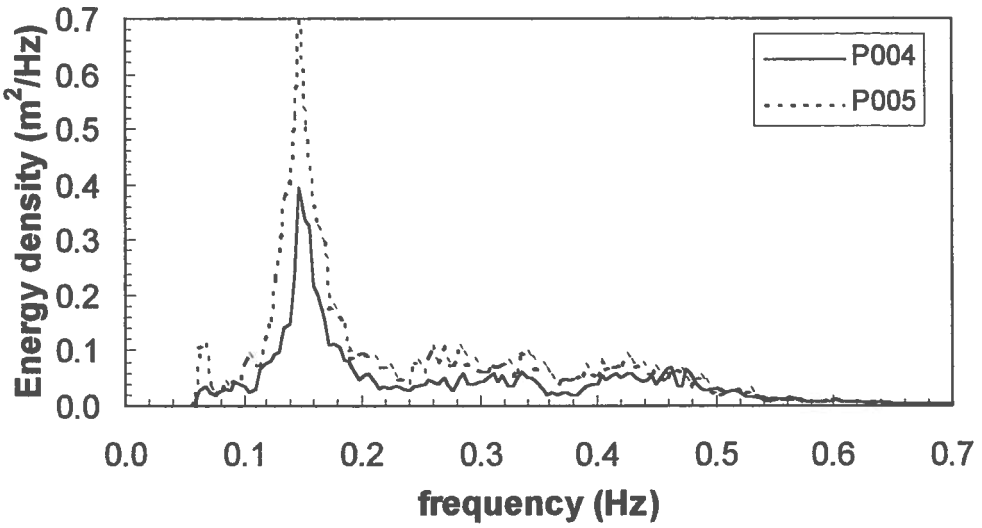

Figure 9. Example of measured transmitted spectra

periods transmitted and offshore was calculated for each test. In general there are two obvious ways to relate these period ratios to an other parameter: as a function of the wave transmission coefficient K_t or the relative crest height, R_c/H_{m0}. The results will be more or less similar as a smaller transmission coefficient often means a larger crest height and vice versa. The full analysis was performed with both parameters, but here only the transmission coefficient will be used. The results were more clear for this parameter.

Figure 10 shows the period ratio T_pt/T_pi as a function of the wave transmission coefficient K_t. The ratio is close to 1, especially for transmission coefficients larger than K_t=0.2. For very small transmission coefficients there is a tendency that the peak period increases after transmission.

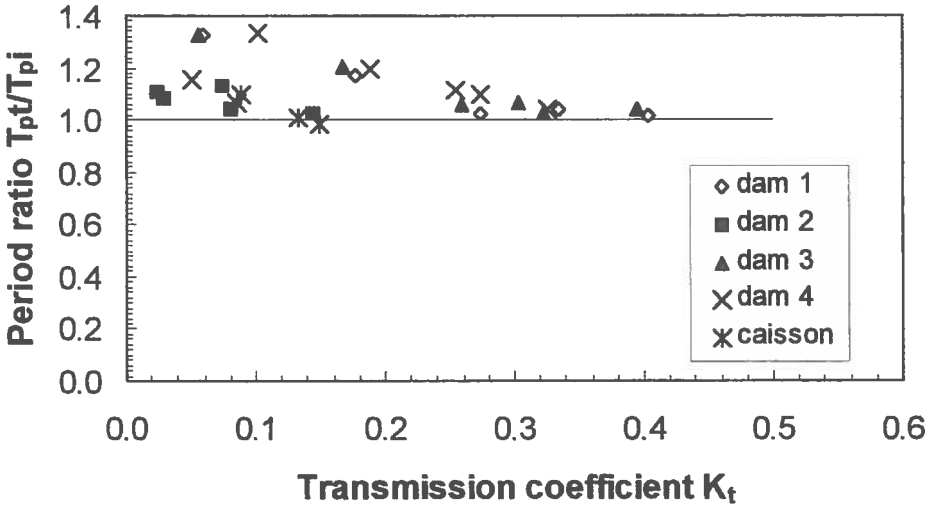

Figure 10. Ratio of peak period transmitted/offshore as a function of transmission

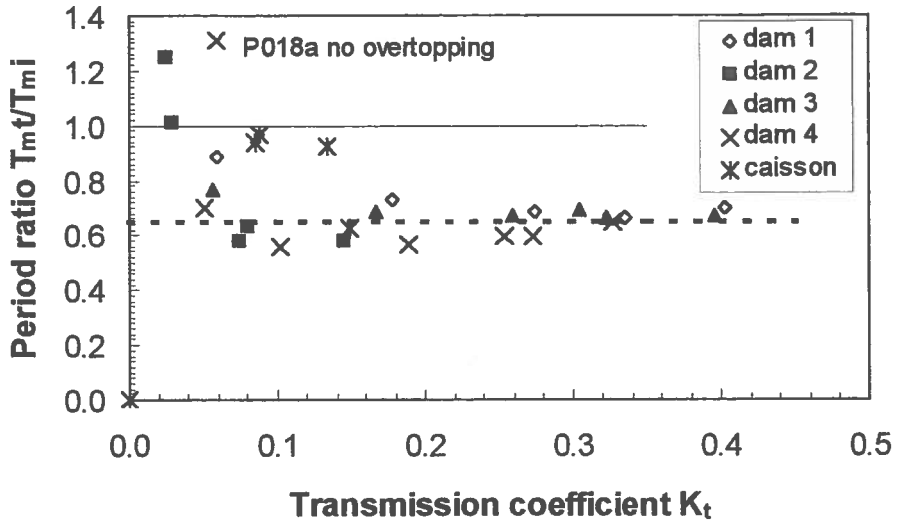

Figure 11. Ratio of mean period transmitted/offshore as function of transmission

The mean period was defined as $T_{m02}=\sqrt{m_0/m_2}$. The ratio of this mean period for transmitted and offshore locations is given in Figure 11. From this figure it is clear that the mean period decreases due to overtopping or transmission. Actually, the waves break on the smooth slope and jump over the crest into the water behind the structure. This jump often will create two waves instead of one and this will decrease the mean period, not the peak period.

Only a few tests showed an increase which was only for very small transmission coefficients. During test 18a there was no wave transmission over the dam as this was blocked in the flume by a vertical plate on top of the crest. The wave transmission measured was due to small transmission underneath the structure through the openings that were created in order to maintain the same water level in front and behind the structure. In average the mean period reduced to about 0.65 of the period offshore, certainly for $K_t>0.15$.

Spectral width. If peak periods, due to transmission or overtopping, remain more or less the same, but mean periods decrease then this is a strong indication that the spectral width also changes. Van Vledder (1992) gives a good overall view of wave group statistics and spectral parameters. The spectral narrowness parameter κ can be calculated both in time and frequency domain, resulting in $\kappa(f)$ and $\kappa(t)$. One is referred to Van Vledder (1992) for definitions. A general meaning is as follows:

Type of spectrum	*κ(f)*	*κ(t)*
very narrow	0.8-0.9	0.8-0.9
Jonswap	0.5-0.7	0.5-0.8
Pierson Moskowitz	0.4-0.6	0.5-0.6
wide	0.2-0.4	0.4-0.5
bi-modal	0.2-0.4	0.4-0.5

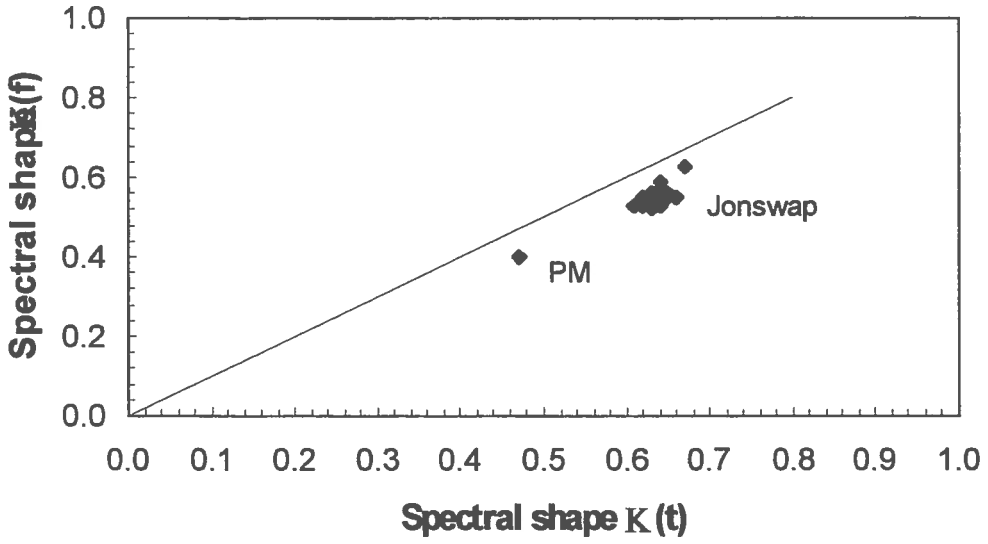

Figure 12. Spectral narrowness parameters measured offshore

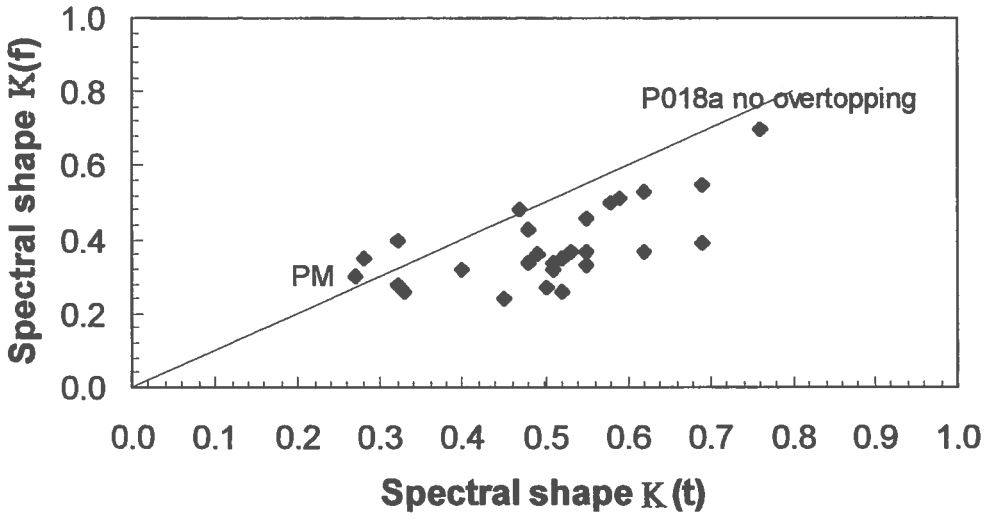

Figure 13. Spectral narrowness parameters measured after transmission

Figure 12 shows both measured spectral narrowness parameters for the offshore location. It is very clear that all Jonswap spectra have the same spectral narrowness and that the only test with a Pierson Moskowitz spectrum is much wider, resulting in a smaller value for the narrowness parameter. A similar graph is shown in Figure 13, but now for the wave spectra after transmission. Now the narrowness is much smaller, indicating that the spectrum is much wider. The smallest value for the Pierson Moskowitz spectrum is still the smallest after transmission. The test without overtopping, but with some energy passing underneath the structure in the flume, shows a very narrow spectrum.

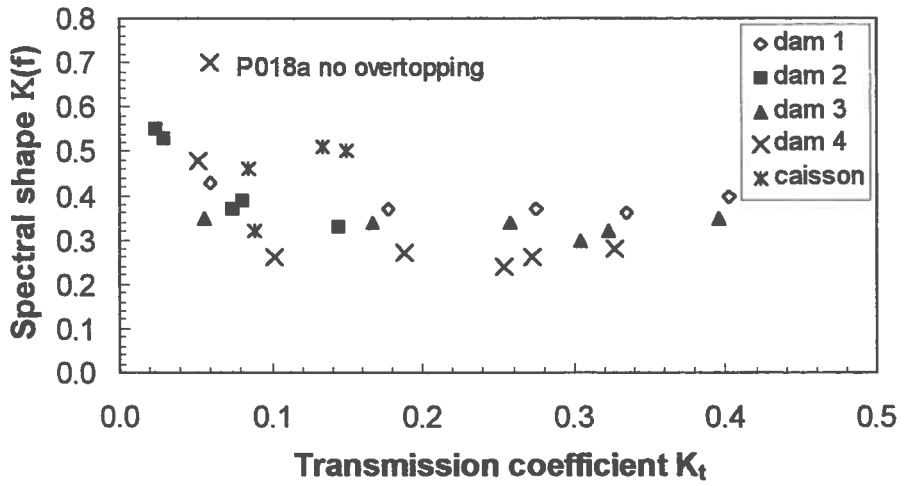

Figure 14. Spectral narrowness after transmission as a function of K_t

Figure 14 shows the spectral narrowness parameter $\kappa(f)$ as a function of the transmission coefficient K_t. For transmission coefficients $K_t>0.15$ it can be concluded that wide spectra are generated by overtopping giving spectral narrowness values of $\kappa(f)=0.25$-0.35.

Energy shift. On the basis of Figure 9 it was concluded that energy was shifted from the peak frequency to higher frequencies and that a fairly constant level of energy was present between 1.5 f_p and 3.5 f_p. The value of 1.5 f_p can be considered as the boundary between "high" and "low" frequency energy. From the transmitted spectra the energy m_0 for frequencies larger than 1,5 f_p was calculated. In Figure 15 this energy is compared with the total energy in the transmitted spectrum.

A clear conclusion can be drawn from this graph: for transmission coefficients $K_t>0.15$ a constant ratio is found of 0.4 (the line in the graph).

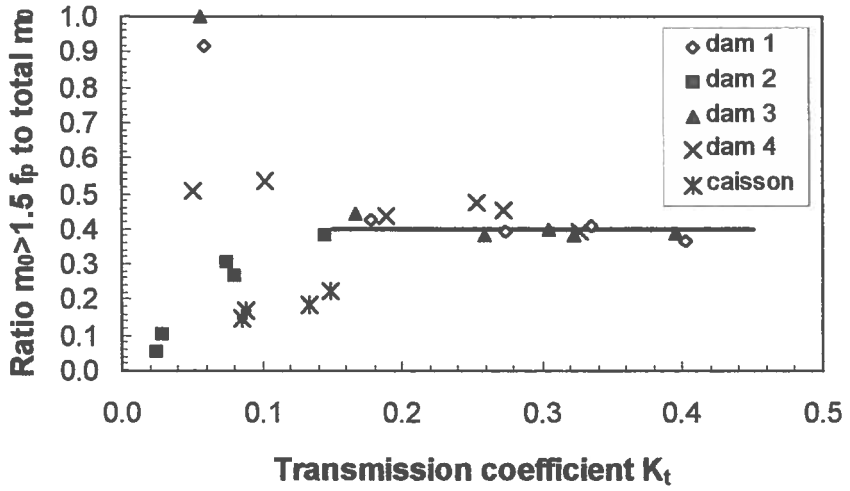

Figure 15. Energy for frequencies larger than1.5 f_p related to total energy m_0

Main conclusions based on the analysis of the tests

The analysis of results of the model tests as described above gives the following conclusions:

- the peak period remains more or less constant
- for wave transmission coefficients K_t > 0.15-0.20 clear trends are found. For lower values the picture is more diffuse and difficult to describe
- for K_t > 0.20 the peak period may increase by not more than 10%
- for K_t > 0.15 the mean period decreases to 0.65 of the incident mean period
- for K_t > 0.15 the spectral narrowness parameter κ_f becomes 0.25-0.35 which indicates a very wide spectrum
- for K_t > 0.15 about 40% of the total transmitted energy is present at the higher frequencies of the spectrum, more specifically between 1.5 f_p and 3.5 f_p.

Method for description of the transmitted spectrum

Conclusions above can be used to develop a prediction method for the spectral shape after wave overtopping or transmission. The basis for this method is the incident spectrum (shape and energy) and the measured or calculated transmission coefficient K_t. For the structures considered here the transmission coefficients in Table 1 or in Figure 7 can be used. The energy of the transmitted spectrum can be calculated by:

$$m_{0,t} = K_t^2 \, m_{0,i} = (0.25 \, K_t \, H_{m0,i})^2 \qquad (2)$$

where t and i stand for transmitted and incident, respectively. The spectral shape remains the same, see Figure 16. In this graph a Pierson Moskowitz spectrum has been assumed with a wave peak period of 6 s. The transmission coefficient was considered to be K_t=0.3, which gives the transmitted spectrum.

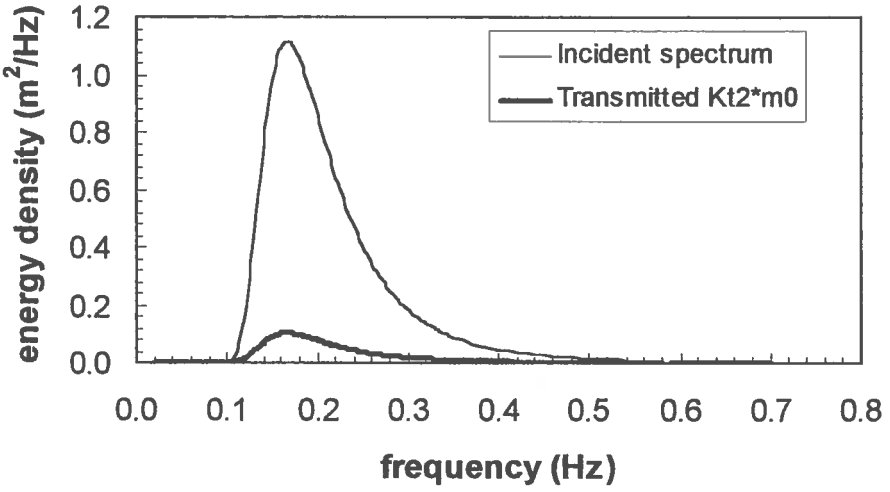

Figure 16. Incident and calculated spectrum, based on the transmission coefficient

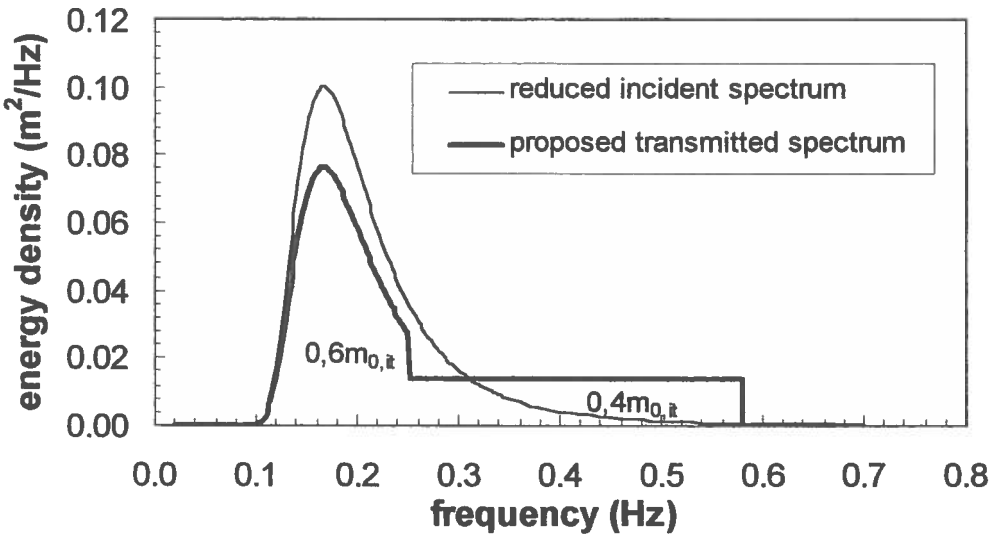

Figure 17. Calculated reduced spectrum and shift of energy resulting in the final transmitted spectrum

Then this total energy is divided and 40% is brought to the higher frequencies, see Figure 17. The division between "long" and "short" energy is taken at 1.5 f_p, in this example at 0.25 Hz. The part of the spectrum with frequencies smaller than 0.25 Hz or 1.5 f_p is similar to the incident spectrum, the total energy is 60% of the total *transmitted* energy. The part of the spectrum with frequencies larger than 1.5 f_p can be described with constant energy up to 3.5 f_p, which means from 0.25 Hz to 0.583 Hz in the example in Figure 17. The bold line in Figure 17 finally shows the transmitted wave spectrum.

Effects on wave run-up and overtopping

The transmitted spectrum has been divided into two parts and can also be treated like that in order to establish wave run-up and overtopping. In fact it can be treated as a bi-modal or double peaked spectrum. See Mendez Lorenzo et al. (2000) for a reference how to deal with double peaked spectra and wave overtopping. The effect will be that less wave overtopping or run-up is expected in comparison to the traditional method, as less energy is present at high periods.

If a certain distance is present between the low-crested structure and the dike, see the situation in Figure 1, local wave generation may play a role too. The effect of the presence of energy especially at high frequencies is that local wave generation by wind can be much faster and higher waves may be expected at the dike than without transmission. In fact the horizontal part in Figure 17 will grow to a second peak by wind.

References

Goda, Y. (1969). Re-analysis of laboratory data on wave transmission over breakwaters. Rep. Port and Harbour Res. Inst., Vol. 8, No. 3, pp. 3-18

Goda, Y. (1985). Random seas and design of maritime structures, Tokyo Press

Lee, D.S, S.W. Park, K.D. Suh and Y.M Oh (1994). Hydraulic experiments for basic design offshore breakwater for protecting artificial island. Proc. Hydro-Port '94, Yokosuka, Japan

Mendez Lorenzo, A.B, J.W. van der Meer and P.J. Hawkes (2000). Effects of bi-modal waves on overtopping: application of UK and Dutch prediction methods. ASCE, proc. 27th ICCE, Sydney, Australia

Raichlen, F., J.C. Cox and J.D. Ramsden (1992). Inner harbor wave conditions due to breakwater overtopping. Proc. ASCE, Coastal Engineering Practice '92. Long Beach, California, US

Tanimoto, K, S. Takahashi and K. Kimura (1987). Structures and hydraulic characteristics of breakwaters – the state of the art of breakwater design in Japan. Report of the Port and Harbour Research Institute, Vol. 26, No. 5

Van der Meer, J.W., 1990. Data on wave transmission due to overtopping. Delft Hydraulics Report H 986

Van der Meer, J.W. and I.F.R. Daemen (1994). Stability and wave transmission at low-crested rubble mound structures. ASCE, Journal of WPC&OE, Vol. 120, No. 1, 1-19

Van Vledder, G.Ph. (1992). Statistics of wave group parameters. ASCE, proc. 23rd ICCE, Venice, Italy. pp. 946-959.

Effects of bi-modal waves on overtopping: application of UK and Dutch prediction methods

A.B. Mendez Lorenzo[1], J.W. van der Meer[2] and P.J. Hawkes[3]

Introduction and background

Sometimes dike sections or seawalls are partially protected by low-crested structures up to one kilometre in front of these coastal defences and more than one kilometre in length. Wave energy may be transmitted over these low-crested structures or dams and waves can penetrate through various openings. These waves have periods similar to the wave periods of the incident waves. Local wave growth of shorter period waves may become important if some fetch is present between dam and coastal defence. Wave spectra in front of the dike sections are often therefore bi-modal. Also sea and swell and/or irregularly shaped wave generation areas may give rise to these bi-modal or double peaked spectra. Until now, little was known about their influence on required dike heights.

A series of physical model studies (conducted at a nominal scale of 1:20) were undertaken by HR Wallingford for the Flood and Coastal Defence with Emergencies Division of the UK Ministry of Agriculture, Fisheries and Food (MAFF). The intention was to provide information on wave breaking behaviour and the impact of bi-modal wave conditions on beaches and coastal structures. This research was described by Coates et al. (1998) and by Hawkes et al. (1998). Wave conditions and wave overtopping were measured for two or three water levels over different bed slopes of 1:50, 1:20 and 1:10.

During a project for the Dutch Public Works Department - IJsselmeer District, Alkyon and Infram studied wave-structure behaviour over low-crested dams and the effect of bi-modal seas on required dike heights. As a part of this project

[1]Ministry of Transport, Public Works and Water Management, Road and Hydraulic Engineering Division, POBox 5044, 2600 GA Delft, the Netherlands; a.mendezlorenzo@dzh.rws.minvenw.nl
[2]Infram, POBox 81, 3890 AB, Zeewolde, the Netherlands; jentsje.vandermeer@infram.nl
[3]HR Wallingford, Howbery Park, Wallingford, Oxfordshire, OX10 8BA, United Kingdom; pjh@hrwallingford.co.uk

Infram visited HR Wallingford and used above research to establish a method for predicting wave overtopping with bi-modal seas for Dutch applications. The research was described (partly) by Van der Meer et al. (2000a). At that time it was recognised that the wave and wave overtopping data measured by HR Wallingford would be interesting to the Dutch Public Works Department for several reasons as they are responsible for establishment of wave boundary conditions and guidelines for safety assessment of the Dutch coastal defences. The actual work consisted of four parts and was described in full depth in Van der Meer et al. (2000b):

- re-analysis of approximately 200 wave flume runs to obtain various time and frequency domain parameters. This work was performed by HR Wallingford
- validation of the SWAN-model and analysis of wave breaking formulations. This work was performed by Alkyon and Delft Hydraulics
- validation of a model on shallow wave height statistics by Delft Hydraulics
- further analysis on wave overtopping by uni- and bi-modal seas, performed by Infram in co-operation with Delft Hydraulics

Only the latter part, the wave overtopping analysis, is the subject of this paper.

Model tests

Wave overtopping on 1:2 and 1:4 uniform and smooth slopes was measured with 1:50, 1:20 and 1:10 beach slopes, see Coates et al. (1998) and Hawkes et al. (1998). About 40 tests with uni-modal spectra and 90 tests with bi-modal spectra were available with overtopping measurements for both slopes. During calibration tests, without a structure in the flume, the waves were measured along the foreshore.

The model scale used was 1:20 and the data are given in prototype values. In general, significant wave heights varied from 1.5 to 4.4 m with peak periods between 5 and 13 s for the uni-modal tests. The significant wave heights for the bi-modal tests varied between 0.6 and 4.4 m. The shortest peak period of the bi-modal spectrum was always close to 6-7 s. The second peak period ranged from 11 to 21 s. Various parameters in both time and frequency domain were calculated and used for further analysis.

Wave deformation over the beach slope

Spectral changes. Figures 1-3 show the spectra from a few selected tests. Each figure shows the spectrum that was generated and measured offshore of the foreshore slope and the spectrum that was measured at the end of the slope (inshore) which was in fact the location of the toe of the slope of 1:2 or 1:4. These waves, however, were measured during the calibration tests with no structure in the flume.

Figure 1 shows a uni-modal spectrum on a foreshore slope of 1:50. The energy at the peak frequency decreased due to wave breaking and some energy was transformed to longer periods. Figure 2 gives an example of a bi-modal spectrum, also on a slope of 1:50. Due to wave breaking, the low-frequency energy reduced a little (around 0.05 Hz) and generated a second harmonic at 0.10 Hz. The second generated peak at 0.14 Hz did not change. The final result in front of the toe of the

slope is a spectrum with three peaks! Figure 3 provides a further example of a bi-modal spectrum with an extremely large difference between the two peaks: 6 and 21 s. On the 1:50 foreshore slope the energy at the long peak period increases due to shoaling, whilst the energy at the short peak period reduces due to wave breaking. The final result is still a bi-modal spectrum, but with altered energy densities at the two peaks.

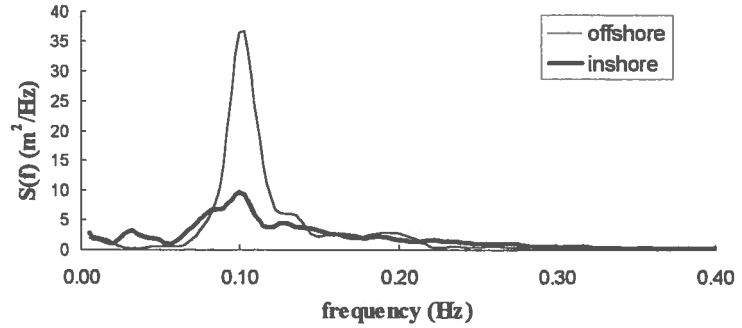

Figure 1. Spectral changes on foreshore slope 1:50; H_{so}=4.4 m and T_p=9.8 s

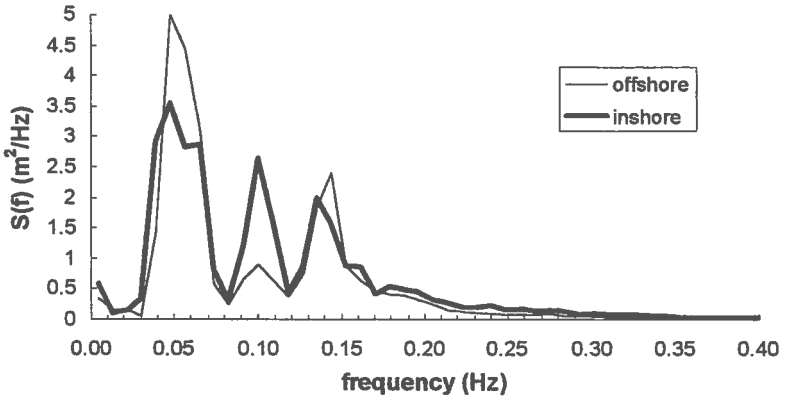

Figure 2. Spectral changes on foreshore slope 1:50; Bi-modal spectrum, H_{so}=1.9 m and T_p=7 and 19 s

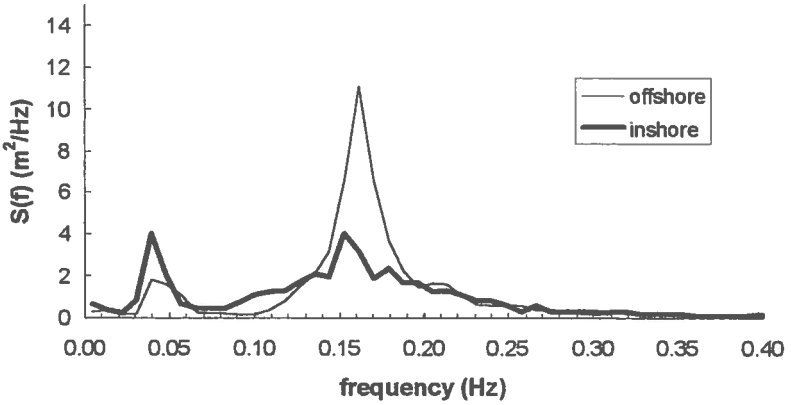

Figure 3. Spectral changes on foreshore slope 1:50; Bi-modal spectrum, H_{so}=2.6 m and T_p=6 and 21 s

It can be concluded that even for uni-modal waves in deep water there may be bi-modal conditions at the toe of the structure. Sometimes the long energy peak is higher than the original peak, shifting the "peak period" drastically. It means that using a peak period at the toe of the structure in overtopping formulae can generate fairly large scatter, simply due to the fact that bi-modal spectra are present. A peak period in deep water could be used for uni-modal spectra, but this ignores the fact that bi-modal spectra may exist at the toe of the structure.

For both uni-modal (breaking) and bi-modal spectra, one peak period is not a sufficient parameter. If the division of energy between the peaks is known, various methods can be used which initially treat the peaks independently and then make an integration. This could even be done for three or more peaks. It would, however, be easier if a spectral period could be chosen, independent of the actual number of peaks. This paper deals with such a spectral period.

Wave breaking. For a few selected tests the wave height evolution along the foreshore has been given in Figures 4-6. The first two figures 4 and 5 give the $H_{1/3}$ along the foreshore for uni-modal waves and different tests. Distance 0 m means at the toe of the structure and positive values are in the offshore direction.

Figure 4 shows the shoaling and breaking on a 1:50 foreshore slope. This slope starts at a distance of 400 m and the water depth at the location of the toe (calibration tests, no structure in the flume!) amounts to 4 m. There is quite some wave breaking for this (small) water depth of 4 m at the toe.

Figure 5 describes the wave breaking on the 1:20 slope with a 6 m water depth at the toe of the structure. Here shoaling and breaking is present over a short distance due to the steep foreshore which starts at a distance of 160 m. The three tests in Figure 5 have more or less the same offshore wave height, but differ in wave period (0f2 means a test with a mean wave steepness of 0.02 and 0f6 with 0.06). The long period test with a mean wave steepness of 0.02 shoals from an offshore wave height $H_{1/3}$=3.8 m to a maximum value of $H_{1/3}$=5.4 m just before breaking!

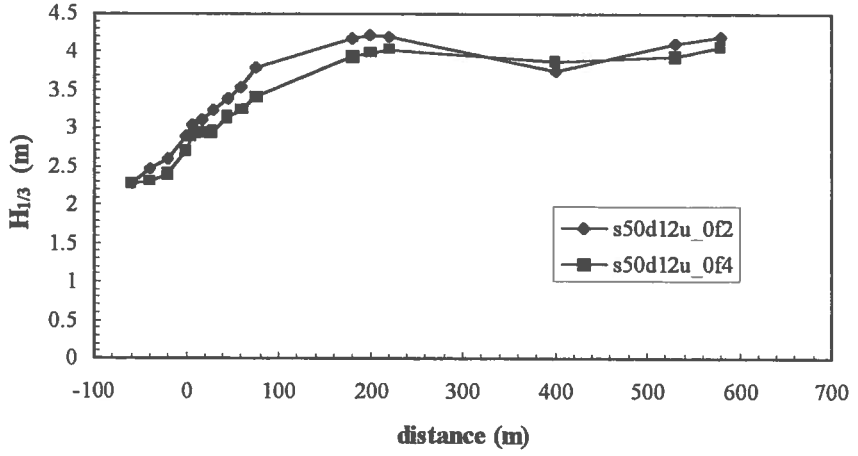

Figure 4. Wave height deformation on a foreshore slope of 1:50. Water depth at the location of the toe 4 m; uni-modal waves

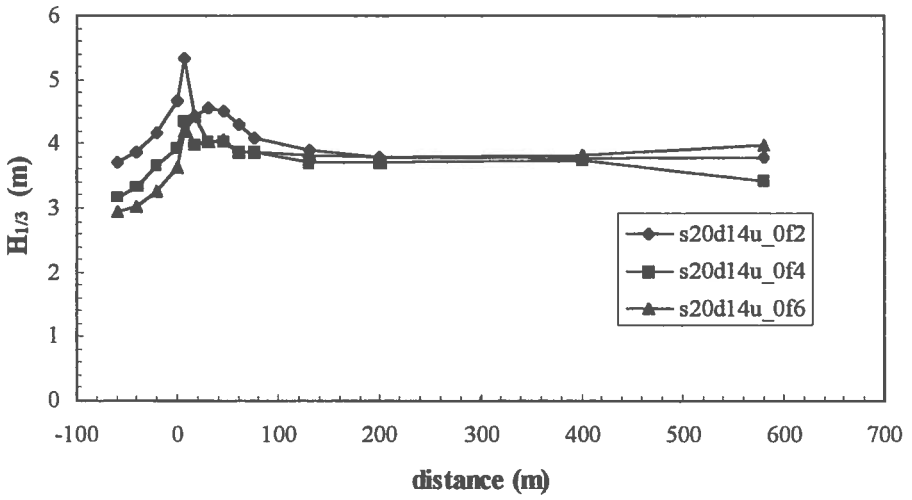

Figure 5. Wave height deformation on a foreshore slope of 1:20. Water depth at the location of the toe 6 m; uni-modal waves

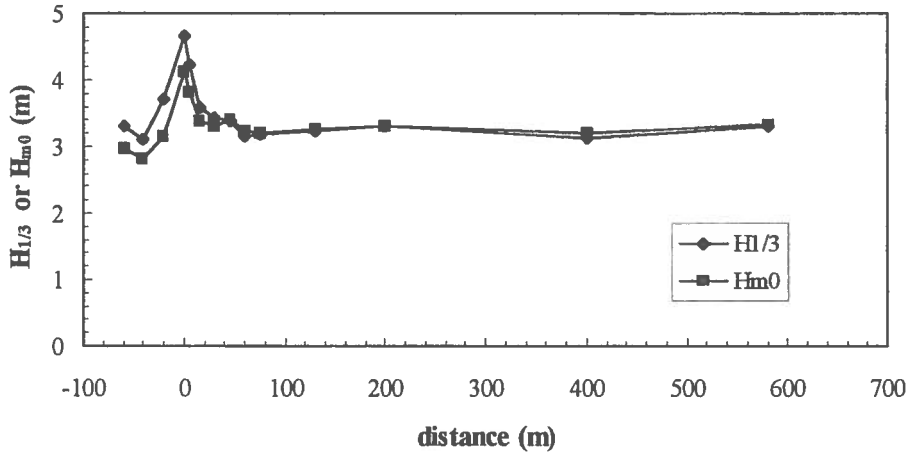

Figure 6. Wave height deformation on a foreshore slope of 1:10. Water depth at the location of the toe 6 m; bi-modal waves

The graph shows that the actual location chosen for the wave height from which to estimate the overtopping rate is quite important. A little shift in location around the toe may result in a significant higher or lower wave height.

Figure 6 gives the behaviour of bi-modal waves on a foreshore slope of 1:10. This slope starts offshore at a distance of 80 m. Now only one test is shown and for this test both the $H_{1/3}$ and H_{m0}. Bi-modal waves show a similar behaviour to uni-modal waves. In the wave breaking area generally the H_{m0} is smaller than the $H_{1/3}$, which can be expected. In *deep water* both the spectral wave height H_{m0} and the statistical wave height $H_{1/3}$ have more or less the same value. In that sense it does not matter which wave height is used in wave overtopping calculation.

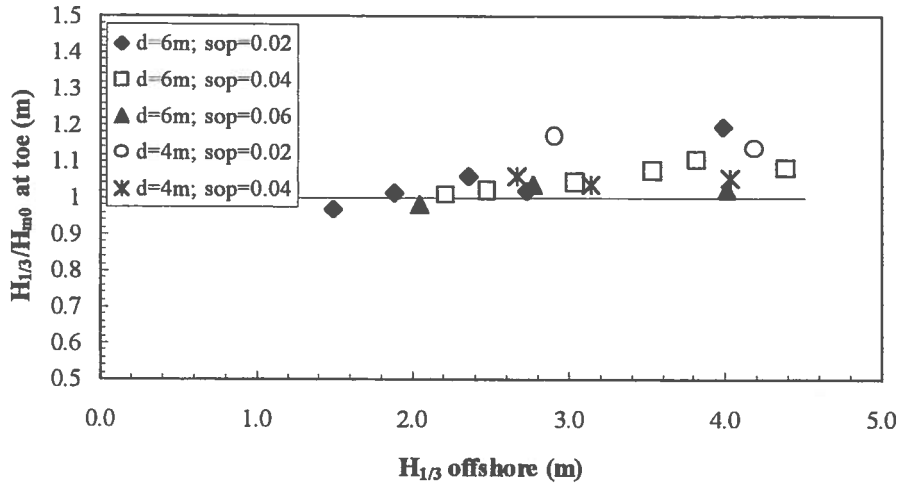

Figure 7. The breaking ratio $H_{1/3}/H_{m0}$ at the location of the toe of the structure during calibration tests. Foreshore slope 1:50, uni-modal tests

Figure 7 gives the $H_{1/3}/H_{m0}$ ratio for all the uni-modal spectra on a foreshore slope of 1:50, the horizontal axis being the $H_{1/3}$ in deep water. The larger the offshore wave height the more wave breaking may be expected and therefore a larger ratio may be expected. This is indeed the case in Figure 7, where for lower wave heights around 2 m a ratio of 1 is found and for larger wave heights a ratio larger than 1. This figure also clearly shows that the ratio increases with decreasing wave steepness. Both tests with the lowest steepness of 0.02 give clearly the largest ratio.

It can be concluded that for steep slopes the location where the wave height is taken to be responsible for the wave overtopping, is quite critical due to the significant changes within a short distance. Furthermore it can be concluded that the spectral and statistical wave height may differ substantially.

Wave periods. A spectral wave parameter close to the peak period (for uni-modal waves) would be preferred as it was proven earlier that a longer period than the mean period may account for differences in spectral shape. Such spectral wave periods are T_{m-10}, T_{m-20} and T_{m-2-1}, where $T_{m\,x1\,x2}=m_{x1}/m_{x2}$ with m_{xx} the frequency moment of the wave spectrum. For a given theoretical spectral shape there is a fixed relationship with the peak period, given in Table 1.

Table 1. Relationship T_p/T_{mx1x2}

	Jonswap	*Pierson Moskowitz*
T_{m-2-1}	1.06	1.08
T_{m-20}	1.08	1.12
T_{m-10}	1.11	1.17
T_{m01}	1.21	1.30
T_{m02}	1.30	1.40

The periods with negative moments give more weight to the energy at the lower frequencies. Due to wave breaking, quite some energy was generated at the toe of the structure, which will tend to increase the first mentioned wave periods in Table 1. In Van Gent (1999) the performance of these wave periods was analysed numerically and it was concluded that the wave period T_{m-10} is the optimal wave period for describing wave run-up and wave overtopping for non uni-modal spectra. And also in Van Gent (2000) this conclusion was confirmed based on physical model tests with wave run-up and wave overtopping.

Wave overtopping

Problem definition. A lot of research on wave overtopping has been performed in (recent) decades. Most of the resulting prediction formulae are based on model tests with not too much wave breaking and with uni-modal waves offshore. The above analysis of wave deformation on foreshore slopes, including bi-modal wave spectra, showed that $H_{1/3}$ and H_{m0} at the toe of the structure may differ [comma] and that a spectral period may be preferred above a peak period. There are various possibilities for the choice of a spectral peak period.

The best choice of parameter would be that which gives the closest agreement with the existing formulae, as in that case there would be no need to develop a new formula with a transition to the existing ones. (This under the requirement that the scatter would be similar as for other choices, and preferably the lowest.)

Overtopping formulae. Two of the main overtopping formulae will be considered here for evaluation against the test data. These are the formula of Owen (1980) and the TAW formulae (Van der Meer et al., 1998).

Owen:
$$\frac{q}{\sqrt{gH_s^3}}\sqrt{\frac{s_m}{2\pi}} = A\exp\left(-B\frac{R_c}{H_s}\sqrt{\frac{s_m}{2\pi}}\right) \qquad (1)$$

TAW:
$$\frac{q}{\sqrt{gH_s^3}}\sqrt{\frac{s_{op}}{\tan\alpha}} = 0.06\exp\left(-5.2\frac{R_c}{H_s}\frac{\sqrt{s_{op}}}{\tan\alpha}\right) \qquad (2)$$

with maximum:
$$\frac{q}{\sqrt{gH_s^3}} = 0.2\exp\left(-2.6\frac{R_c}{H_s}\right) \qquad (3)$$

with:

q	= average overtopping discharge	m^3/s per m width
g	= acceleration of gravity	m/s^2
H_s	= significant wave height, $H_{1/3}$ or H_{m0}	m
s_m	= wave steepness with mean period T_m	-
R_c	= crest freeboard	m
s_{op}	= wave steepness with peak period T_p	s
tanα	= slope angle	-

Table 2. A and B coefficients in the Owen formula (equation 1)

Slope	A	B
1:1	7.94×10^{-3}	20.1
1:1.5	8.84×10^{-3}	19.9
1:2	9.39×10^{-3}	21.6
1:2.5	1.03×10^{-2}	24.5
1:3	1.09×10^{-2}	28.7
1:3.5	1.12×10^{-2}	34.1
1:4	1.16×10^{-2}	41.0
1:4.5	1.20×10^{-2}	47.7
1:5	1.31×10^{-2}	55.6

A and B are coefficients in the Owen formula (equation 1) given for each slope (slopes of 1:1; 1:2; and 1:4 were measured, for other slopes an interpolation was performed). The coefficients were slightly changed later on by HR Wallingford and are given in Table 2. In fact the Owen formula was developed further during the TAW-work (around 1990) when Owen's original data were re-used. The main differences or developments were:

- include $\tan\alpha$, as this will lead to one set of formulae instead of a table of coefficients for distinct slopes
- change to T_p, as it was found that a longer period than T_m gave similar results for different spectral shapes, where T_m gave deviations
- include a maximum for non-breaking waves. It was found that there was no or hardly any influence of $\tan\alpha$ and T_p if the waves did not break on the slope.

The TAW formulae also include reduction factors for roughness, berms, oblique wave attack, and walls on top of a dike. As this paper deals with uniform slopes only, these factors (which can also be applied to the Owen formula) will not be treated here.

There is another difference between the Owen and TAW formulae. Owen (1980) gives a figure for the breaking index of the wave height in shallow water. Actually, one should take the significant wave height and mean period at deep water, apply the figure with the breaker index and apply the resulting wave height in the formula. The TAW formulae were mainly based on relatively deep water waves and the wave height to be used is the wave height at the toe of the structure. This implies that one should have a method available to predict this wave height at the toe of the structure.

Analysis of wave overtopping. The TAW formulae consider breaking and non-breaking waves on a slope. For non-breaking waves there is no influence of slope angle or wave period , but only of wave height and crest freeboard (equation 3). The test series include long periods that give non-breaking conditions for the 1:4 slope. At the 1:2 slope the conditions are always non-breaking. This means that in tests where waves are non-breaking on both slopes, the wave overtopping can be compared directly. Figure 8 gives these data.

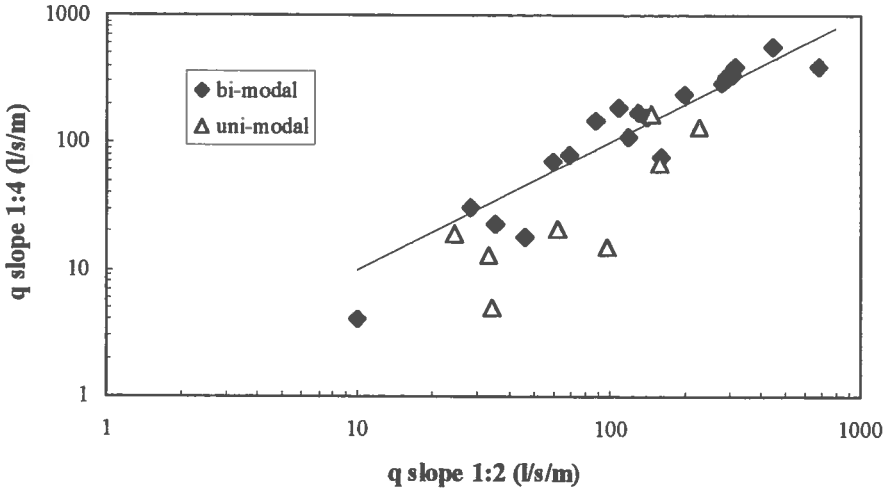

Figure 8. Direct comparison of wave overtopping for 1:2 and 1:4 slopes for non-breaking waves on the slope

For the uni-modal tests, generally the 1:2 slope gives more overtopping than the 1:4 slope, especially for lower overtopping rates. The bi-modal tests, however, show a clear correlation between the two slopes, supporting the conclusion that there is hardly any influence of slope angle on wave overtopping for non-breaking conditions. At present there is no explanation as to why uni- and bi-modal tests give different results.

Figures 9 and 10 give the measurements together with the predictions by Owen, equation 1 (together with the original data of Owen). Here the $H_{1/3}$ at the toe of the structure was taken together with T_m in deep water.

Figure 9 gives the results for the slope of 1:2. The bi-modal waves show more scatter than the uni-modal waves. This can be expected as the mean period, instead of a larger period, will increase the scatter for different spectral shapes, which occur

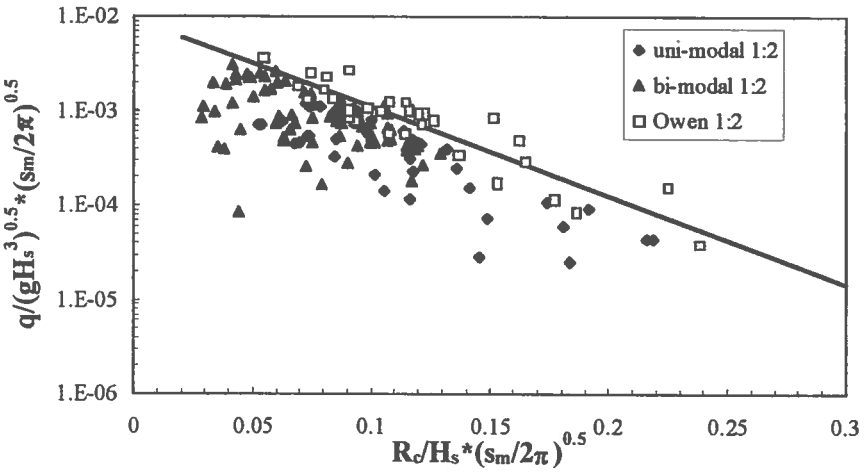

Figure 9. Wave overtopping with Owen formula for slope 1:2

particularly in the case of bi-modal waves. Moreover, the average trend gives less overtopping than predicted by Owen. This may partly be explained by the presence of longer wave periods than were used in development of the formula, but actually have no or minor influence. Still the deviation between measurements and predictions is quite large, especially for the uni-modal waves, although it is reassuring to note that the original data of Owen lie close to the line.

Figure 10 gives the data, together with the Owen formula for the slope of 1:4. Here the data are around the line, with more scatter for the bi-modal spectra, which can be expected as the mean period has been used to characterise the bi-modal spectrum.

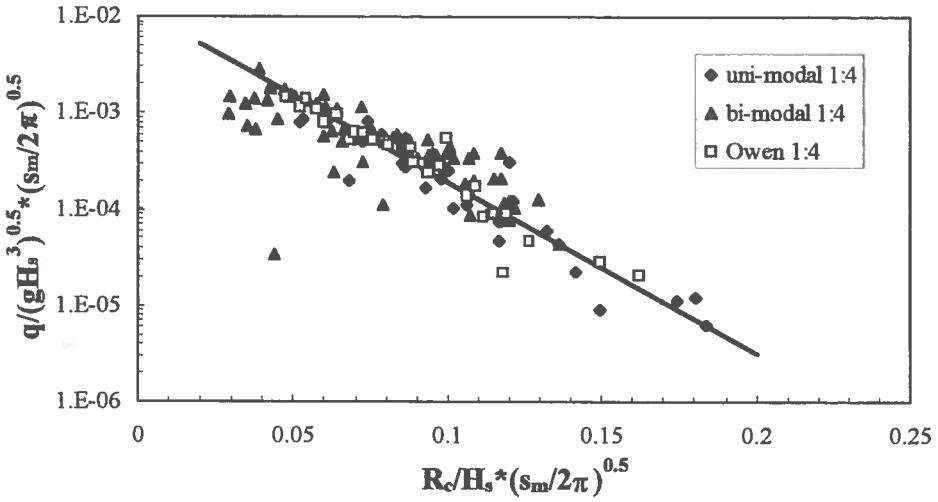

Figure 10. Wave overtopping with Owen formula for slope 1:4

It can be concluded that the steep slope of 1:2 shows a deviation from the predicted line. For both structure slopes the bi-modal spectra are not well described by the mean period, as the scatter is larger than for uni-modal waves.

For the TAW formulae (equations 2 and 3) various definitions of wave height and wave period were used. The data were plotted with $H_{1/3}$ or H_{m0} at the toe of the structure in combination with T_{m-10}, T_{m-20} or T_{m-2-1}, also measured at the toe of the structure. As shown in Table 1 there is a difference between the peak period and the spectral wave parameters. The spectral wave parameters for uni-modal waves are normally a little smaller than the peak period. For an objective comparison one should include the spectral wave period in the prediction. For simplicity it is assumed that a Jonswap spectrum represents most of the earlier tests in deep water, and therefore the following relationships were used to modify the TAW formulae or the prediction lines in the figures: $T_p = 1.11\ T_{m-10} = 1.08\ T_{m-20} = 1.06\ T_{m-2-1}$.

Not all the graphs can be given in this paper. After thorough analysis the final conclusion is that the data support the use of $H_{1/3}$ and T_{m-10} at the toe of the structure, which is consistent with conclusions mentioned earlier by Van Gent (2000). Only the graphs with these parameters are given here. Figure 11 shows the data for breaking waves, together with equation 2, adapted for use of T_{m-10} by using a factor $T_p=1.11T_{m-10}$. The data show the same trend as the line, but are on average a little

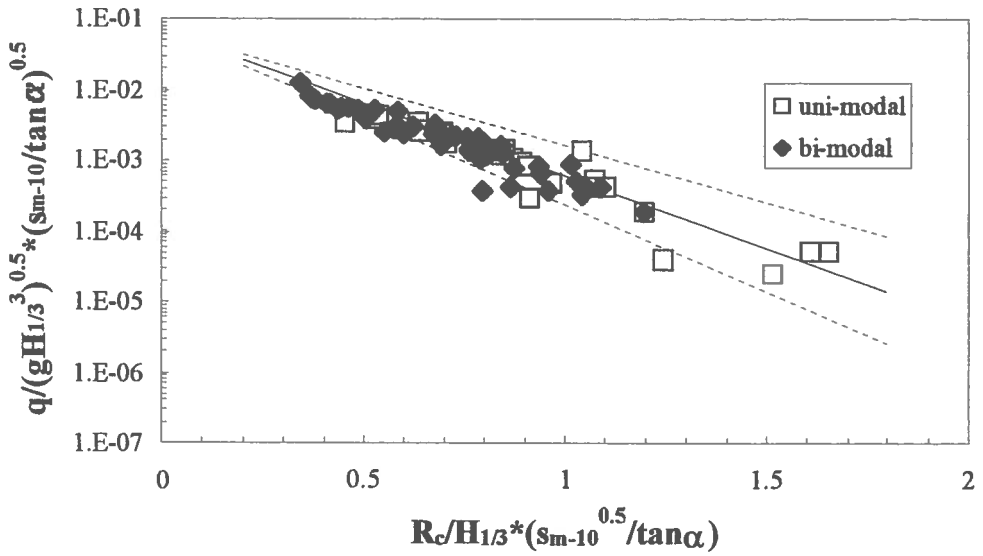

Figure 11. Wave overtopping data with TAW formula for breaking waves (equation 2) with the use of $H_{1/3}$ and T_{m-10} (the best choice)

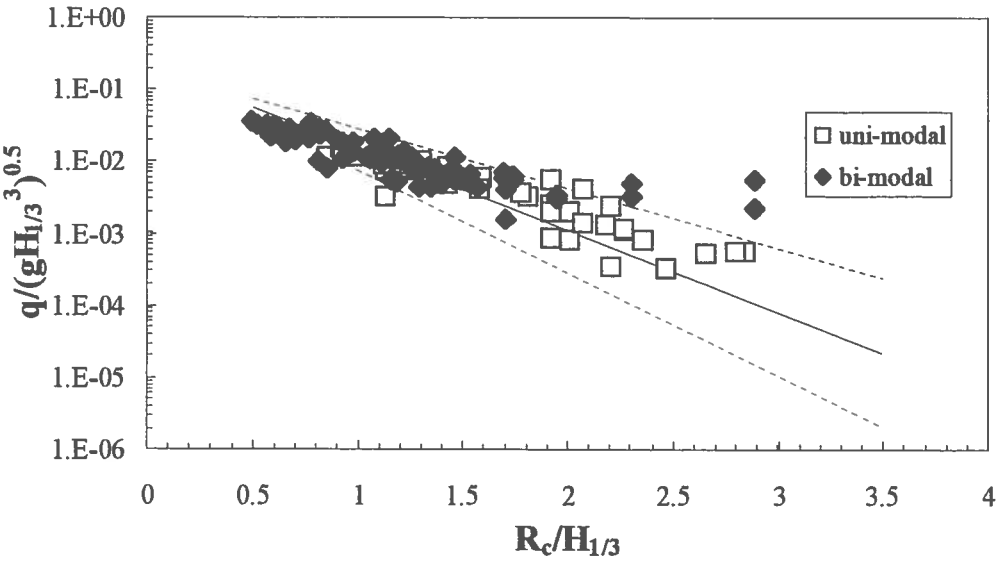

Figure 12. Wave overtopping data with TAW formula for non-breaking waves (equation 3) with the use of $H_{1/3}$ (and T_{m-10} for definition of breaking or non-breaking)

lower than this line, certainly for larger overtopping rates. This suggests a slightly conservative prediction method, but the differences are small.

Figure 12 shows the data for non-breaking waves on the slopes. On average the data are present around the line, but the data shows less overtopping for larger discharges and more overtopping for smaller discharges (the right side of the graph). It appears that the trend should be gentler than given by the prediction line. In fact the same was found with the original data of Owen (1980) for slopes 1:1 and 1:2, but

together with data from other sources, the average line is closer to the equation, see for instance Van der Meer et al. (1998).

For application of the TAW formulae, preference should be given to the use of $H_{1/3}$ and T_{m-10} for non-uni-modal wave spectra (bi-modal, more peaks or a wide spectrum due to wave breaking). This conclusion holds only for not too severe wave breaking (say not more than 50% reduction in wave height by breaking) and fairly steep foreshore slopes. Very severe wave breaking on gentle foreshores has been described by Van Gent (2000) and may include the effects of surf beat, resulting in increased wave overtopping. For application of the TAW formulae, $T_p = 1.11\ T_{m-10}$ should be used. (An alternative would be to rewrite the TAW formulae with T_{m-10} instead of T_p.)

Application of results

Scientific approach. Analysis thus far has focussed on the use of a spectral wave period which includes all kinds of spectral shapes. This has resulted in the conclusion to use T_{m-10} in the TAW formulae with a correction factor between T_p and T_{m-10}. The approach can be summarised as follows:

- Establish $H_{1/3}$ and T_{m-10} at the toe of the structure
- Use $T_p = 1.11\ T_{m-10}$
- Use the TAW formulae

This approach is called a scientific approach as it is still fairly complicated to establish the correct T_{m-10}. SWAN is not able to predict this period. First research shows (Van Gent and Doorn, 2000) that Boussinesq type models may be able to do this, but these type of models are still in use mainly by researchers and are not available for most practising engineers. The measurements in the tests give directly the desired wave period and height at the toe of the structure. Figure 13 shows the predicted against measured overtopping discharges for the slope 1:4, using the measured wave heights and periods at the toe for the predictions.

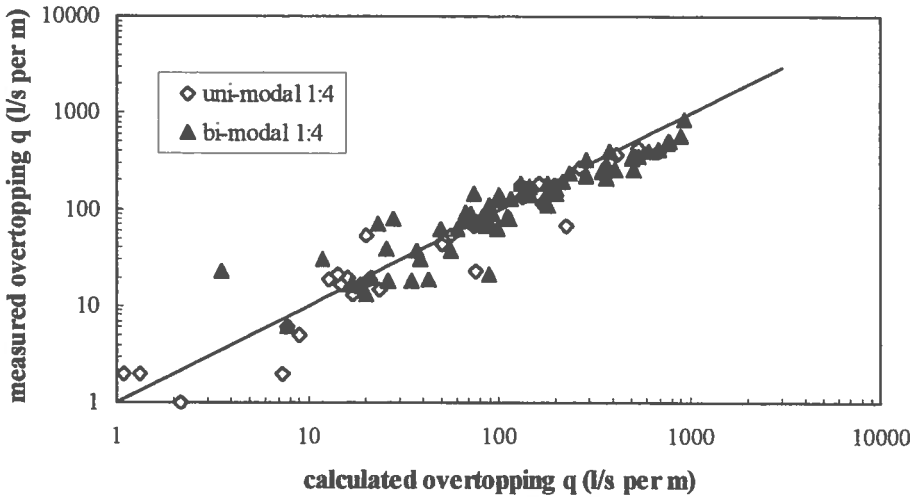

Figure 13. Scientific approach: use of $H_{1/3}$ and T_{m-10} at toe of structure; all data on slope 1:4; measured overtopping versus predicted

In Figure 13 only data for a slope of 1:4 have been plotted. Results for the 1:2 slope are comparable both for uni- and bi-modal waves, for the scientific approach as well as for the practical approach described below, as in each approach the maximum overtopping discharge for non-breaking waves is reached, which means that there is no influence of wave period.

Practical approach. Most standard methods for estimation of overtopping rate under uni-modal wave conditions are based on the use of a single offshore wave height and wave period. A potential problem arises if the spectrum becomes bi-modal before arrival at the structure where (at least) two peak periods may then be present. Bearing in mind that the offshore spectrum is often known, either from measurements or predictions, a simple approach was suggested by HR Wallingford (Hawkes et al., 1998) using the two (or more) separate offshore periods in separate overtopping predictions, before combining them into a single overall prediction. This idea was developed further and provides the basis for the practical approach given here. The method for bi-modal spectra can be summarised as follows:

- Establish the peak periods of both peaks *offshore*, T_{p1} and T_{p2}, with corresponding wave heights H_{s1} and H_{s2}, being the spectral wave heights $4\sqrt{m_{01}}$ or $4\sqrt{m_{02}}$ *offshore*
- Establish H_{m0} at the toe of the structure with a (simple) energy model
- Calculate $H_{1/3}$ using H_{m0} above by the method described in Battjes and Groenendijk (2000)
- Calculate breaker parameters ξ_{op1} and ξ_{op2} with respectively T_{p1} and $H_{1/3}$ and T_{p2} and $H_{1/3}$, where $\xi_{op}=\tan\alpha/\sqrt{2\pi H_s/(gT_p^2)}$
- Calculate the equivalent breaker parameter:
  $$\xi_{op}(eq) = (\xi_{op1} H_{s1}^2 + \xi_{op2} H_{s2}^2)/(H_{s1}^2 + H_{s2}^2) \quad (4)$$
- Calculate the overtopping discharge for with equation 2 and 3, using $\xi_{op}(eq)$.
- Equation 2 can be rewritten to:

$$\frac{q}{\sqrt{gH_s^3}} = 0.06\xi_{op}/\sqrt{\tan\alpha}\exp\left(-5.2\frac{R_c}{H_s}\frac{1}{\xi_{op}}\right) \quad (5)$$

This is called the practical approach as the (bi-modal) wave spectrum offshore is used, and a simple model to predict the wave height at the toe of the structure. Figure 14 gives the calculated and measured overtopping discharges for this approach, which can directly be compared with the results of the scientific approach, Figure 13.

Comparison of the two figures results in the following conclusion: the 1:4 slope with uni-modal spectra shows a slightly smaller scatter for the practical approach than for the scientific approach. The 1:4 slope with bi-modal spectra is slightly better predicted by the scientific approach as the practical approach gives mainly under predictions for small overtopping discharges. In general it can be concluded that the practical approach does not differ much from the scientific approach for the situations which were considered here, ie not too much wave breaking and fairly steep foreshores.

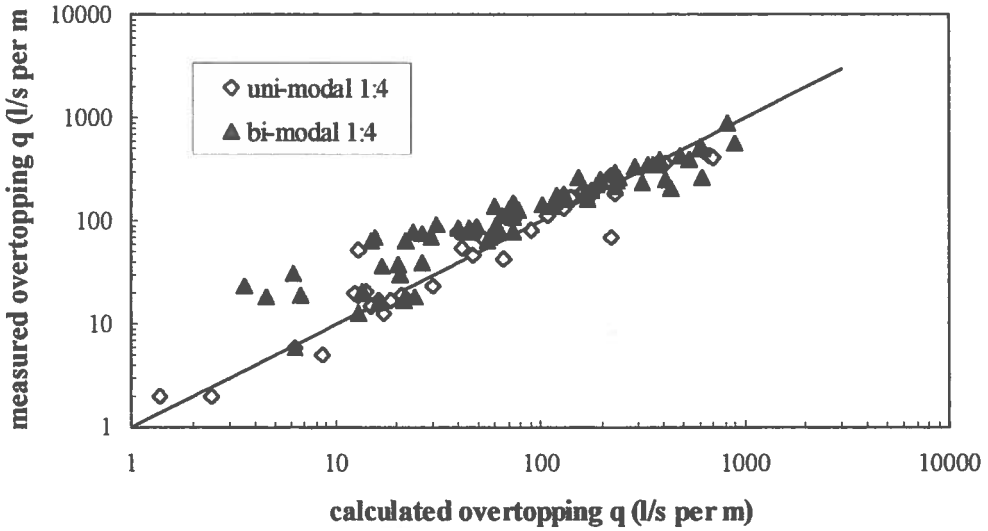

Figure 14. Practical approach: use of $H_{1/3}$ at the toe and peak periods offshore; all data on slope 1:4; measured overtopping versus predicted

References

Battjes, J.A. and H.W. Groenendijk (2000). Wave height distributions on shallow foreshores. Journal of Coastal Engineering, Volume 40, Number 3, 161-182

Coates, T.T., R.J. Jones and P. Bona (1998). Wave flume studies on responses to wind/swell and steep approach slopes. Research Report TR 24, HR Wallingford

Hawkes, P.J., T.T. Coates and R.J. Jones (1998). Impact of bi-model seas on beaches and control structures. Research report SR 507, HR Wallingford

Owen, M.W. (1980). Design of seawalls allowing for wave overtopping. Hydraulics Research Station, Report No EX 924

Van der Meer, J.W., P. Tönjes and J.P. de Waal (1998). A code for dike height design and examination. Coastlines, Structures and Breakwaters. ICE, pp. 5-19. Editor N.W.H. Allsop, Thomas Telford, London, UK

Van der Meer, J.W., E. Regeling and J.P. de Waal (2000a). Wave transmission: spectral changes and its effect on run-up and overtopping. ASCE, Proc. 27th ICCE, Sydney, Australia

Van der Meer, J.W., D.P. Hurdle, G.Ph. van Vledder, M.R.A. van Gent and R.C. Ris (2000b). Uni- and bi-modal wave spectra on steep foreshores. Validation of the SWAN-model, wave height statistics and wave overtopping, based on HR Wallinford data. Report i230 / A509 / H3510 of Infram, Alkyon and Delft Hydraulics

Van Gent, M.R.A. (1999). Wave run-up and wave overtopping for double-peaked wave energy spectra. Delft Hydraulics Report H3351, January 1999, Delft

Van Gent, M.R.A. (2000). Wave run-up on dikes with shallow foreshores. ASCE, Proc. 27th ICCE, Sydney, Australia

Van Gent, M.R.A. and N. Doorn (2000). Numerical model investigations on coastal structures with shallow foreshores. Delft Hydraulics Report H3351, Delft

Infram publication no. 13

Oblique wave transmission over low-crested structures

Jentsje W. van der Meer[1]
Baoxing Wang[2]
Ard Wolters[3]
Barbara Zanuttigh[4]
Morten Kramer[5]

[1]Infram, POBox 81, 3890 AB Zeewolde, NL, jentsje.vandermeer@infram.nl
[2]UNESCO-IHE, Institute for Water Education; former MSc-student, Westvest 7, 2611 AX Delft NL
[3]Ministry of Transport, Public Works and Water Management; Road and Hydraulic Engineering Division, POBox 5044, 2600 GA Delft, NL
[4]Università di Bologna, DISTART Idraulica, viale Risorgimento 2, 40136 Bologna, IT
[5]Aalborg University, Sohngaardsholmvej 57, 9000 Aalborg, DK

Paper presented at Coastal Structures 2003, August, Portland, USA

Oblique wave transmission over low-crested structures

Jentsje W. van der Meer[1], Baoxing Wang[2], Ard Wolters[3], Barbara Zanuttigh[4] and Morten Kramer[5]

Introduction

Wave transmission over low-crested structures has often been subject for research, as the wave field behind these structures determines what will happen in this area. Detached low-crested structures are often parallel to the coastline and in most cases wave attack will be perpendicular to this coastline and therefore, perpendicular to the structure. This situation can be simulated by small scale physical modeling in a wave flume. Results have been given by Van der Meer and Daemen (1994) and d'Angremond, van der Meer and de Jong (1996). Recent research, including all data of the above given references and new extensive data sets, has enlarged the insight on the topic, see Briganti et al. (2003). The results from 2D tests are:

- prediction formulae for the wave transmission coefficient K_t
- a description of change of spectral shape due to wave transmission

In quite some situations low-crested structures are not parallel to the coast. T-shaped groynes are an example, but also breakwaters for a harbour where only under very extreme storm surge the structure can be considered as low-crested. In these situations wave attack is very often not perpendicular to the alignment of the structure and in many situations even quite oblique wave attack and transmission occurs. But what will be the difference with perpendicular attack? More in detail:

- Are the prediction formulae for K_t still valid?
- Is the spectral change (more energy to high frequencies) similar to perpendicular wave attack?
- Is there any influence of short-crestedness of waves?
- Are wave directions similar in front of the structure and after transmission?

Only a three-dimensional investigation in a short-crested wave basin can give answer to these questions. Within the EU-project DELOS these tests have been performed and are the subject of this paper.

---

[1]Infram, POBox 81, 3890 AB Zeewolde, NL, jentsje.vandermeer@inframn.nl
[2]UNESCO-IHE, Institute for Water Education; former MSc-student, Westvest 7, 2611 AX Delft, NL [3]Ministry of Transport, Public Works and Water Management; Road and Hydraulic Engineering Division, POBox 5044, 2600 GA Delft, NL
[4]Università di Bologna, DISTART Idraulica, viale Risorgimento 2, 40136 Bologna, IT
[5]Aalborg University, Sohngaardsholmvej 57, 9000 Aalborg, DK

Test set-up and programme

Basin and layout. The three-dimensional wave transmission tests were carried out in the short-crested wave basin (9.0 m × 12.5 m × 0.9 m) at Aalborg University, Denmark. Two structures were tested, a rubble mound structure and a smooth structure made out of plywood. The rubble mound structure had an armour layer of rock. In reality smooth structures have a cover layer of asphalt or placed block revetments, a type of structure quite common in the Netherlands.

The structures were placed on a horizontal plateau, which was 0.16 m higher than the bottom of the basin. This created a larger depth in front of the wave generator and made it easier to generate the required waves. Three layouts were constructed for each structure: 0° (perpendicular wave attack, structure parallel with the wave generator), 30° and 50°. Figure 1 shows the layout of the smooth structure, which was constructed under an angle of 30° with the wave generator and Figure 2 shows the layout for the rubble mound structure under 50°. The two lowest horizontal lines in both figures give the area between the deeper water in front of the wave generator and the 0.16 cm higher plateau.

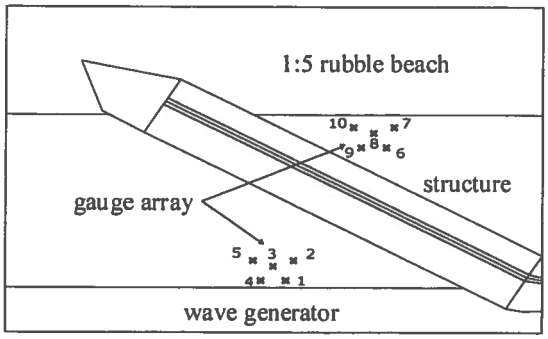

Figure 1. Smooth structure under 30° angle

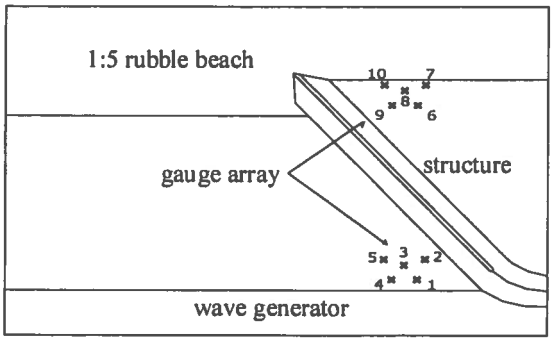

Figure 2. Rubble mound structure under 50° angle

Cross-sections. The rubble mound structure was 25 cm high. It had a seaward slope of 1:2 and a leeward slope of 1:1.5, see Figure 3. The crest width was 10 cm. The core consisted of B-rock with D_{n50} = 0.031 m and the bottom layer of C-rock with D_{n50} = 0.016 m. The armour layer consisted of A-rock with W_{50} = 0.269 kg, D_{n50} = 0.0466 m and a grading of D_{85}/D_{15} = 1.25. The shape of the armour rock can be described by L/H and the blockiness coefficient; where L = the largest dimension of the rock, H = the smallest dimension, B = the third dimension, V = the volume of the rock and the blockiness coefficient is defined as V/(LxBxH). The shape can be described by two values: the percentages of rock exceeding 2L/H and 3L/H. These values were 50% and 4%, respectively. The blockiness coefficient was 0.42 (see also Stewart et al. 2002).

The smooth structure had gentler slopes than the rubble mound structure, which is also the case in reality. The seaward slope was 1:3 and the leeward slope 1:2. The structure height was 0.30 m and the crest width 0.20 m.

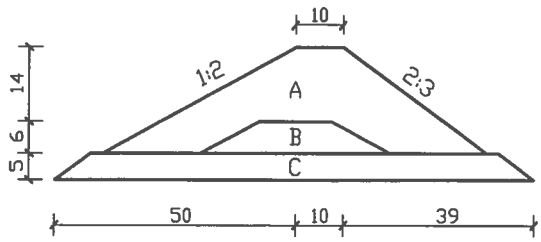

Figure 3. Rubble mound structure

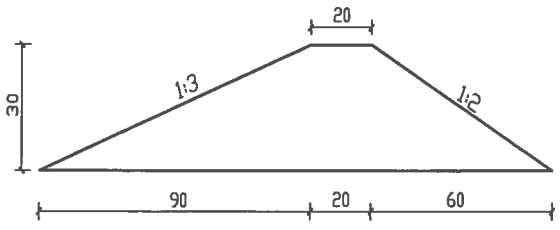

Figure 4. Smooth structure

Test programme. For both the rubble mound structure as well as for the smooth structure 84 tests were performed. Table 1 gives an overall view. Three crest freeboards were tested with two wave steepnesses and for each wave steepness three wave heights. The main angles of attack were 0°, 30° and 50°, but as the multi-directional wave generator could also generate waves under an angle, a limited number of tests were performed with 20°, 40° and 60°. Only 10 of the 84 tests were performed with long-crested waves.

Table 1 Overall view of test programme

Tests per structure	84 (10 long-crested, 74 short-crested)
Crest freeboard	+0.05 m; 0.0 m; -0.05 m
Dimensionless freeboard R_c/H_s	-0.7 to +0.8
Wave height H_s	0.07 m to 0.14 m
Wave steepness s_{op}	0.02 and 0.04
Angles of wave attack β	**0°**, 20°, **30°**, 40°, **50°** and 60°

Data processing. A Jonswap spectrum with γ=3.3 was used for the tests. The short-crested tests were performed with a $\cos^{2s}$ spreading function, where s=50. In fact the testing was quite simple, as only incident and transmitted wave conditions were required. A wave gauge array of 5 gauges was placed in front of the structure to measure the incident waves and a similar array behind the structure to measure the transmitted waves, see also Figures 1 and 2.

The PADIWA package for directional wave analysis, as available at Aalborg University, was used to analyze the measured wave signals. The Bayesian Directional Spectrum Estimation Method (BDM) was used to estimate the directional wave spectrum. Also analysis on individual wave gauges was performed, both in time and frequency domain. The processing resulted in: incident and transmitted wave heights H_{m0i}, excluding reflection from structure or 1:5 spending beach; wave periods like the peak period T_p, the mean period T_m and the spectral period $T_{m-1,0}$, wave directions β and spectral shapes. Finally, the ratio of transmitted wave height to incident wave height resulted in the transmission coefficient $K_t = H_t/H_i$.

Data analysis

Long-crested versus short-crested waves. The first question to consider is whether similar results are found for long-crested and short-crested waves. In theory it should

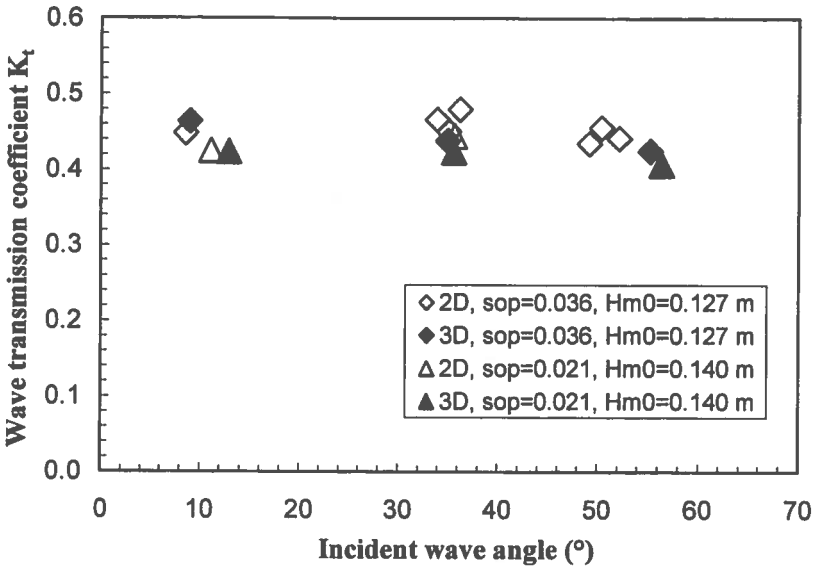

Figure 5. Comparison of long-crested and short-crested waves for rubble structures

be similar for perpendicular wave attack ($\beta = 0°$), but differences may occur for angled wave attack. For wave run-up and overtopping on dikes, for example, short-crested waves gave less reduction for larger wave angles than long-crested waves, see Van der Meer et al. (1998).

Figure 5 gives a comparison for the rubble mound structure. Tests were selected which were similar in both cases. This resulted in wave steepnessess of $s_{op} = 0.036$ and 0.021 with wave heights of respectively $H_{mo} = 0.127$ m and 0.140 m. In the graph the wave transmission coefficient has been given as a function of the incident wave angle. Similar shape of symbols give similar wave conditions and these should be compared with each other. Open symbols give long-crested waves and solid symbols give short-crested waves. The trend of the data points is not important at this stage, only the direct comparison of similar open and solid symbols for the same angle of wave attack.

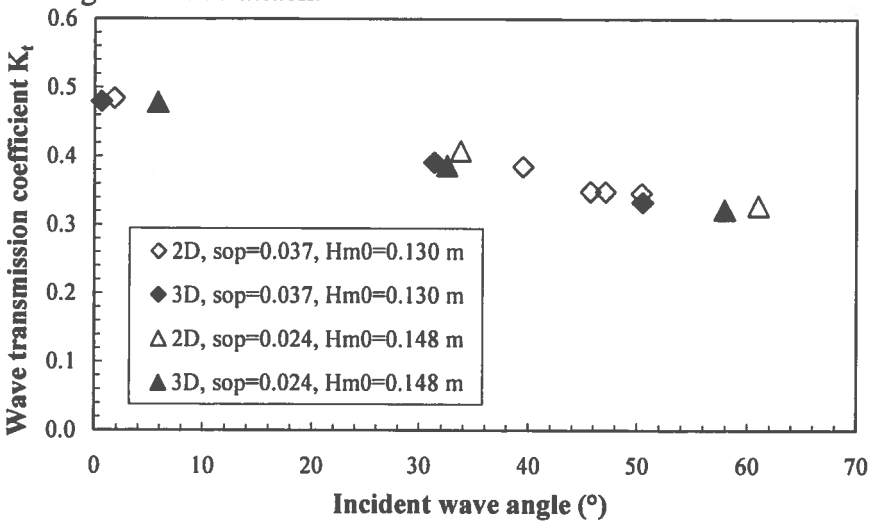

Figure 6. Comparison of long-crested and short-crested waves for smooth structures

The conclusion from Figure 5 is that long-crested and short-crested waves give similar overtopping for rubble mound structures, although in average the short-crested waves give 1%–2% lower values.

Figure 6 gives similar results for the smooth structure. The graph shows a clear influence of the angle of wave attack on transmission, but this aspect will be treated later. Direct comparison of similar symbols give the same conclusion as for rubble mound structures: there is no or only a marginal difference between long-crested and short-crested waves.

Change of wave direction. Another important question is whether transmitted waves have the same direction as the incident waves. Figure 7 gives the results for the rubble mound structure. First of all this graph shows that perpendicular generated waves did in fact not reach the structure completely perpendicular, but in average under an angle of about -10°. This was caused by a slightly different layout with a roundhead at one of the ends of the structure.

The figure shows clearly that for rubble mound structures the transmitted wave direction is smaller than the incident one. The reason for this could be that roughness and porosity of the structure cause dissipation of energy in such a way thatthe waves do not go on in the same direction. A simple straight line fits all data points quite well and leads to the conclusion that the transmitted wave angle is about 80% of the incident wave angle, or:

$\beta_t = 0.80\ \beta_i$ for rubble mound structures

Figure 8 shows the results for the smooth structure. The conclusions now are quite different from the one for rubble mound structures. Up to 45° transmitted and incident waves have similar directions. For larger incident angles than 45° this

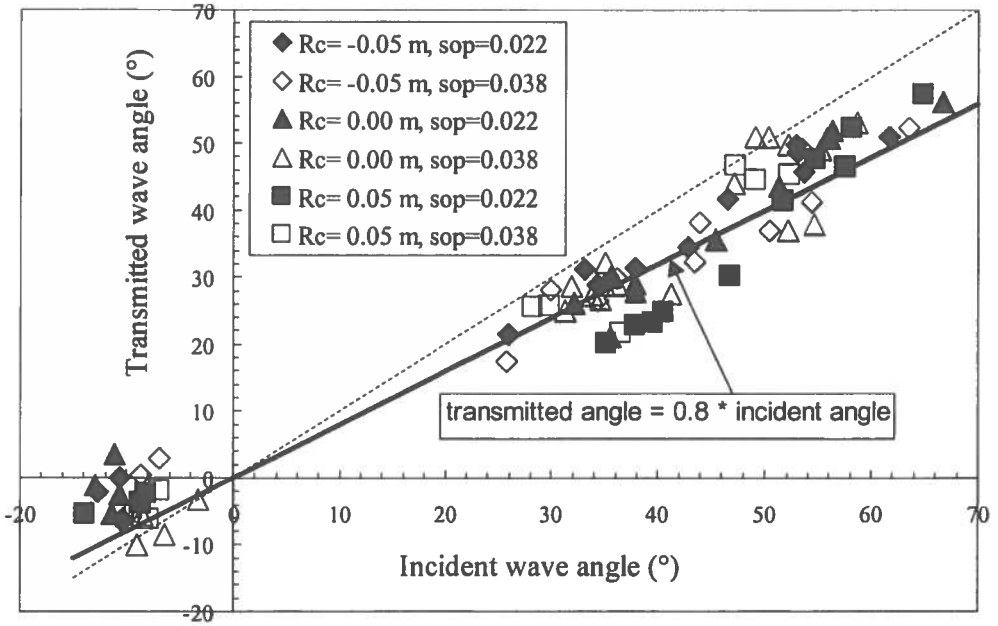

Figure 7. Transmitted wave angle versus incident angle. Rubble mound structure

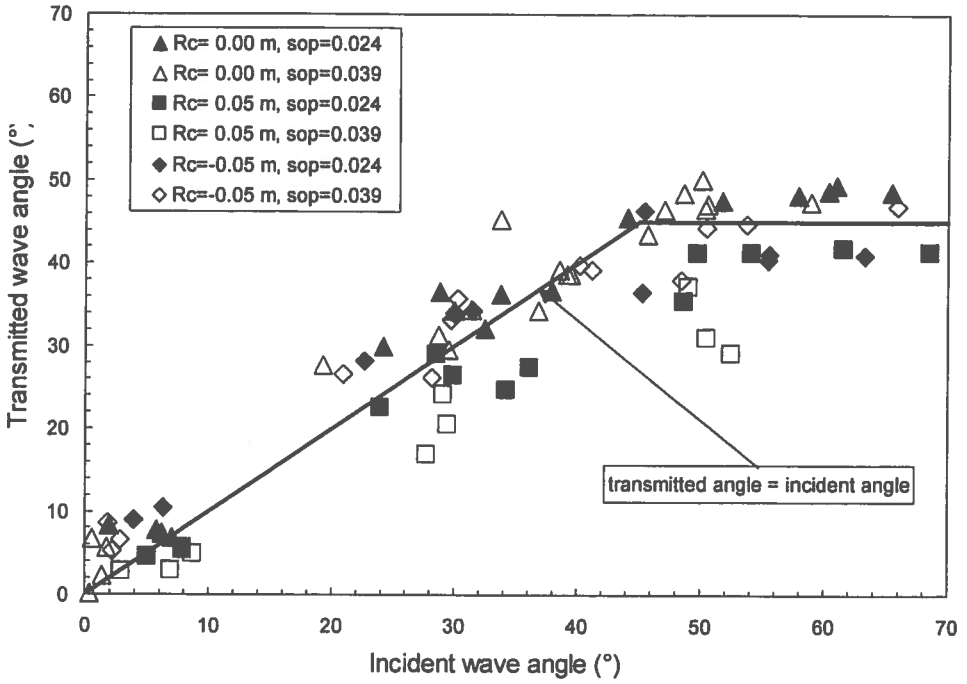

Figure 8. Transmitted wave angle versus incident wave angle. Smooth structure

changes: the transmitted wave angle remains 45°. Probably the smooth structure works in such a way that for larger angles the waves run along the crest of the structure and generate always a transmitted angle of 45°. There is also a tendency that for lower wave transmission (the data points for R_c = 0.05 m) the transmitted wave angle is a little smaller than the incident one. For smooth structures the behaviour can be described by:

$\beta_t = \beta_i$ for $\beta_i \leq 45°$
$\beta_t = 45°$ for $\beta_i > 45°$ for smooth structures

Influence of angle of wave attack on transmission coefficient. Transmission coefficients are mostly obtained by 2D flume testing where the angle of wave attack is always perpendicular to the structure. But is this still true if the angle of wave attack is oblique? Figure 9 gives the answer for rubble mound structures. The transmission coefficients are given for 3 groups of data points (the 3 different crest levels) and within each group a distinction has been made for the wave steepness. Of course a lower crest level gives larger transmission, which is according to 2D research.

The main objective in Figure 9, however, is to look at the trend within each group of data points with respect to the incident wave angle. For the two lowest crest heights, the upper part of the graph, there is a very small tendency that the transmission coefficient decreases with increasing angle of wave attack. But within the scatter of the data it is only marginal. For the highest crest height the trend seems a little more pronounced, but even there no influence is found for incident wave angles between 30° and 60°.

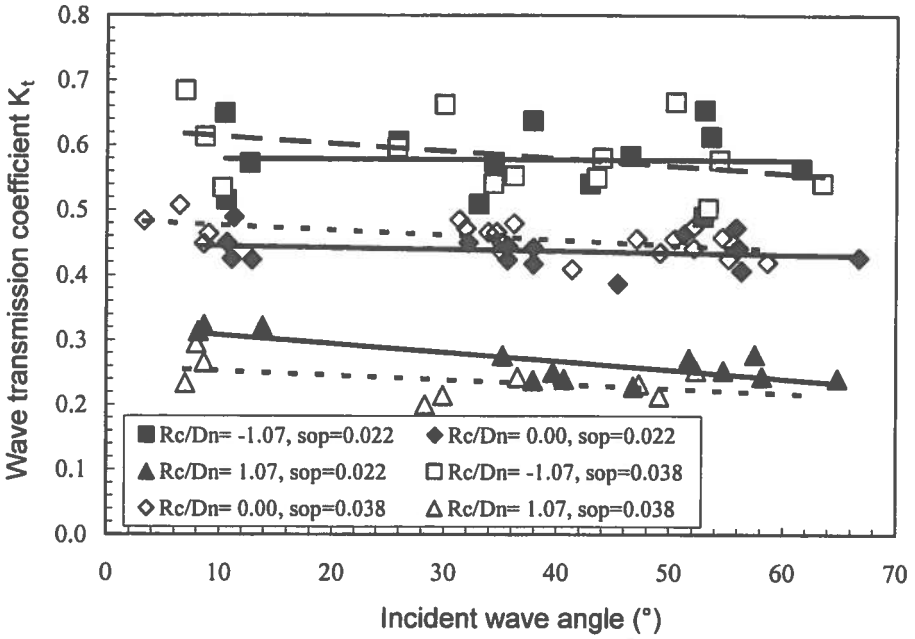

Figure 9. Influence of wave angle on wave transmission coefficient K_t for rubble mound structures

For rubble mound structures it can be concluded that the angle of wave attack has no or only marginal influence on the wave transmission coefficient. This leads also to the conclusion that earlier 2D research, resulting in prediction formulae for transmission at rubble mound structures, is valid for oblique wave attack. One restriction may be that it is only valid for rubble structures with a small crest width.

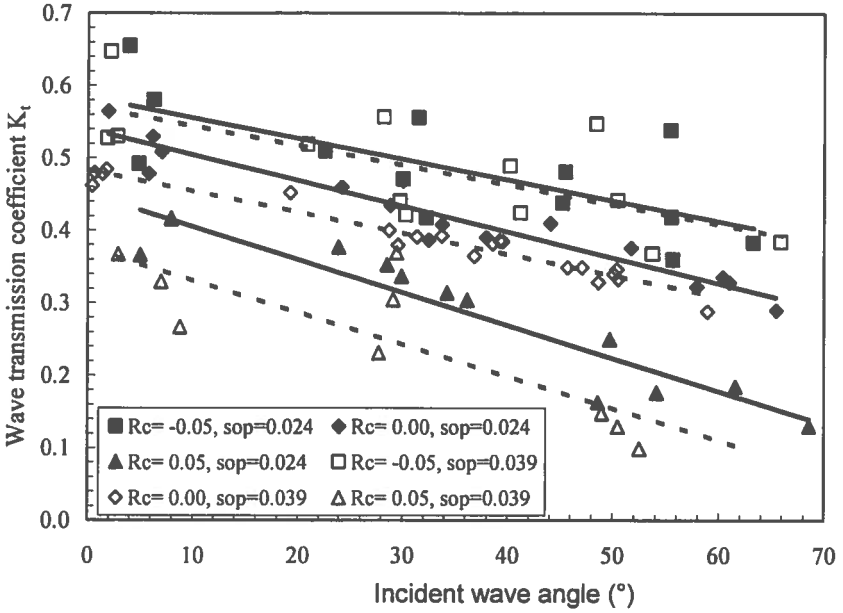

Figure 10. Influence of wave angle on wave transmission coefficient K_t for smooth structures

Figure 10 shows a similar graph as Figure 9, but now for the smooth structure. The conclusions, however, are completely different! It is very clear that for smooth structures the wave transmission coefficient decreases significantly with increasing angle of wave attack. It means also that if 2D prediction formulae for smooth structures are used for oblique wave attack, the predicted wave transmission is quite conservative. Further analysis is required to come up with a prediction formula on the influence of the angle of wave attack on transmission, see the next section.

2D wave transmission on smooth structures. d'Angremond et al. (1996) with as basis De Jong (1996) came up with a formula for wave transmission on smooth structures. The formula is as follows:

$$K_t = -0.4R_c/H_i + [B/H_i]^{-0.31} * [1 - \exp(-0.5\xi)] * 0.80 \qquad (1)$$

with as minimum $K_t = 0.075$ and maximum $K_t = 0.8$.

This formula has a similar shape as the one for rubble mound structures, only one coefficient is different, ie 0.80 is 0.64 for rubble mound structures. The formula for smooth structures at that time was only based on a limited data set. Now new data are available: Van der Meer et al. (2000) and the data within the present project with perpendicular wave attack.

The comparison of all data on smooth structures with the formula of d'Angremond et al. (1996), equation 1, is given in Figure 11. The total picture gives data well distributed around the line, but in detail the conclusion is different. The original data (open symbols) are in average located above the line, where the new data (solid symbols) are below the line. Therefore a new analysis was performed on the data in order to come up with an improved method for smooth structures.

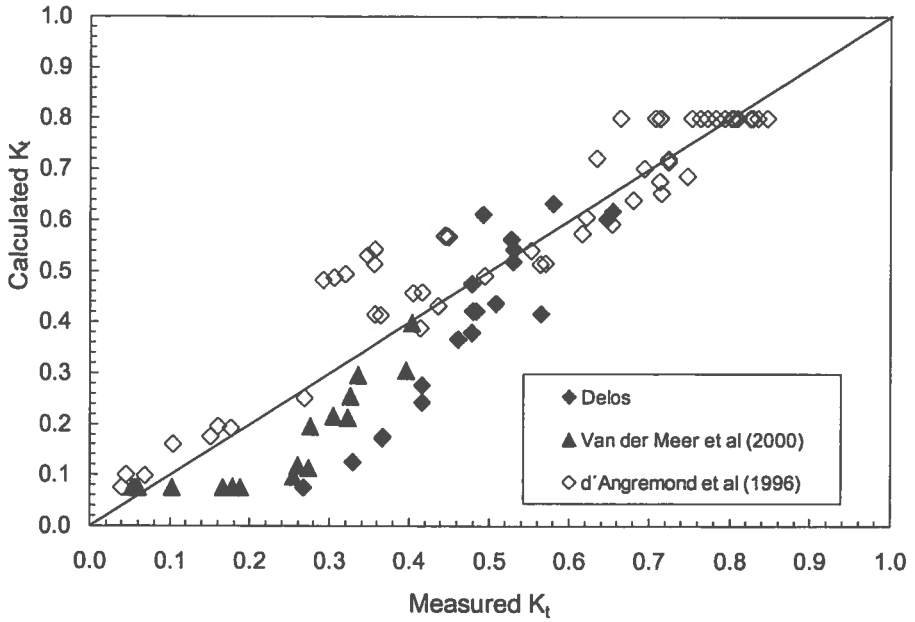

Figure 11. All data on smooth structures compared with equation (1)

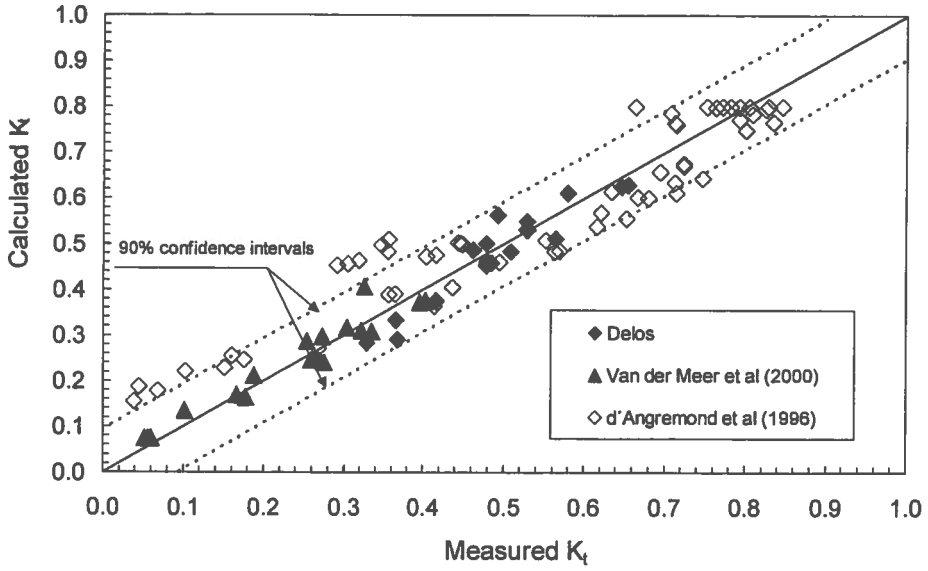

Figure 12. All data on smooth structures compared with new equation (2)

In equation (1) there is quite a strong influence of the crest width on wave transmission. This expression in (1) was based on rubble mound structures, where indeed a permeable and rough crest with a large width has a tremendous effect on transmission. Van der Meer et al. (2000) tested smooth structures with different crest widths and it was very clear that for smooth structures there was hardly any influence of crest width, if the seaward slope was quite gentle. The waves broke on the seaward slope and jumped over the smooth crest without any energy dissipation on the crest. The first conclusion for a new analysis is that the crest width B has no or hardly influence on transmission. This could be different for non-breaking waves (large ξ-values) and structures with very wide submerged crests.

With above conclusion a new analysis was done on the total data set, keeping the structure of the original formula similar. The formula was divided in two parts, one for breaking waves ($\xi_{op} < 3$), where the influence of the crest width was not present and one for non-breaking waves with the same structure as equation (1). The same lower and upper boundaries for K_t were used. The result is given as equation (2). The comparison between measured and calculated K_t is shown in Figure 12.

Modified formula for smooth structures:

$$K_t = -0.3R_c/H_i + 0.75[1 - \exp(-0.5\xi)] \qquad \text{for } \xi_{op} < 3$$

$$K_t = -0.3R_c/H_i + [B/H_i]^{-0.31} * [1 - \exp(-0.5\xi)] * 0.75 \text{ for } \xi_{op} \geq 3 \qquad (2)$$

with as minimum $K_t = 0.075$ and maximum $K_t = 0.8$.

3D wave transmission on smooth structures. With a good formula for 2D wave transmission on smooth structures it is possible to make a straight forward analysis on the effect of oblique waves. Equation (2) was used as a reference and for each test

condition the K_t for perpendicular wave attack was calculated. The ratio measured K_t over calculated K_t for $\beta = 0°$ was then plotted versus the incident wave angle β. This graph is shown in Figure 13.

Although Figure 13 shows some scatter, the trend is very clear that wave transmission decreases with increasing incident wave angle. An easy way to include the effect of oblique waves is to add a $\cos^{2/3}\beta$ function to the 2D equation (2). This leads to the final prediction formula for smooth structures:

$$K_t = [-0.3R_c/H_i + 0.75[1 - \exp(-0.5\xi)]] \cos^{2/3}\beta \qquad (3)$$

with as minimum $K_t = 0.075$ and maximum $K_t = 0.8$.

and limitations: $1 < \xi_{op} < 3$ $0° \leq \beta \leq 70°$ $1 < B/H_i < 4$

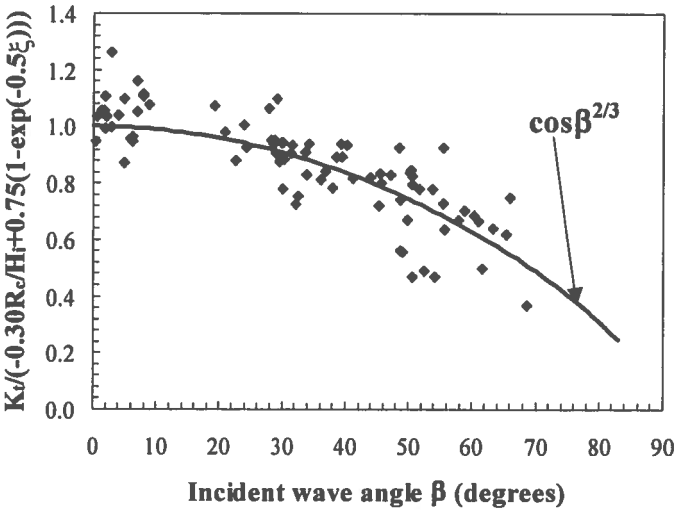

Figure 13. Influence of oblique wave attack on smooth structures

Spectral change due to wave transmission.

Transmitted spectra are often different from incident spectra. Waves breaking over a low-crested structure may generate two or more transmitted waves on the lee side. The effect is that more energy is present at higher frequencies than for the incident spectrum. In general the peak period is quite close to the incident peak period, but the mean period may decrease considerably. A first analysis on this topic can be found in Van der Meer et al. (2000).

The wave transmission coefficient only contains information about the wave heights behind the structure. It is the spectrum which contains wave period information. Very often information is required on both wave heights and periods, for example for wave run-up or overtopping at structures behind a low-crested structure, or for calculation of morphological changes.

Figure 14 shows an example of a transmitted spectrum for a smooth structure and gives clearly the picture that energy is present more or less a similar level up to

high frequencies. Based on this a simple and rude model was developed by Van der Meer et al. (2000), which is shown in Figure 15. In average 60% of the transmitted energy is present in the area of $< 1.5f_p$ and the other 40% of the energy is evenly distributed between $1.5f_p$ and $3.5f_p$.

It are these assumptions of division of energy in 60%/40% parts and the frequency of $f_{max} = 3.5f_p$, which were only based on a limited number of tests, that can be more elaborated with new data. Analysis showed that there was no clear dependency on wave direction, so all data were taken together. The results are given in Table 2.

Table 2. Average results on spectral shape compared with Van der Meer etal (2000)

	proposed method	rubble mound	smooth structure
f_{max}/f_p	3.5	3.2 (2.1-4.3)	3.8 (2.9-5.6)
$E_{1.5fp-fmax}/E_{total}$	40%	34% (20%-51%)	42% (30%-60%)

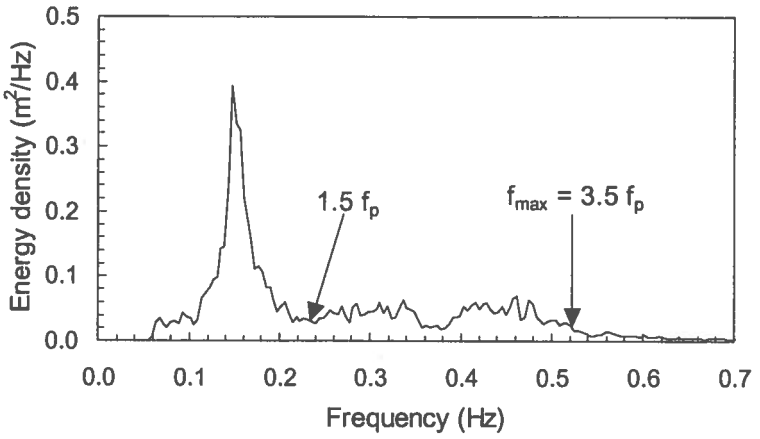

Figure 14. Example of transmitted spectrum with energy at high frequencies

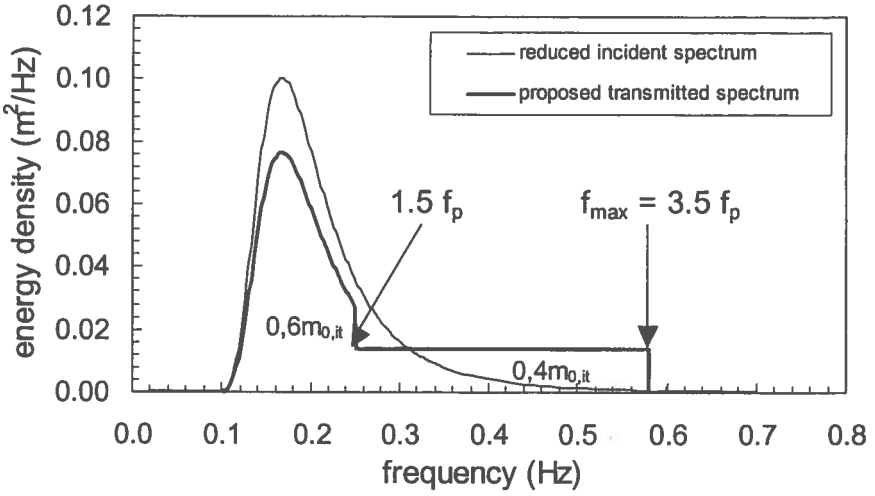

Figure 15. Proposed method by Van der Meer et al. (2000) for transmitted spectrum

The overall results are similar to the proposed method, although rubble mound structures give a little smaller values than smooth structures. Briganti et al. (2003) have taken this a little further and come to the conclusion that rubble mound and smooth structures do not give a similar behaviour. The method is also applicable for submerged rubble mound structures, but not for emerged ones. In the latter case much less energy goes to the higher frequencies and f_{max} may become close to 2.0. More research is needed to improve the method as described above.

Conclusions

***General* conclusions.** The first conclusion is that rubble mound structures have a completely different behaviour than smooth structures. The structures are of course also quite different. Gentle smooth slopes cause the waves to break, where steep rubble mound slopes give no breaking, but a lot of energy dissipation through the permeability and roughness of the structure. Although d'Angremond et al. (1996) developed a similar wave transmission prediction formula for rubble mound and smooth structures, it is better to treat both structures independently.

Another general conclusion is that long-crested and short-crested waves give similar wave transmission.

Transmitted wave angle. Incident and transmitted wave angles are not always similar. The conclusions are:

$\beta_t = 0.80\ \beta_i$		for rubble mound structures
$\beta_t = \beta_i$	for $\beta_i \leq 45°$	for smooth structures
$\beta_t = 45°$	for $\beta_i > 45°$	

Transmission coefficient. The influence of the wave angle on the transmission coefficient is non to marginal for rubble mound structures. This means that the most recent and well calibrated formulae of Briganti et al. (2003) can be taken for 3D situations. A new formula was developed for smooth structures, where the angle of wave attack has large influence on the transmission coefficient:

$$K_t = [-0.3R_c/H_i + 0.75[1 - \exp(-0.5\xi)]]\ \cos^{2/3}\beta \qquad (3)$$

with as minimum $K_t = 0.075$ and maximum $K_t = 0.8$.
and limitations: $1 < \xi_{op} < 3$ $0° \leq \beta \leq 70°$ $1 < B/H_i < 4$

Spectral change. Results on spectral change were not conclusive, but in general results were according to an earlier proposed method (Van der Meer et al. (2000)). Emerged rubble mound structures show a different behaviour and more research is required on this aspect.

Acknowledgements
This work has been performed within the EU-funded project DELOS with contract number EVK3-2000-00038.

References

Briganti, R., J.W. van der Meer, M. Buccino and M. Calabrese (2003). "Wave transmission behind low crested structures". *ASCE, Proc. Coastal Structures, Portland, Oregon.*

d'Angremond, K., J.W. van der Meer and R.J. de Jong, (1996). "Wave transmission at low crested structures". *ASCE, Proc. ICCE, Orlando, Florida,* 3305-3318.

De Jong, R.J., (1996). "Wave transmission at low-crested structures. Stability of tetrapods at front, crest and rear of a low-crested breakwater". MSc-thesis, *Delft University of Technology.*

Stewart, T.P., S.D. Newberry, J.D. Simm and J.P. Latham, (2002). "The hydraulic performance of tightly packed rock armour layers". *ASCE, proc. ICCE, Cardiff.* 1449-1461.

Van der Meer, J.W. and I.F.R. Daemen, (1994). "Stability and wave transmission at low crested rubble mound structures". *J. of WPC&OE, ASCE, 1994, 1, 1-19.*

Van der Meer, J.W., P. Tönjes and J.P. de Waal, (1998). "A code for dike height design and examination". *ICE, Proc. Coastlines, structures and breakwaters. Londen.* 5-19.

Van der Meer, J.W., H.J. Regeling and J.P. de Waal, (2000). "Wave transmission: spectral changes and its effect on run-up and overtopping". *ASCE, Proc. ICCE, Sydney, Australia.* 2156-2168.

Wang, B., (2003). "Oblique wave transmission at low-crested structures". MSc-thesis HE 133. *UNESCO-IHE, Institute for Water Education, Delft.*

Infram publication no. 20

Wave transmission at low-crested structures, including oblique wave attack

J.W. van der Meer[1]
R. Briganti[2]
B. Wang[3]
B. Zanuttigh[4]

[1] Infram, POBox 16, 8316 ZG Marknesse, the Netherlands; jentsje.vandermeer@Infram.nl
[2] Dipartimento di Scienze dell'Ingegneria Civile University of Roma Tre, IT
[3] Former MSc-student UNESCO-IHE, POBox 3015, 2601 DA Delft, NL PhD-student University of Plymouth, PL4 8AA, UK
[4] Università di Bologna, 40136 Bologna, IT

Paper presented at the International Conference on Coastal Engineering,
ASCE, ICCE 2004, Lisbon

WAVE TRANSMISSION AT LOW-CRESTED STRUCTURES, INCLUDING OBLIQUE WAVE ATTACK

JENTSJE W. VAN DER MEER

Infram, PO. Box 16, 8316 ZG Marknesse, NL, jentsje.vandermeer@infram.nl

RICCARDO BRIGANTI

Dipartimento di Scienze dell'Ingegneria Civile University of Roma Tre, IT, briganti@uniroma3.it

BAOXING WANG

Former MSc-student UNESCO-IHE, POBox 3015, 2601 DA Delft, NL
PhD-student University of Plymouth, PL4 8AA, UK; baoxing.wang@plymouth.ac.uk

BARBARA ZANUTTIGH

Università di Bologna, 40136 Bologna, IT, barbara.zanuttigh@mail.ing.unibo.it

A part of the DELOS research focused on wave transformation at low-crested structure and is summarised in this paper. Several flume tests have been carried out within the project to analyse wave transmission on rubble mound structures and simultaneously an existing database has been extensively increased by receiving data from other researchers in the world. This new database consists of more than 2300 tests and has been used to come up with the best 2D wave transmission formula for rubble mound LCS. Oblique wave attack on LCS was a second objective within DELOS. Small scale model results were produced and analysed leading to new transmission formulae for smooth LCS and to conclusions on 3D effects for both rubble mound and smooth LCS.

1. Introduction

Waves coming from deep water may reach a structure after refraction, shoaling and breaking. As soon as waves reach a structure, such as a low-crested structure – (LCS), a lot of processes start. The waves may break on the structure, overtop it, generate waves behind the structure and reflect from the structure. Another effect may be wave penetration through openings between structures and diffraction around the head of structures. Both wave penetration and diffraction do not depend on the fact whether the structure is low-crested or not and, therefore, one is referred to handbooks for these items. The process of wave transmission over and through a structure, permeable and impermeable, in 2D and 3D conditions, is subject of this paper.

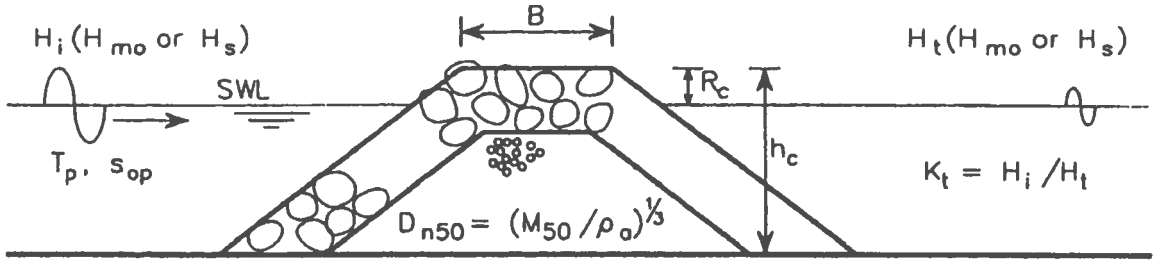

Figure 1. Definitions of governing parameters involved in wave transmission

The main parameters describing wave transmission have been given in Figure 1, here for a rubble mound structure. These are:

H_i = incident significant wave height, preferably H_{m0i}, at the toe of the structure

H_t = transmitted significant wave height, preferably H_{m0t}

T_p = peak period

s_{op} = wave steepness, $s_{op} = 2\pi H_i/(gT_p^2)$

R_c =crest freeboard

h_c = structure height

K_t =transmission coefficient H_t/H_i

ξ_{op} = breaker parameter $\xi_{op} = \tan\alpha/(s_{op})^{0.5}$; α = slope angle of structure

2. 2D wave transmission at rubble mound LCS

2.1. *Database*

Wave transmission and overtopping are the two phenomena that allow wave energy to pass over or through LCS. As these structures are commonly employed in coastal defence interventions, the prediction of the amount of energy transmitted behind them is a crucial point in design practice. Research in the past has led to various design formulae for wave transmission that are now commonly used in engineering practice, but each contain their own limitations.

A first effort made within the EU-funded project DELOS has been both to perform new tests on LCS and to gather many existing datasets on wave transmission and build an extensive database. A second effort was to perform a review and an upgrading of the existing approaches by means of this extensive database. More details are given in Briganti et al. (2003).

A wide database concerning experiments on wave transmission at low-crested structures in wave flumes has been collected. Earlier work by Van der Meer and Daemen (1994) and d'Angremond et al. (1996) has been used as the starting point of the present work. They began to collect and reanalyse data from different sources, giving a description of the various phenomena, which led to two different formulae. The gathered database, made up of 2337 tests, includes

the data previously described and analysed by Van der Meer and Daemen (1994) and by d'Angremond et al. (1996), that will be referred to as the "old database" here after. This database includes rubble mound rock structures as well as tetrapod and accropode armour layers. The range of the tested parameters is shown in Table 1.

Table 1. Summary of the ranges of parameters involved in 2D wave transmission tests at LCS

Database	Armour type	Rc/Hi	B/Hi	B/Lop	ξop	Hi/Dn50	Hi/h	sop	Tests #
Old database	various	-8.7	0.37	0.009	0.7	0.3	0.03	2*10-4	398
		4.0	43.48	0.51	8.26	6.62	0.62	0.06	
UCA	rubble mound	-1.5	2.67	0.04	3.97	0.84	0.1	0.002	53
		1.53	30.66	0.4	12.98	2.42	0.37	0.02	
UPC	rubble mound	-0.37	2.66	0.07	2.69	2.65	0.17	0.02	24
		0.88	8.38	0.24	3.56	4.36	0.33	0.034	
GWK	rubble mound	-0.76	1.05	0.02	3	1.82	0.31	0.01	45
		0.66	8.13	0.21	5.21	3.84	0.61	0.03	
M & M	core locks	-8.2	1.02	0.02	2.87	0.68	0.05	0.01	122
		8.9	7.21	0.13	6.29	4.84	0.5	0.054	
Seabrook	rubble mound	-3.9	1.38	0.04	0.8	0.78	0.11	0.01	632
		0	74.47	1.66	8.32	3.2	0.58	0.06	
Aquareef	aquareef	-4.77	1.24	0.02	1.78	0.59	0.1	0.01	1063
		-0.09	102.12	2.1	5.8	4.09	0.87	0.08	

Within the DELOS project series of 2D random wave tests have been carried out in 2001 at the University of Cantabria, Spain, (referred as UCA here after) and at the Polytechnic of Catalonia, Spain, (referred to as UPC), described in Gironella et al. (2002). Both narrow and large crests have been tested, in particular in the UCA tests the parameter B/H_i ranged from 2.6 to 30, allowing a detailed analysis on the influence of this parameter. Large-scale tests in the Large Wave Channel (GWK), of the Coastal Research Centre (FZK), in Hanover (Germany), have been performed and analysed by the University of Naples, Italy, Calabrese et al. (2002). The main objective of these tests was to look at low-crested and submerged breakwaters in presence of broken waves on a beach.

Furthermore, tests from Seabrook and Hall (1998) have been included in the database. Structures tested in this study are classical rubble mound submerged breakwaters. Both the relative freeboard and the relative crest width have been varied within a wide range. In particular B/H_i reaches values of 74. Also tests results from Hirose et al. (2000) concerning a new type of concrete armour units, Aquareef, designed for submerged structures, have been added to the dataset. Similar to the Seabrook and Hall (1998) tests, the relative crest width has been varied from very small values up to $B/H_i = 102$. Both datasets have submerged structures only. Finally, experimental data coming from Melito and Melby's

(2000) (M & M hereafter) investigation on hydraulic response of structures armoured with coreloc have been considered. These tests have been performed both on submerged and emerged structures with the relative freeboard varying in a wide range.

Before starting any analysis it is worthwhile to take a look at Figure 2, which shows the overall picture on transmission coefficient versus the relative freeboard. In these graphs the old database has been shown jointly with UPC, UCA and GWK data, while the other three datasets have been shown separately. The range of R_c/H_i plotted is limited to $-5 < R_c/H_i < 5$. It is clear that structures armoured with Aquareef show higher maximum values of K_t compared to the other structures, probably due to the high permeability of the armour layer or due to the definition of the crest height (top of the aquareef unit). Moreover, these large values are reached at relatively large values of R_c/H_i.

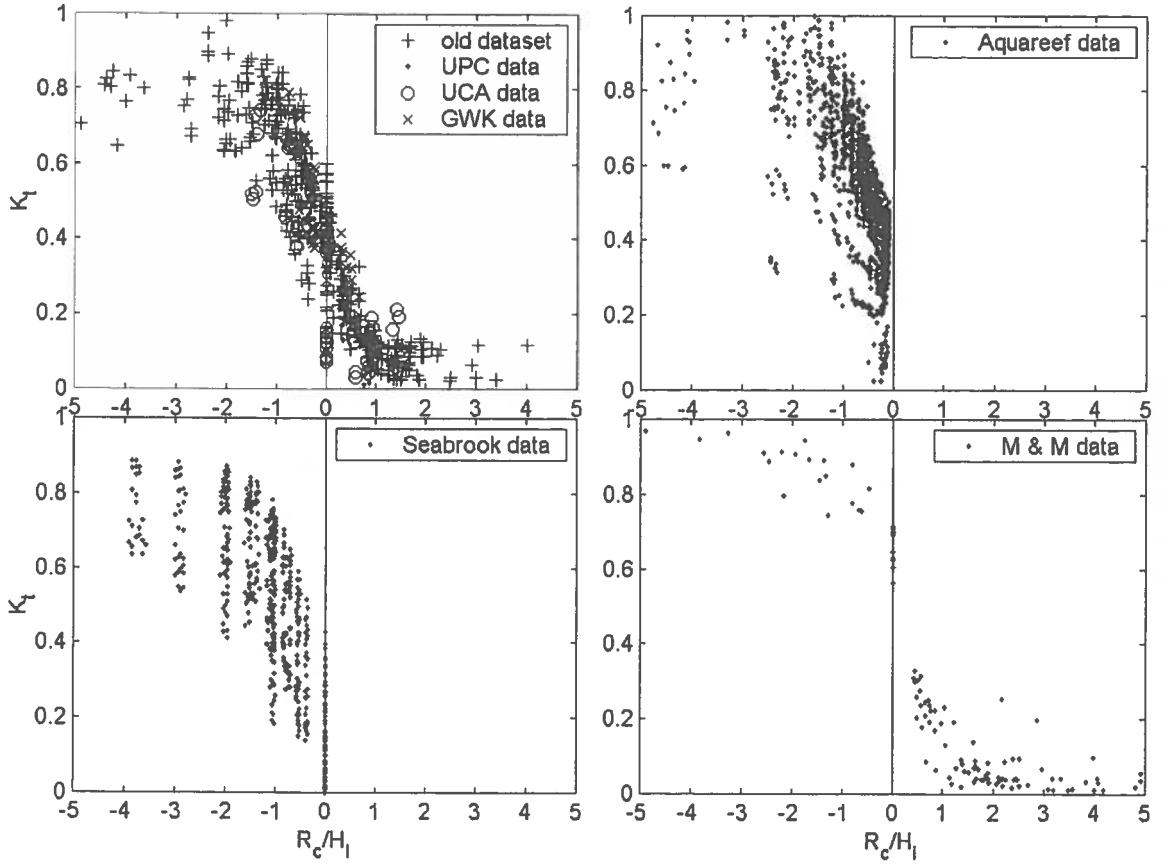

Figure 2. Wave transmission coefficient versus relative freeboard for the four sub-datasets used in this study.

2.2. *Improvement of existing formulae*

Van der Meer and Daemen (1994) and d'Angremond et al. (1996) proposed two different design formulae for K_t, which gives the starting point of the present analysis. The first reference considers the use of the nominal diameter D_{n50} in order to describe the influence of crest height on wave transmission; the second

reference relates the crest freeboard directly to the incident wave height. This enables a description of impermeable smooth structures too and not only rubble mound structures. Both formulae of above references include the influence of the non-dimensional crest freeboard, R_c/D_{n50} or R_c/H_i, the wave length L_{op} (or steepness, s_{op}) and the crest width B. In both formulae a linear dependency of K_t on the relative freeboard is assumed in the sharply varying region for K_t. The influence of crest width is included to explain the behaviour of K_t if $R_c = 0$.

The Van der Meer and Daemen formula for traditional breakwaters reads:

$$K_t = a\, R_c/D_{n50} + b \qquad (1)$$

where:
$a = 0.031H_i/D_{n50} - 0.024$ and
$b = -5.42s_{op} + 0.0323H_i/D_{n50} - 0.017(B/D_{n50})^{1.84} + 0.51$

The d'Angremond et al. (1996) formula reads:

$$K_t = -0.4R_c/H_i + 0.64(B/H_i)^{-0.31} * (1 - \exp(-0.5\xi_{op})) \qquad (2)$$

Both formulae have been limited with two values for K_t, which are K_t=0.75 and K_t=0.075 in Van der Meer and Daemen (1994) and K_t=0.8 and K_t=0.075 in d'Angremond et al.'s formula.

Equations 1 and 2 have been applied to the present database, keeping in mind that the parameter ranges are sometimes different from the ones investigated in the two original studies. It is obvious that if any formula is used outside the range in which it has been inferred, the accuracy of the estimate will decrease. In particular the influence of crest width described in equations 1 and 2 relies on a limited number of data, so it was expected that this variable might be crucial for the accuracy of the formula.

In this study an attempt to improve the formulae has been done by using two different relations, one for structures with B/H_i<10 and one for structures with larger relative crest width. The relationship for $B/H_i > 10$ has been obtained by simply refitting the structure of equation 2 on data with relative crest width belonging to this class. The result is:

$$K_t = -0.35R_c/H_i + 0.51(B/H_i)^{-0.65} * (1 - \exp(-0.41\xi_{op})) \qquad (3)$$

For structures with B/H_i <10 equation 2 has been considered still accurate.

It is useful to limit the maximum value in equation 3 in analogy with the two aforementioned studies. The definition of a maximum independent from B/H_i would lead to an inaccurate estimation of K_t. Therefore, a maximum function has been derived instead of a constant value. The average values of K_t corresponding to $R_c/H_i < -2$ have been considered for the six classes of B/H_i analysed in Figure

2 and the influence of the relative crest width has been studied. The upper limit, K_{tu}, can be described by assuming a linear dependency from the relative crest width:

$$K_{tu} = -0.006B/H_i + 0.93 \quad (4)$$

The lower limit, K_{tl}, of the formula has been kept constant and equal to $K_{tl} = 0.05$. The measured values of K_t have been compared with the ones predicted with equations 2 and 3, making use of the proposed limiting relationship 4, see Figure 3. The performances of the equations 1 - 4 may be evaluated in terms of round mean square error (RMSE) and R^2. Equations 1 and 2 show a RMSE of 0.112 and 0.072 and R^2 equal to 0.81 and 0.91, respectively for $B/H_i < 10$. Hence the d'Angremond et al's formula may be considered more accurate in this range. Eqaution 4 shows a RMSE equal to 0.082 and R^2 equal to 0.90 for $B/H^i > 10$ which represents its range of application. The standard deviation is 0.05 for equation 2 and 0.06 for equations 3 and 4.

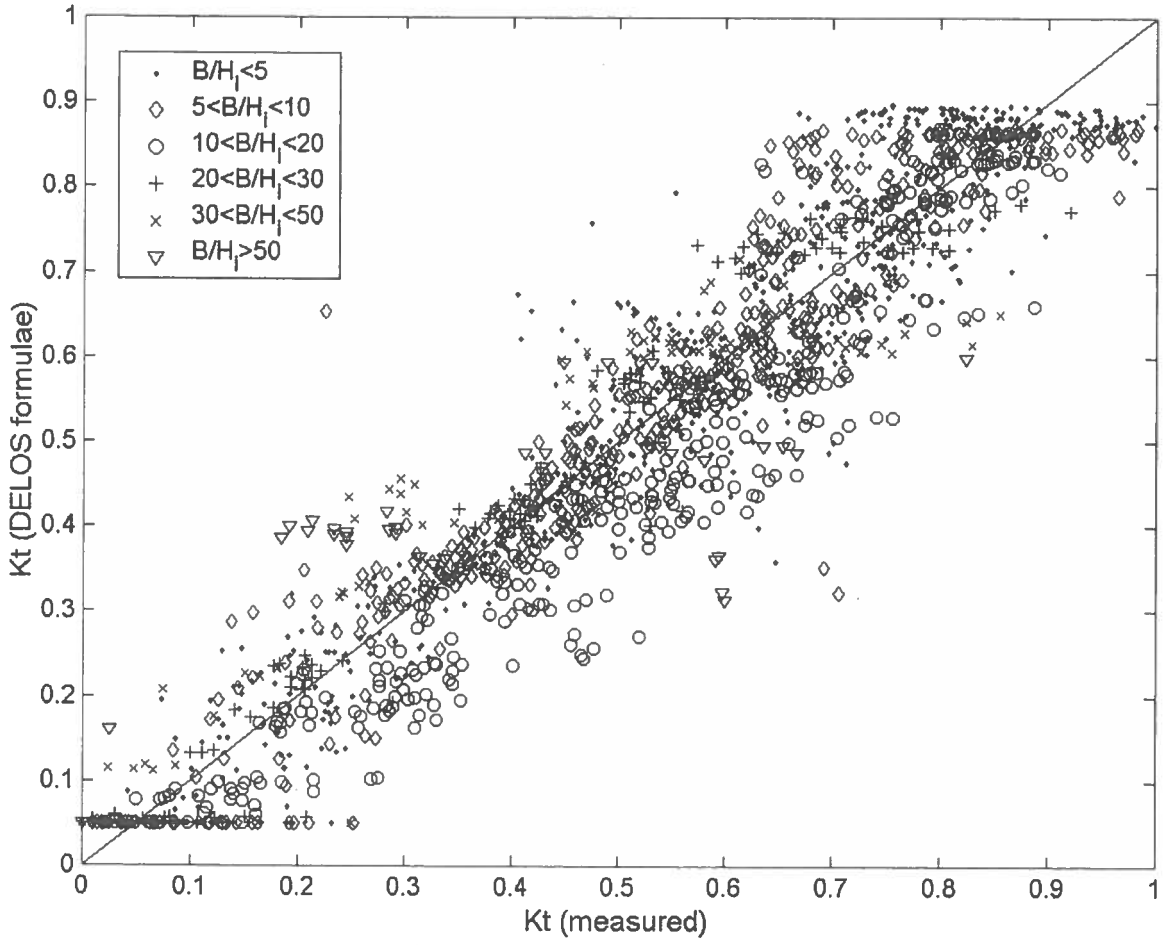

Figure 3. Comparison between calculated and measured values of the transmission coefficient using the proposed equations 2 – 4.

3. 3D effects on rubble mound LCS

In quite some situations low-crested structures are not parallel to the coast. T-shaped groynes are an example, but also breakwaters for a harbour where only under very extreme storm surge the structure can be considered as low-crested. In these situations wave attack is very often not perpendicular to the alignment of the structure and in many situations even quite oblique wave attack and transmission occurs. But what will be the difference with perpendicular attack?

More in detail:

- Are the prediction formulae for K_t still valid?
- Is there any influence of short-crestedness of waves?
- Are wave directions similar in front of the structure and after transmission?
- Is the spectral change (more energy to high frequencies) similar to perpendicular wave attack?

Three-dimensional tests on wave transmission were performed under DELOS in the short-crested wave basin at Aalborg University, Denmark to answer these questions, see Van der Meer et al. (2003).

3.1. *Long-crested versus short-crested waves*

The first question to consider is whether similar results are found for long-crested and short-crested waves. In theory it should be similar for perpendicular wave attack ($\beta = 0°$), but differences may occur for angled wave attack. For wave run-up and overtopping on dikes, for example, short-crested waves gave less reduction for larger wave angles than long-crested waves, see Van der Meer et al. (1998). The conclusion from the present research, however, is that long-crested and short-crested waves give similar overtopping for rubble mound structures, although in average the short-crested waves give 1%–2% lower values. For more details see Van der Meer et al. (2003).

3.2. *Change of wave direction*

Another important question is whether transmitted waves have the same direction as the incident waves. Figure 4 gives the results for the rubble mound structure. First of all this graph shows that perpendicular generated waves did in fact not reach the structure completely perpendicular, but in average under an angle of about -10° (the cloud of data points in the lower left corner of Fig. 4).

This was caused by a slightly different layout with a roundhead at one of the ends of the structure. The figure shows clearly that the transmitted wave direction is smaller than the incident one. The reason for this could be that roughness and porosity of the structure cause dissipation of energy in such a way that the waves do not go on in the same direction. A simple straight line fits all

data points quite well and leads to the conclusion that the transmitted wave angle is about 80% of the incident wave angle, or:

$$\beta_t = 0.80\ \beta_i \quad \text{for rubble mound structures} \tag{5}$$

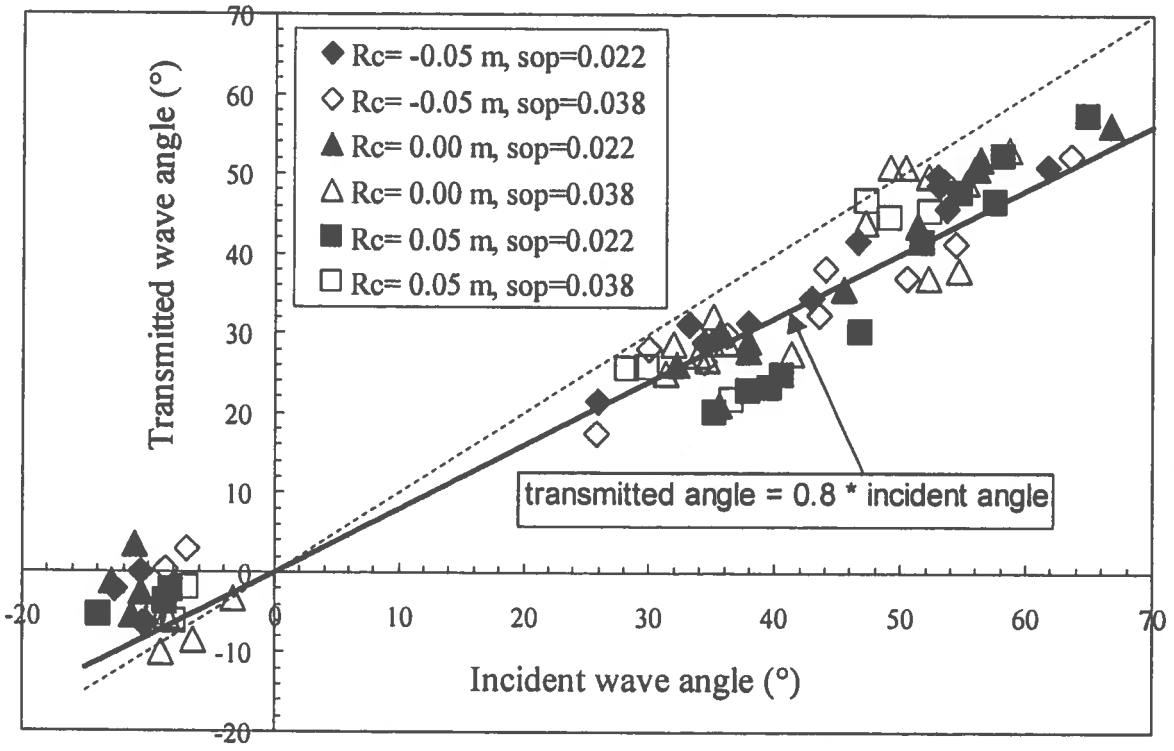

Figure 4. Transmitted wave angle versus incident angle. Rubble mound structure.

3.3. *Influence of angle of wave attack on transmission coefficient*

Transmission coefficients are mostly obtained by 2D flume testing where the angle of wave attack is always perpendicular to the structure. But are the coefficients still valid if the angle of wave attack is oblique? Figure 5 gives the answer for rubble mound structures.

The transmission coefficients are given for 3 groups of data points (the 3 different crest levels) and within each group a distinction has been made for the wave steepness. Of course a lower crest level gives larger transmission, which is according to 2D research. The main objective in Figure 5, however, is to look at the trend within each group of data points with respect to the incident wave angle. For the two lowest crest heights, the upper part of the graph, there is a very small tendency that the transmission coefficient decreases with increasing angle of wave attack. But within the scatter of the data it is only marginal.

For the highest crest height the trend seems a little more pronounced, but even there no influence is found for incident wave angles between 30° and 60°.

For rubble mound structures it can be concluded that the angle of wave attack has no or only marginal influence on the wave transmission coefficient. This leads also to the conclusion that prediction formulae for transmission at rubble mound structures, such as equations 2-4, are valid for oblique wave attack as well. One restriction may be that it is only valid for rubble structures with a small crest width and up to an angle of about 60°.

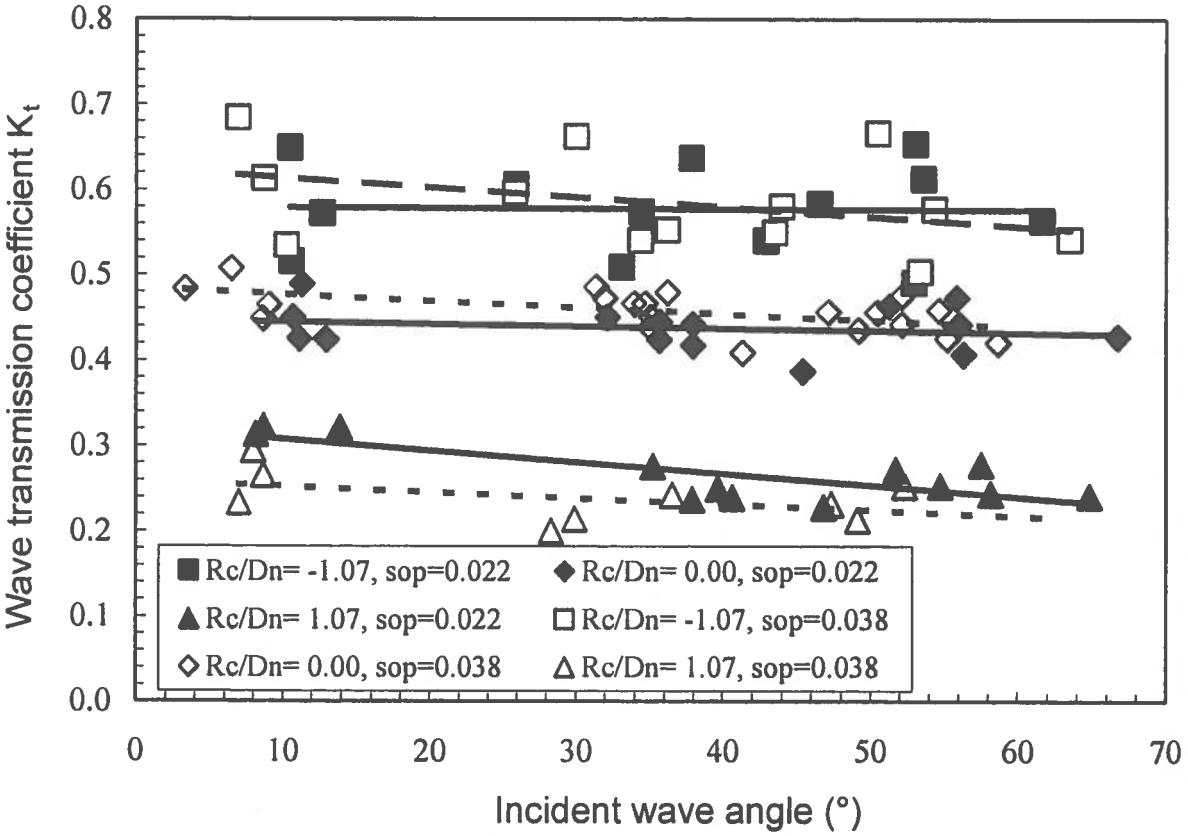

Figure 5. Influence of wave angle on wave transmission coefficient K_t for rubble mound structures

4. Wave transmission at smooth and impermeable LCS

4.1. *Normal wave attack*

Not all low-crested structures are of the rubble mound type. Sometimes smooth and impermeable structures exist, for example low-crested structures covered with asphalt or armoured with a block revetment. Often the slope angles of the structure are gentler (1:3 or 1:4) than for rubble mound structures, mainly for construction reasons.

Wave transmission over smooth low-crested structures is completely different from rubble mound structures. First of all, the wave transmission is larger for the same crest height, simply because there is no energy dissipation by friction and porosity of the structure. Furthermore, the crest width has less or even no influence on transmission, as also on the crest there is no energy

dissipation, which is completely different from rubble mound structures. Only for very wide (submerged) structures there could be some influence on the crest width, but this is not a case that will often be present in reality as asphalt and block revetments are mainly constructed in the dry and not under water. The presence of tide makes it possible to construct these kind of structures above water.

Equation 2 in this paper, given by d'Angremond et al., 1996, appeared to be a good formula for rubble mound structures. An almost identical formula was given for smooth structures, but now with a coefficient 0.80 instead of 0.64. At that time it was assumed on limited data, that rubble mound and smooth structures perform more or less the same. The opposite is true as already stated above and, therefore, smooth structures are treated independently from rubble mound structures. A re-analysis was done on all smooth structure data available and this led to the following equation to be used for 2D wave transmission at smooth LCS:

$$K_t = -0.3R_c/H_i + 0.75[1 - \exp(-0.5\xi_{op})] \qquad \text{for } \xi_{op} < 3$$

$$K_t = -0.3R_c/H_i + [B/H_i]^{-0.31} * [1 - \exp(-0.5\xi_{op})] * 0.75 \qquad \text{for } \xi_{op} \geq 3 \qquad (6)$$

with as minimum $K_t = 0.075$ and maximum $K_t = 0.8$.

4.2. *Influence of angle of wave attack on transmission coefficient*

In contrast to rubble mound structures, smooth LCS showed a strong dependency between transmission coefficient and angle of wave attack. With a good formula for 2D wave transmission on smooth structures (equation 6) it is possible to make a straight forward analysis on the effect of oblique waves. Equation 6 was used as a reference and for each test condition the K_t for perpendicular wave attack was calculated. The measured to calculated K_t ratio for $\beta = 0°$ was then plotted versus the incident wave angle β, see Figure 6.

Although Figure 6 shows some scatter, the trend is very clear that wave transmission decreases with increasing incident wave angle. An easy way to include the effect of oblique waves is to add a $(\cos\beta)^{2/3}$ function to the 2D-equation 6. This leads to the final prediction formula for smooth structures, including obliquity:

$$K_t = [-0.3R_c/H_i + 0.75[1 - \exp(-0.5\xi_{op})]] (\cos\beta)^{2/3} \qquad (7)$$

with as minimum $K_t = 0.075$ and maximum $K_t = 0.8$, and limitations:

$$1 < \xi_{op} < 3 \qquad 0° \leq \beta \leq 70° \qquad 1 < B/H_i < 4$$

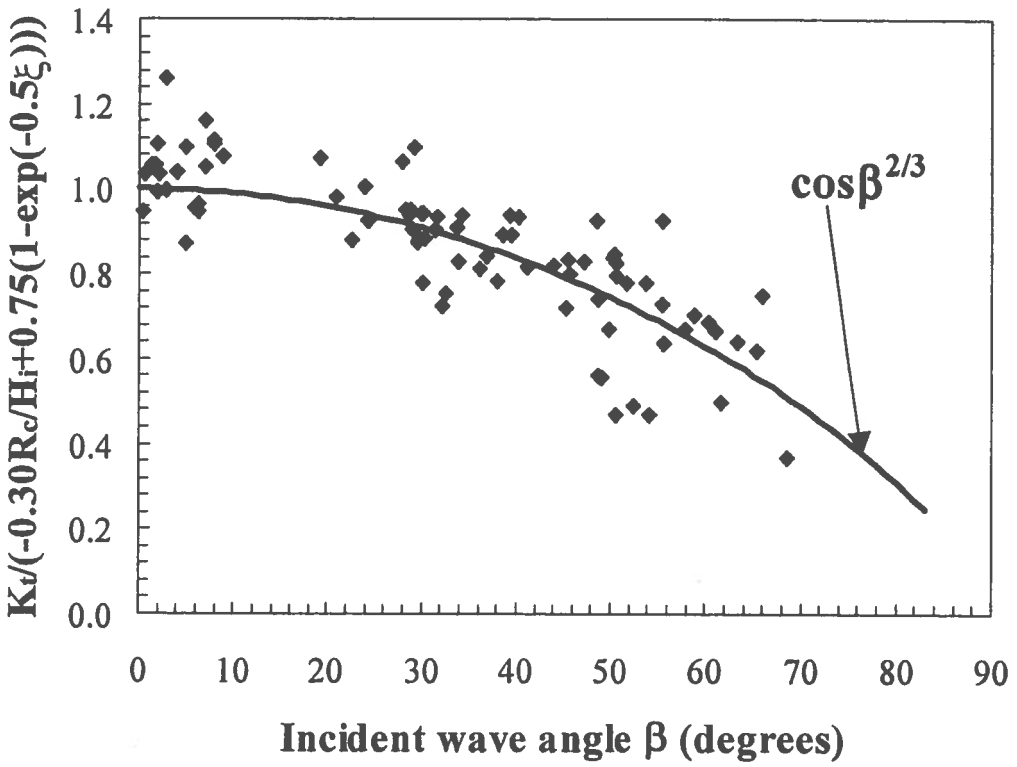

Figure 6. Influence of oblique wave attack on smooth structures.

4.3. *Long-crested versus short-crested waves*

Comparsion of long-crested and short-crested results on smooth slopes gave the same conclusion as for rubble mound structures: there is no or only a marginal difference between long-crested and short-crested waves. See for more details Van der Meer et al. (2003).

4.4. *Change of wave direction*

Figure 7 shows the results of change of wave direction for the smooth structure in a comparable way as in Figure 4 for the rubble mound LCS.

The conclusions now are quite different from the one for rubble mound structures. Up to 45° transmitted and incident waves have similar directions. For larger incident angles than 45° this changes: the transmitted wave angle remains 45°. Probably the smooth structure works in such a way that for larger angles the waves run along the crest of the structure and generate always a transmitted angle of 45°. There is also a tendency that for lower wave transmission (the data points for R_c = 0.05 m) the transmitted wave angle is a little smaller than the incident one. For smooth structures the behaviour can be described by:

$$\beta_t = \beta_i \qquad \text{for } \beta_i \leq 45°$$

$$\beta_t = 45° \quad \text{for } \beta_i > 45° \qquad \text{for smooth structures} \tag{8}$$

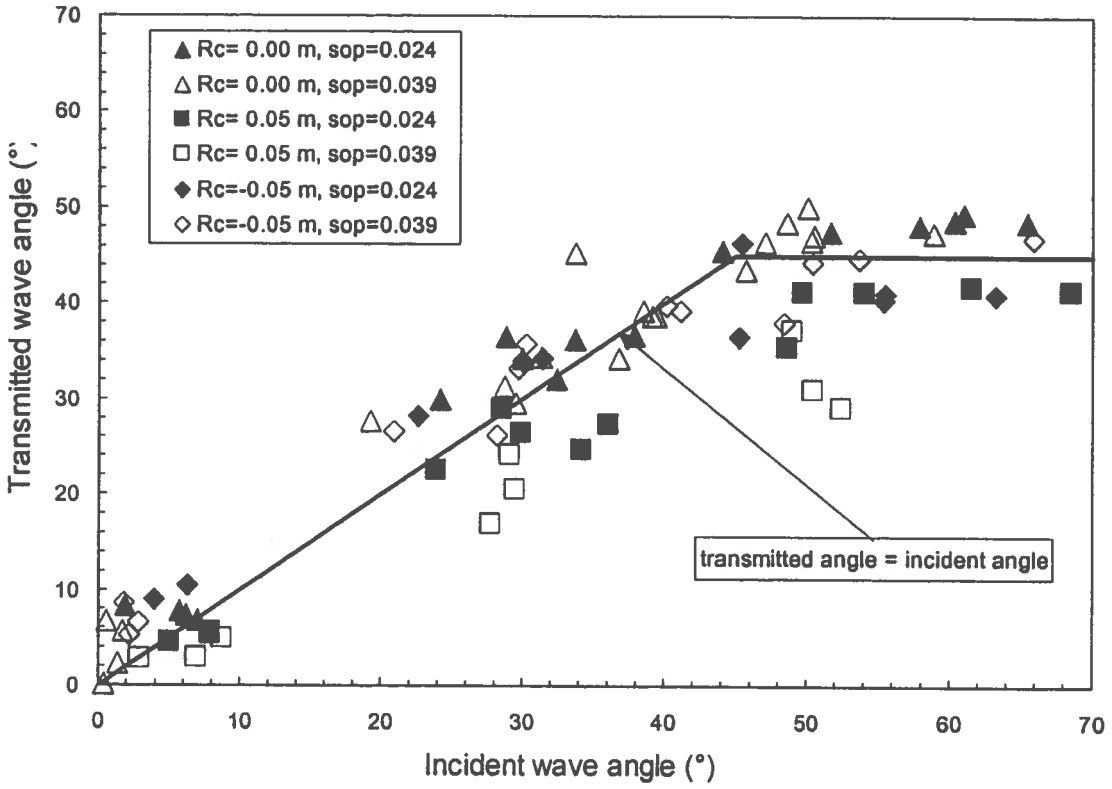

Figure 7. Transmitted wave angle versus incident angle. Smooth structure

Conclusions

Within the EU funded project DELOS 2D and 3D experiments at permeable and impermeable LCS have been carried out and an extensive database of 2D wave transmission at LCS has been collected. The gathered results have been reanalysed and used to improve the prediction of the transmission coefficient.

The outcome of this analysis consists in two new design formulae: for rubble-mound structures, eqs. (3)-(4), which are respectively d'Angremond et al. (1996) formula for relatively small crest widths ($B/H_i < 10$) and a new formula for large to very large crest widths; for smooth structures, eq. (6) gives different expression depending on the breaking parameter.

Incident and transmitted wave angles are not always similar: for rubble mound structures, the transmitted wave angle is about the 80% of the incident one, whereas for smooth structures the transmitted wave angle is equal to the incident one for incident wave angles less than 45° and is equal to 45° for incident wave angles larger than 45°.

The influence of the wave angle on the transmission coefficient is small for rubble mound structures, whereas smooth structures show a clear influence on the wave angle which can be described by a cosine function, see eq. (7).

Acknowledgments

This work has been performed within the EU-funded projects DELOS (EVK3-2000-00041). The authors would like to thank Prof. Kevin Hall (Queens University, Canada), Norikazu Hirose (Tetra co. ltd, Japan) and Dr. Jeffrey Melby (USACE) for making available their valuable datasets.

References

Briganti, R., J.W. van der Meer, M. Buccino and M. Calabrese (2003). Wave transmission behind low crested structures. Proc. Coastal Structures, Portland, Oregon, USA.

d'Angremond K., J.W. van der Meer and R.J. de Jong (1996). Wave transmission at low crested structures. Proc. 25th Int. Conf. on Coastal Engineering, ASCE, 3305-3318.

Calabrese M., V. Vicinanza and M. Buccino (2002). Large scale experiments on the behaviour of low crested and submerged breakwaters in presence of broken waves. Proc. 28th Int. Conf. on Coastal Engineering, ASCE, 1900-1912.

Gironella X., A. Sànchez-Arcilla, R. Briganti, J.P. Sierra and L. Moreno (2002). Submerged detached breakwaters: towards a functional design. Proc. 28th Int. Conf. on Coastal Engineering, ASCE, 1768-1777.

Hirose, N., A. Watanuki and M. Saito (2002). New Type Units for Artificial Reef Development of Ecofriendly Artificial Reefs and the Effectiveness Thereof. Proc. 30th International Navigation Congress, PIANC, 2002.

Melito, I and J.A. Melby (2002) Wave runup, transmission, and reflection for structures armoured with CORE-LOC. J. of Coastal Engineering 45, 33 – 52. Elsevier.

Seabrook S.R. and K.R. Hall (1998). Wave transmission at submerged rubble mound breakwaters. Proc. 26th Int. Conf. on Coastal Engineering, ASCE, 2000-2013.

Van der Meer J.W. and I.F.R. Daemen (1994). Stability and wave transmission at low crested rubble mound structures. J. of Waterway, Port Coastal and Ocean Engineering, 1, 1-19.

Van der Meer, J.W., P. Tönjes and de J.P. de Waal (1998). A code for dike height design and examination. Coastlines, Structures and Breakwaters. ICE, pp. 5-19. Ed. N.W.H. Allsop, Thomas Telford, London, UK.

Van der Meer, J.W., A. Wolters, B. Zanuttigh. and M. Kramer (2003). Oblique wave transmission over low-crested coastal defence structure. Proc. Coastal Structures, Portland, Oregon, USA.

KEYWORDS – ICCE 2004

WAVE TRANSMISSION AT LOW-CRESTED STRUCTURES, INCLUDING OBLIQUE WAVE ATTACK

Van der Meer, J.W., R. Briganti, B. Wang and B. Zanuttigh

Abstract number 388

Low-crest
Transmission
Oblique attack
Rubble structure
Smooth structure
Experiments 2D, 3D
Database